



Technology Maturation

Holly Trelue
Technical Area Lead
For Tech. Mat.

March 3, 2022

LA-UR-22-21890

Outline

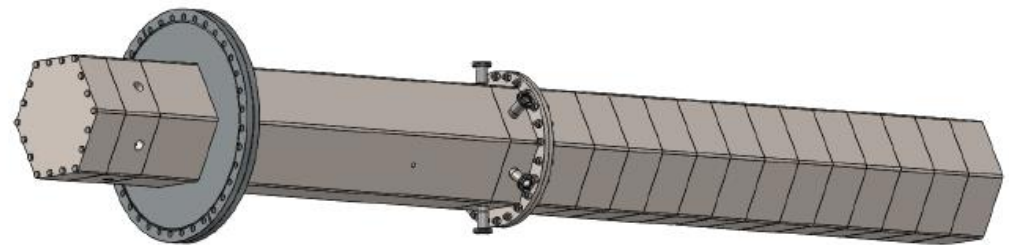
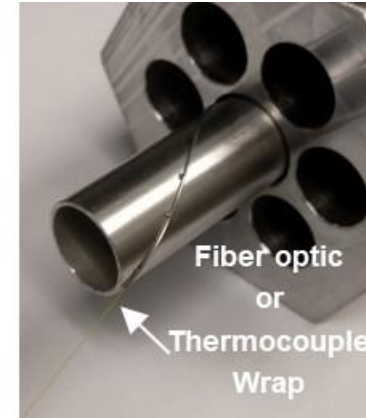
- Overview
- High Temperature Moderator Material
- Instrumentation and Sensors
- Heat Transfer/37 Heat Pipe Test Article
- NEUP – Structural Integrity
- NEUP – Heat Pipe Failures
- NEUP – Heat Exchanger Technology
- Future Work/Wrap-Up

How Technology Maturation Meets Program Objectives

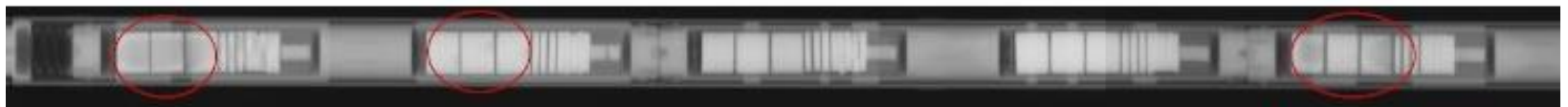
- Through cross-cutting research and development and technology demonstration support, achieve technological breakthroughs for key features of microreactors, examine:
 - Moderation to reduce required fuel mass
 - Instrumentation and sensors
 - Advanced heat transfer
- Meet critical R&D needs of existing developers that require national lab or university expertise or capabilities.
 - Develop and irradiate samples of moderating material
 - Build and test non-nuclear test articles
- Develop advanced technologies and concepts for next-generation microreactor applications and systems.
 - Design and fabricate state-of-the-art technology.
 - Understand performance of systems with instruments.
- Enable future microreactor applications
 - Coupling of the above components.

Three control areas are currently supported

- High Temperature Moderator Material
 - INL (Chase Taylor)
 - LANL (Erik Luther)
- Instrumentation and Sensors
 - ORNL (Chris Petrie)
 - INL (Troy Unruh)
 - LANL (TJ Ulrich)
- Heat Transfer
 - LANL (Bob Reid)
- 4-5 journal articles in special issue of Nuclear Technology



Hydrogen loss in the moderator



Cracked can

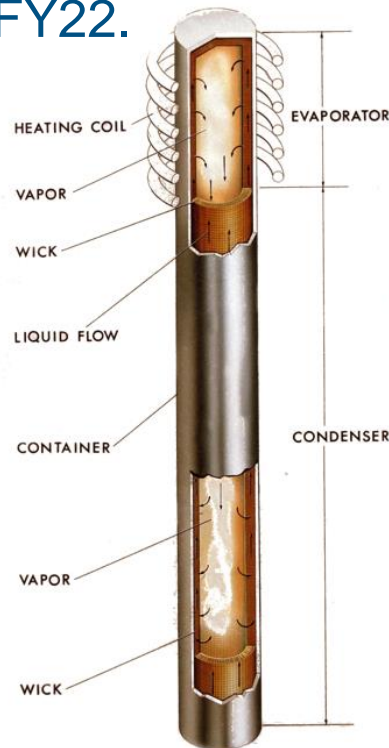
High Temperature Moderator Material

- FY20: Fabricated samples of yttrium hydride.
- FY21: Samples were irradiated in ATR.
- FY22: Initiated PIE on irradiated samples.
- FY22: Performed neutron imaging to understand hydrogen migration with temperature
- FY21: Initiated cladding and containment analysis for hydrides.
- FY21: Performed critical experiment on YH.



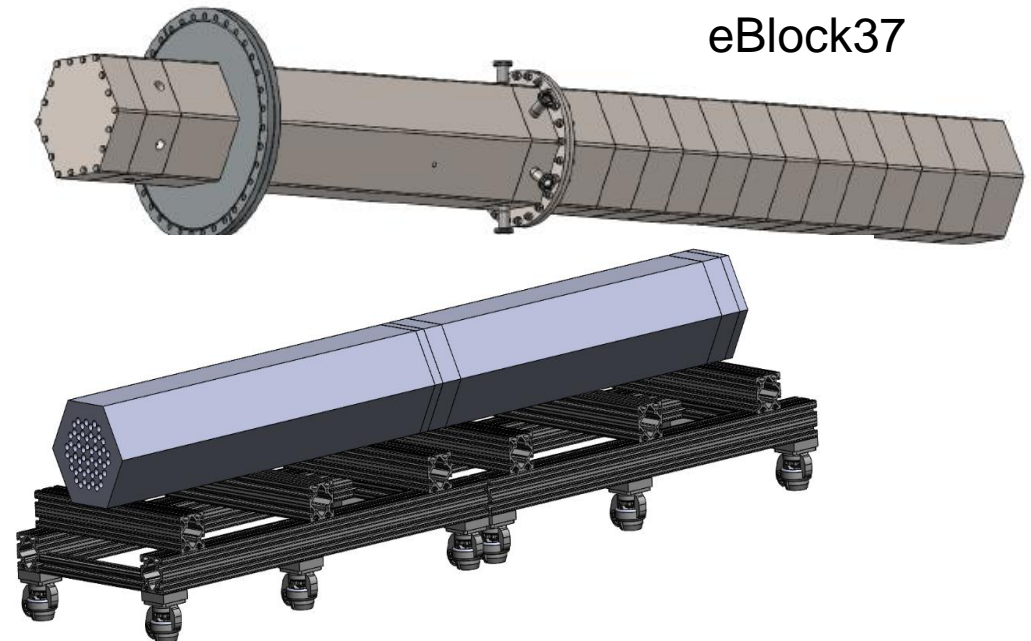
Heat Transfer – focus on heat pipes

- 37 heat pipe article is being fabricated.
 - Core block components are being joined then combined with heat exchanger part.
 - High fidelity wicks fabricated; need to be added to the 2 m long article, then filled with sodium.
 - Final step is laser weld system at LANL then ship to INL.
- Fuel rods will be simulated with cartridge heaters and combined heat pipe/heat exchanger article will be tested at MAGNET in FY22.



HEAT PIPE

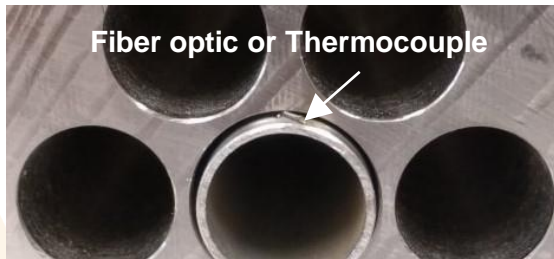
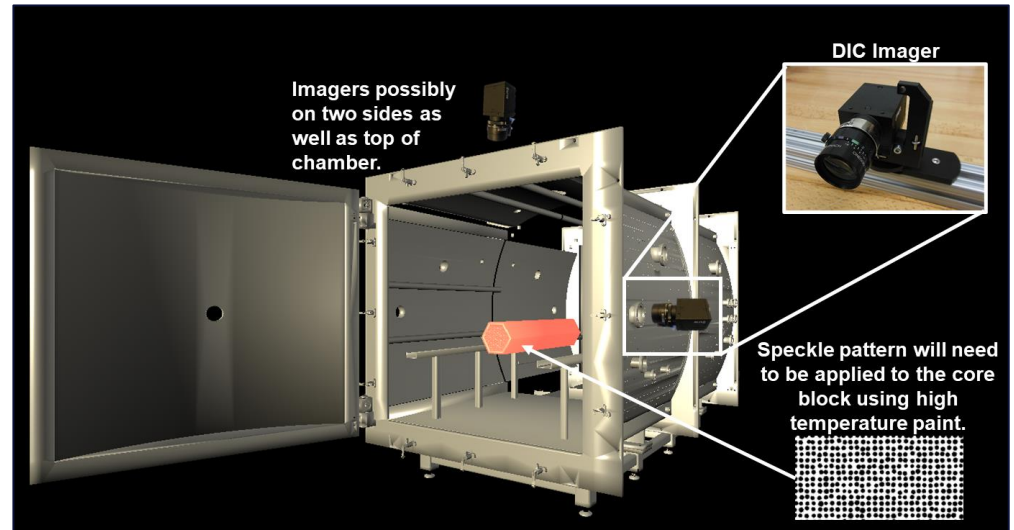
LANL



Test Article on Handling Cart

Instrumentation and Sensors

Fiber optics, Digital Image Correlation, Thermocouples, and More



Distributed temperature sensor measurement mockup



Thermocouple weld mockup

Work packages	\$	Milestones	Due Date
AT-22OR080401 – ORNL Instrumentation and Sensors	\$113k	Perform test on article with embedded sensors	7/29/22 On track
AT-22IN080402 – Instrumentation and Sensors – INL	\$100k	Test sensors - SPHERE Test sensors - MAGNET Final Annual Report	(4/26/22) 7/28/22 8/31/22 On track
AT-22LA080403 – Instrumentation and Sensors – LANL	\$89k	Report on proposed structural health measurements	9/30/22
AT-22LA080404 – Heat Transfer – LANL	\$948k (\$200k)	Document progress Complete assembly of 37 heat pipe article Ship article to INL	1/31/22 6/30/22 (delayed) 7/31/22
AT-22LA080405 – High Temperature Moderator – LANL	\$415k	Report on neutron imaging Advanced Handbook v2	8/31/22 9/30/22
AT-22IN080406 – High Temperature Moderator - INL	\$958k	Ship capsules for PIE Disassemble capsules Complete ½ PIE	11/30/21 2/28/22 8/30/22

Conclusions

- Upcoming presentations will give technical details
- Followed by discussion of future work needs



High temperature moderator material

March 3, 2022

Chase N. Taylor, Idaho National Laboratory

Eric P. Luther, Los Alamos National Laboratory

Objective

- Presence of moderator significantly decreases overall mass of fuel required in a microreactor by thermalizing neutrons and increasing probability of fission.
- Investigate materials performance, fabrication, and testing of moderators. FY22 work involved yttrium hydride (YH_x).
- High temperature moderator work in FY22 focused on two main technical activities:
 - Post irradiation examination of YH_x irradiated in the Advanced Test Reactor (ATR).
 - Neutron imaging measurements at the Los Alamos Neutron Science Center (LANSCE) to determine hydrogen diffusion with temperature.



Yttrium hydride microreactor moderators

March 3, 2022

Chase N. Taylor, M. Nedim Cinbiz, Thomas A. Johnson,

Idaho National Laboratory

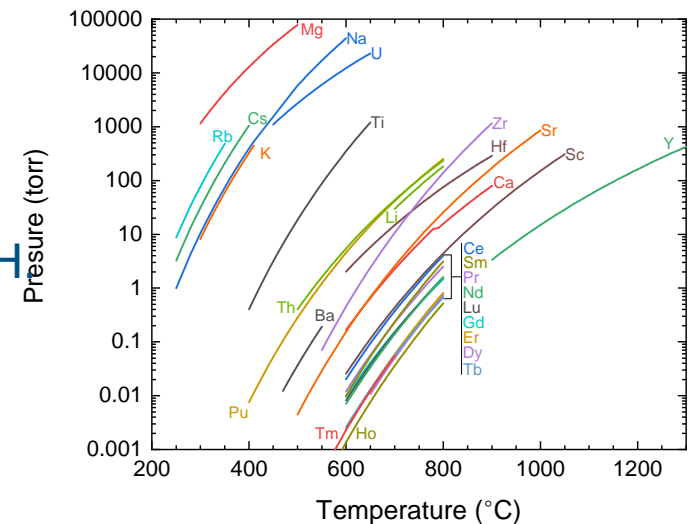
Eric P. Luther, Aditya P. Shivprasad

Los Alamos National Laboratory

Introduction

- Advanced neutron moderators are required for microreactors due to the:
 - Lower fuel enrichment of HALEU (<20%) instead of high enriched uranium.
 - Compact size.
 - High efficiency/high temperature requirements.
- Hydrogen is the best moderator as it has a low Z number.
 - Metal hydrides have exceptionally high hydrogen density.
 - Yttrium hydride YH has the highest temperature stability of metal hydrides.
- Legacy experiments proved that YH can be an extremely effective moderator, but no quantitative post-irradiation data exists for YH.

Hydride	Attainable hydrogen density	
	10^{22} atoms H/cm ³	g H/cm ³
TiH ₂	9.1	0.152
ZrH ₂	7.3	0.122
LiH	5.8	0.095
YH ₂	5.8	0.097
ThH ₂	4.9	0.082
H ₂ O	6.6	0.110
ThZr ₂ H ₇	7.7	0.129
ThTi ₂ H ₆	8.8	0.147



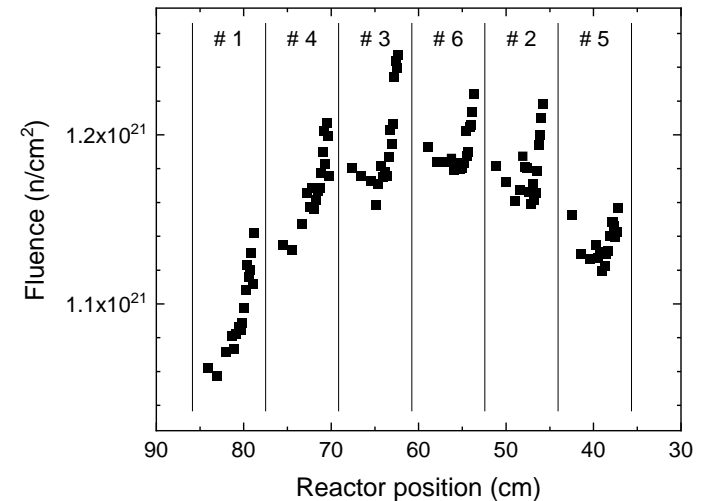
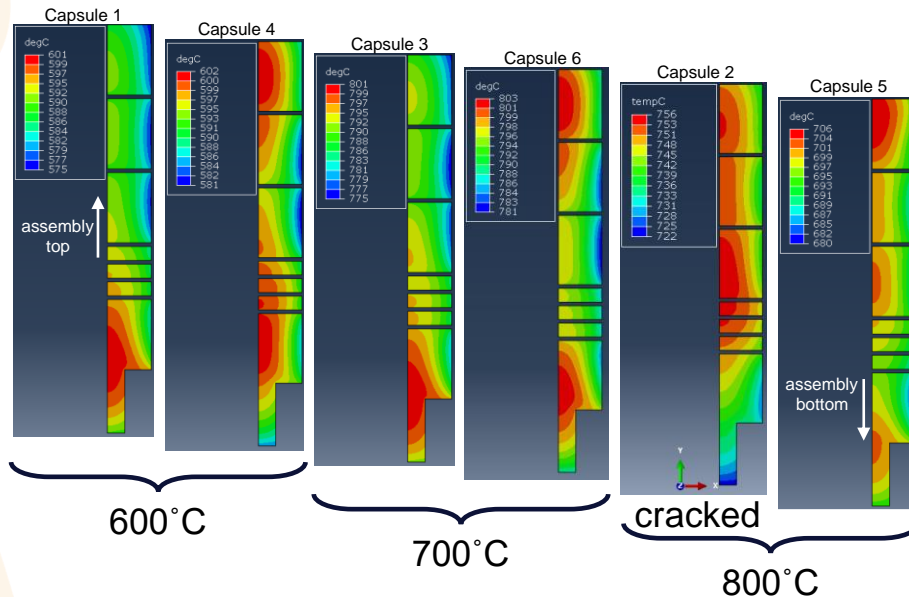
Objective

- Obtain the properties of irradiated YH.

Summary of project progress

(...since February 2021)

- February 19, 2021 – Advanced Test Reactor (ATR) irradiation of yttrium hydride samples commenced
- April 19, 2021 – ATR irradiation completed.



Summary of project progress

(...since February 2021)

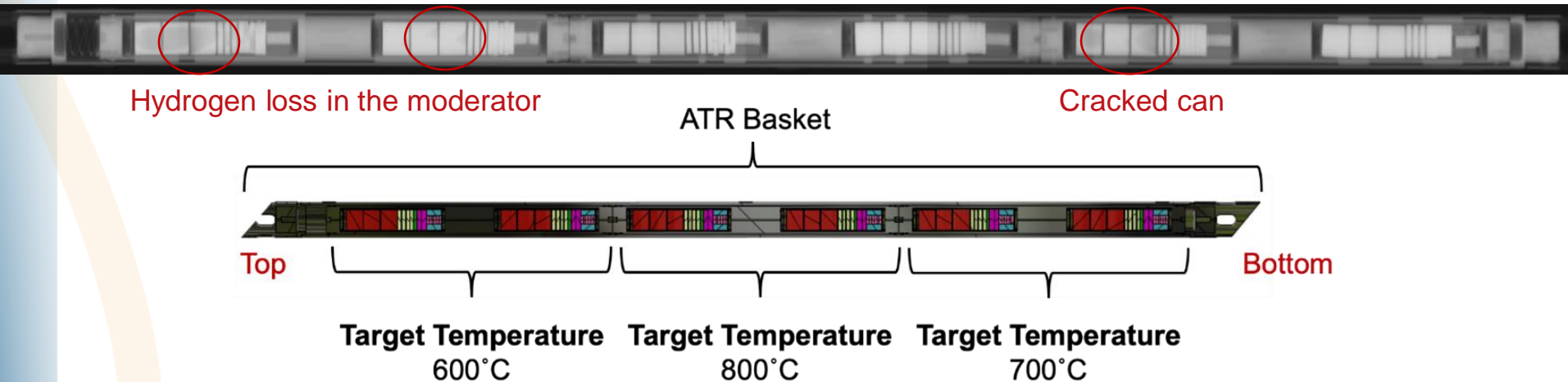
- February 19, 2021 – Advanced Test Reactor (ATR) irradiation of yttrium hydride samples commenced
- April 19, 2021 – ATR irradiation completed.
- June 16, 2021 - Irradiation assembly shipped from ATR to the Hot Fuels Examination Facility (HFEF) at Materials and Fuels Complex (MFC).



Summary of project progress

(...since February 2021)

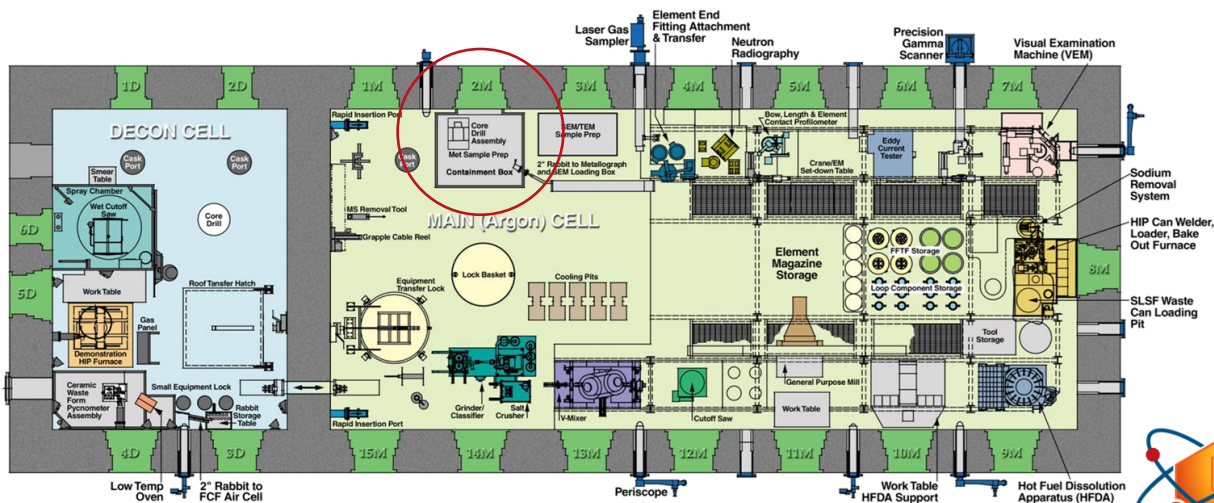
- February 19, 2021 – Advanced Test Reactor (ATR) irradiation of yttrium hydride samples commenced
- April 19, 2021 – ATR irradiation completed.
- June 16, 2021 - Irradiation assembly shipped from ATR to the Hot Fuels Examination Facility (HFEF) at Materials and Fuels Complex (MFC).
- September 2, 2021 – Neutron radiography performed.



Summary of project progress

(...since February 2021)

- February 19, 2021 – Advanced Test Reactor (ATR) irradiation of yttrium hydride samples commenced
- April 19, 2021 – ATR irradiation completed.
- June 16, 2021 - Irradiation assembly shipped from ATR to the Hot Fuels Examination Facility (HFEF) at Materials and Fuels Complex (MFC).
- September 2, 2021 – Neutron radiography performed.
- October 6, 2021 – Irradiation assembly disassembled.



Summary of project progress

(...since February 2021)

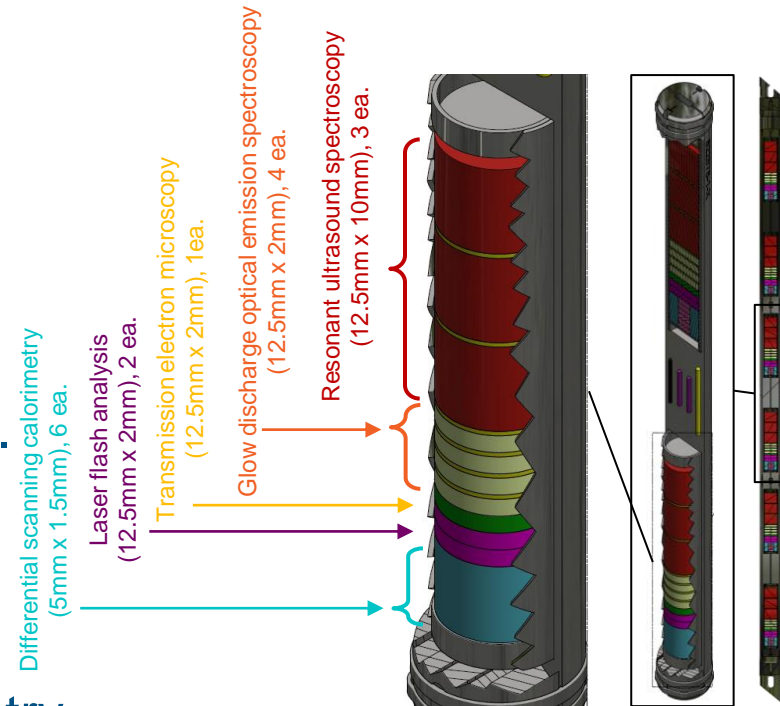
- February 19, 2021 – Advanced Test Reactor (ATR) irradiation of yttrium hydride samples commenced
- April 19, 2021 – ATR irradiation completed.
- June 16, 2021 - Irradiation assembly shipped from ATR to the Hot Fuels Examination Facility (HFEF) at Materials and Fuels Complex (MFC).
- September 2, 2021 – Neutron radiography performed.
- October 6, 2021 – Irradiation assembly disassembled.
- November 8, 2021 – First batch of samples (19) transferred from HFEF to the Analytical Research Laboratory for extended PIE.
- January 31, 2022 – Moving the samples from the contaminated KGTs to the clean KGTs.
- February 16, 2022 – Gamma spectroscopy results on radioactive constituents.

Milestones

- M3 (11/30/2021): Transfer LANL capsules from HFEF to analytical laboratory
 - Complete
- M4 (2/28/2021): Disassembly of the LANL capsules
 - Complete
- M2 (8/30/2022): Complete at least half of post irradiation examination activities for YH irradiated in ATR.
 - Higher than expected radiation and contamination levels are introducing significant delays.
 - Path forward to completion identified.

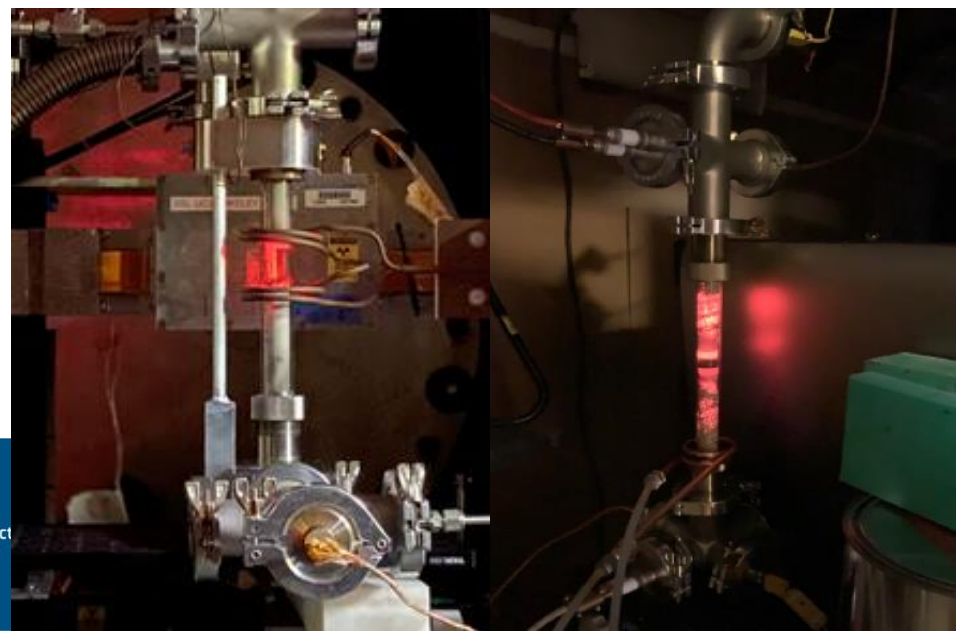
Future work

- Continue PIE activities
 - Non-destructive examination:
 - Optical
 - Dimensional
 - Volumetric
 - Mass characterization.
 - Fluence wire characterization.
 - Begin thermal characterization:
 - Hydrogen analysis
 - Thermal diffusivity
 - Differential scanning calorimetry
- FY23 PIE will include:
 - SEM, TEM, nanoindentation, XRD, elastic properties, GD-OES.
 - Continue thermal characterization (including thermal expansion).
 - PIE on TZM foils.



Building up Capabilities to Characterize Hydrogen in YH_{2-x} with Neutron Radiography at LANL

Alexander Long, Travis Carver, Erik Luther, Vedant Mehta, Caitlin Taylor, James Torres, Aditya Shivprasad, Holly Trelue, and Sven Vogel

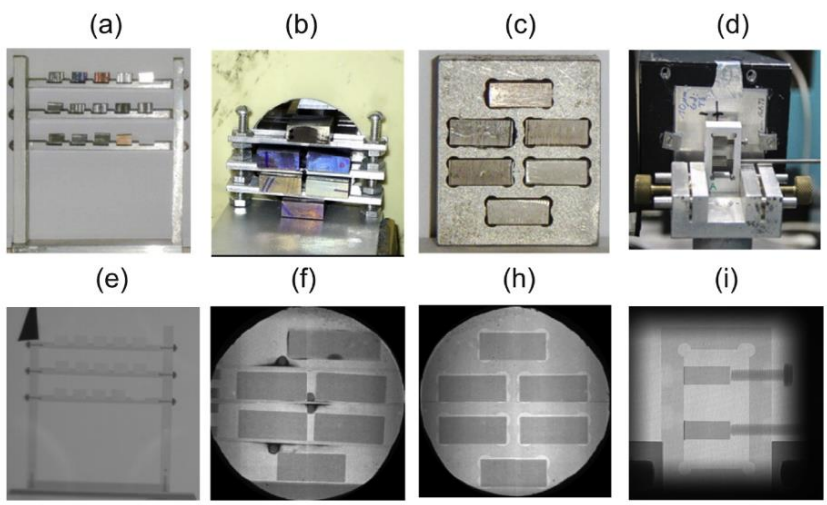
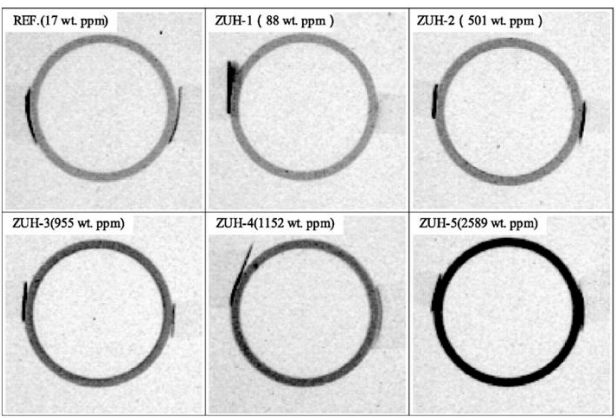


Previous Works of Neutron Imaging to Probe H-concentrations

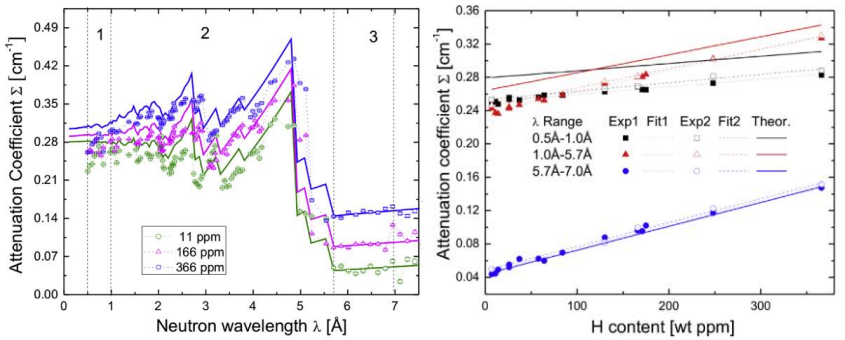
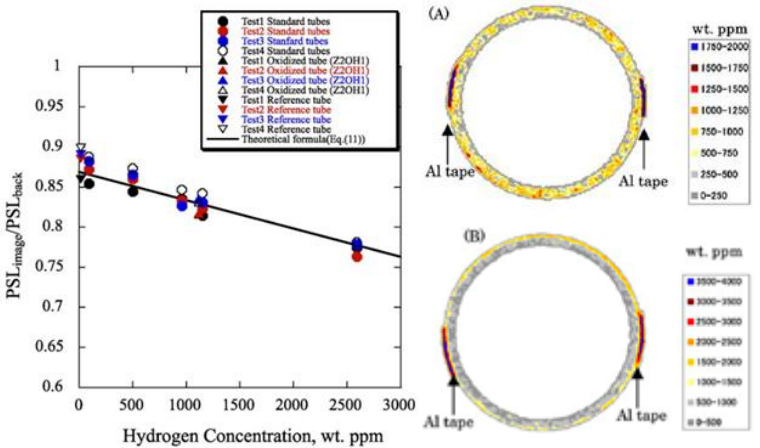
Most Neutron imaging measurements to date have looked at H-concentrations in Zirconium alloys.

$$T(x, y, E_n) = \exp(-z_H(x, y) \Sigma(x, y, E_n))$$

Measure Determine Calibrate/Model
 $T(x, y, E_n)$ $z_H(x, y)$ $\Sigma(x, y, E_n)$



If neutron source is pulsed, then **Energy Resolved Neutron Imaging (ERNI)** measurements can be performed. ERNI measurements have been shown not need calibration sample and to resolve H-concentrations down to 5ppm %wt.

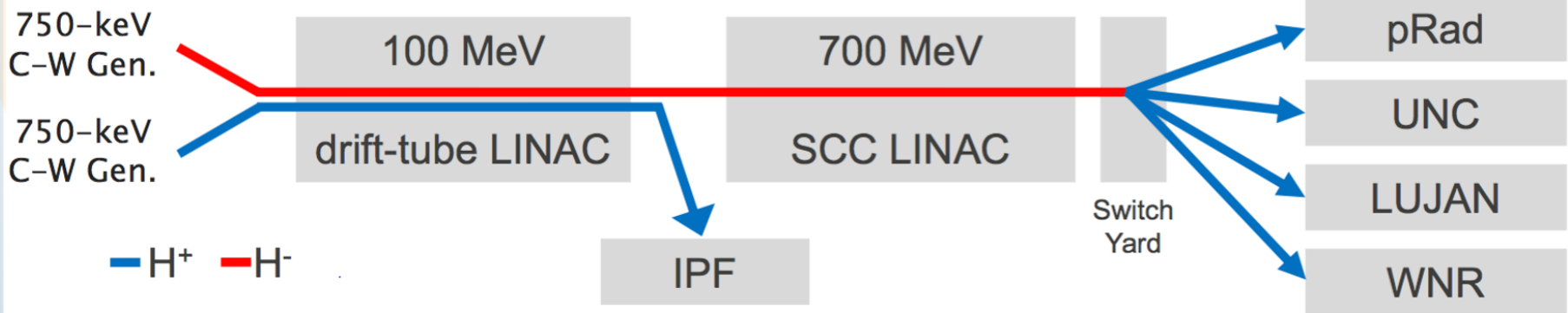
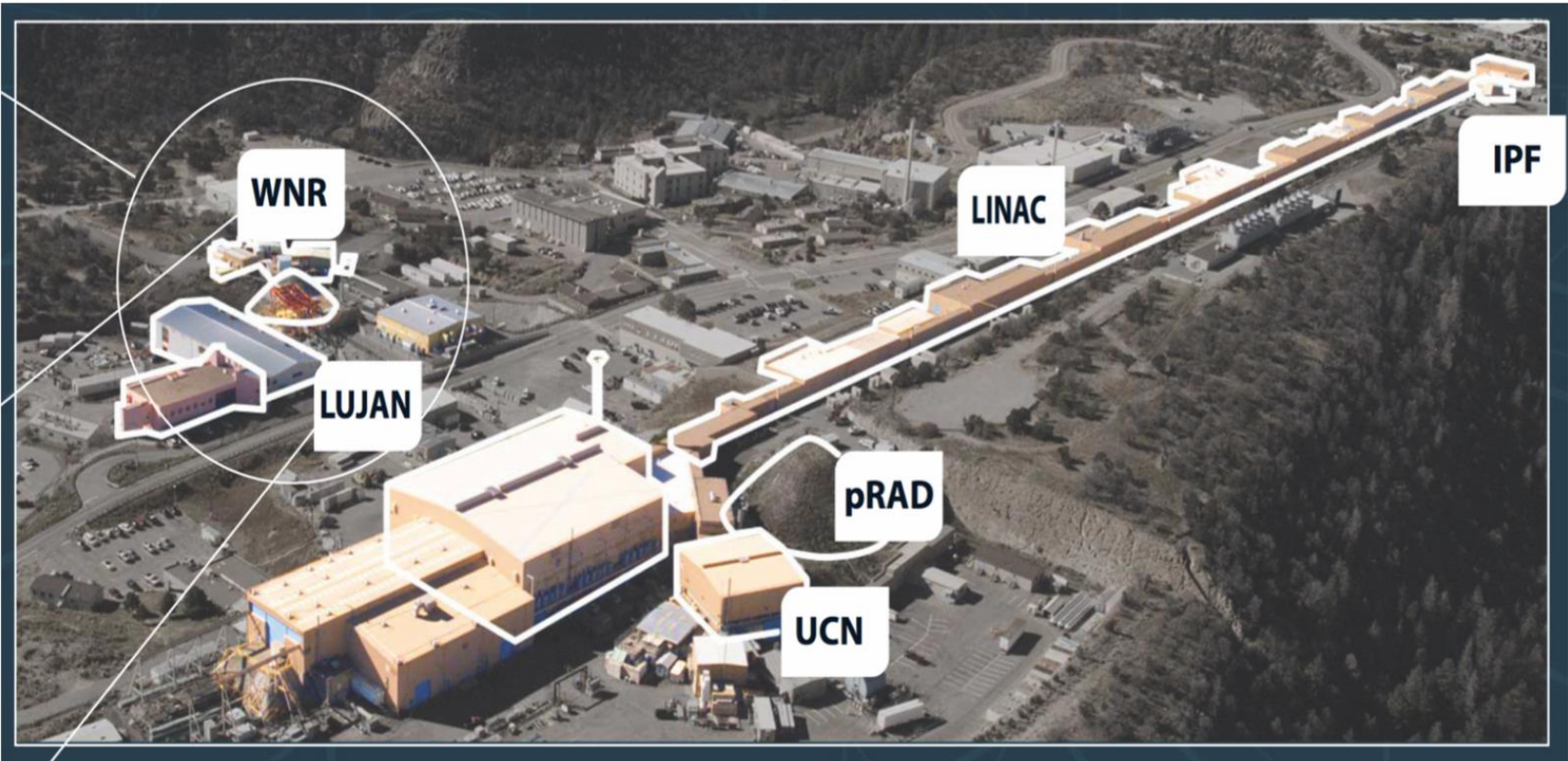


Our work aims to set up similar capabilities at LANSCE to measure H-concentrations in YH metals, both at ambient and extreme (applied temperature gradient) conditions.

R. Yasuda et. al. Journal of Nuclear Materials 320 (2003) 223-230
 N.L Buitrago et. al. Journal of Nuclear Materials 503 (2018) 98-109

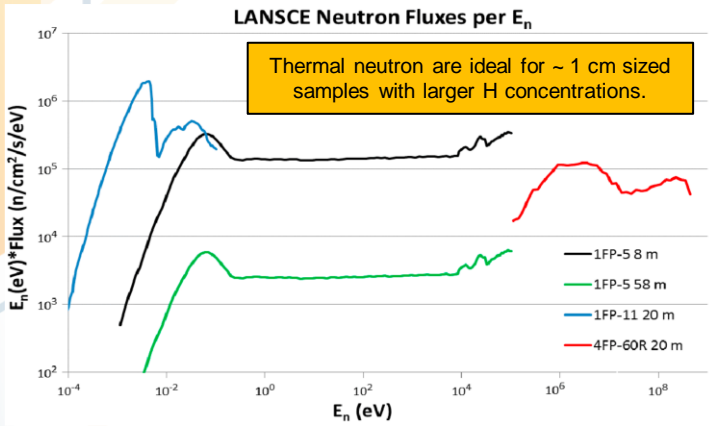


The Los Alamos Neutron Science Center (LANSCE)



Measuring H-Concentrations on Flight Path 5 at LANSCE

FP5 views pulsed thermal neutrons from the 1L target

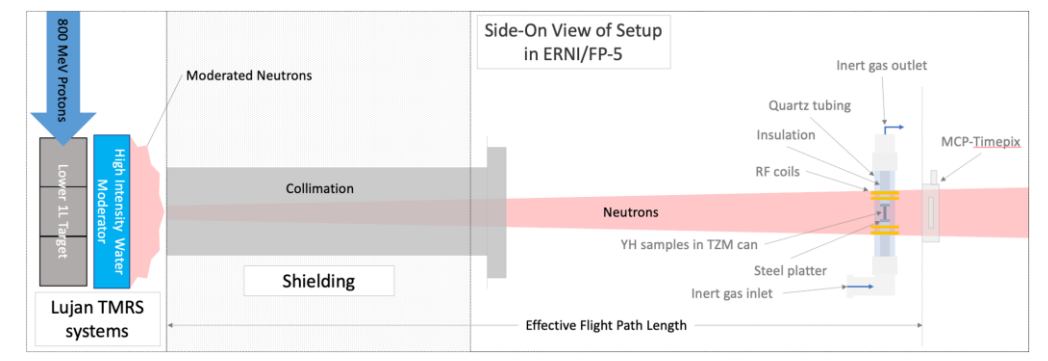


Goals and Approach

Measure H-Diffusion coefficients at various conditions (stoichiometry, temperatures, phase fractions) in YH samples.

- Build up similar neutron radiography capabilities to quantify and map out H-concentrations.
- Build a sample environment capable of inducing high temperature gradients.

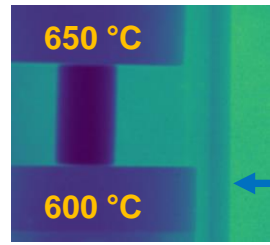
General neutron imaging setup of FP5



Compact dual zone furnace for in-situ heating

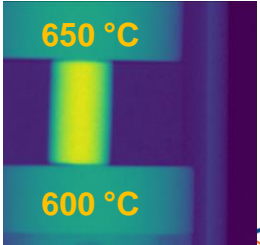


YH_{2-x} samples fabricated @ LANL



Measure $T(x,y,E_n) = \exp(-z_H(x,y) \Sigma(x,y,E_n))$

Determine Calibrate/Model



Use models to extract diffusion flux

$$J_{net} = J_{VC} + J_{VT} + J_{V\sigma}$$

J_{VC} Fickian (Concentration)
 J_{VT} Soret (Temperature)
 $J_{V\sigma}$ Stress (Temperature)

2021 in-Situ YH Measurements with Temp Gradient

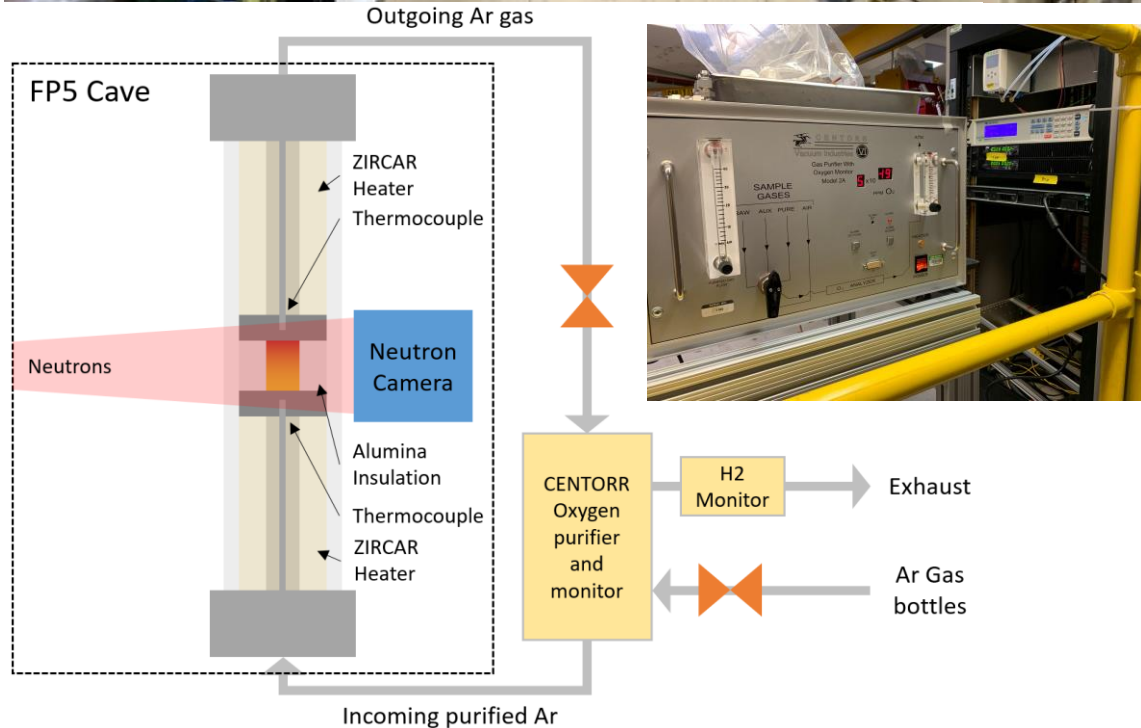
Neutron Imaging measurements were performed on FP5 during Nov. 2021

- Single heating measurement took about 24 hours.
- Selected sample YH_{1.9} “178-1”
- Used Compact Dual-Zone (CDZ) furnace (developed in house)
- Use ATIK 490ex CCD camera coupled with 200um thick ZnS screen
- Selected temperature profiles that would increase from 300°C to 900°C in 50°C increments.
- Included extra auxiliary diagnostics
 - Oxygen analyzer on furnace outlet
 - H₂ analyzer on exhaust

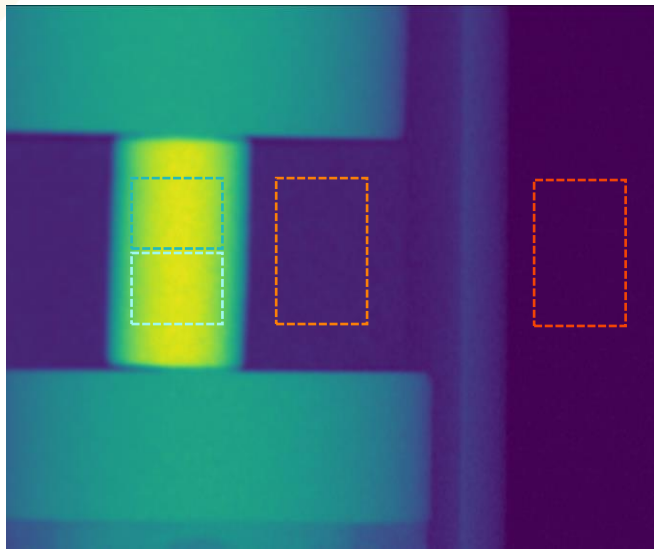
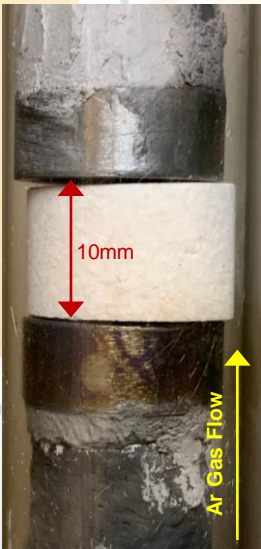


Compact Dual-Zone Furnace

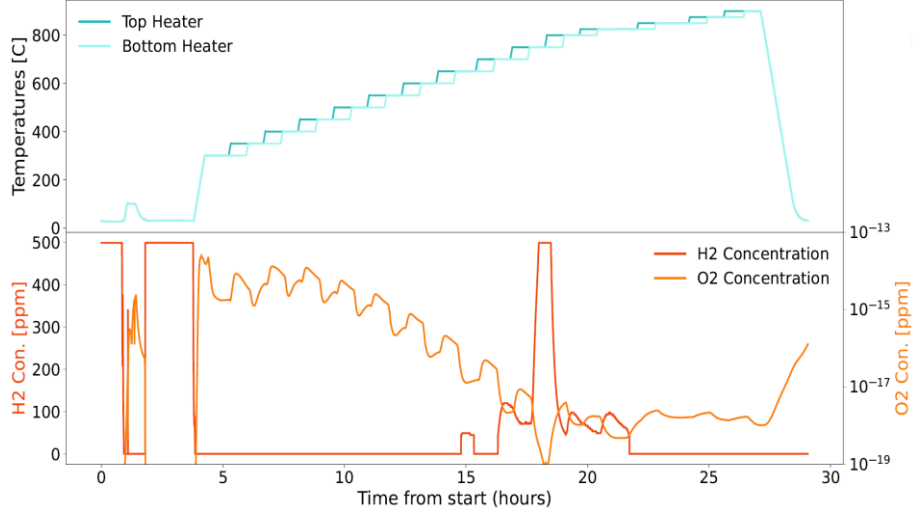
- Using two independent heating elements to induce temperature gradients.
- Max temperatures of ~1100°C
- Sample, insulation, and heater all fit within a 1" diameter tube (reducing geometric image blur).
- Using purified Ar gas flow from bottom to top.
- During testing, we were able to induce 200°C (700-900) gradient across a steel surrogate sample.



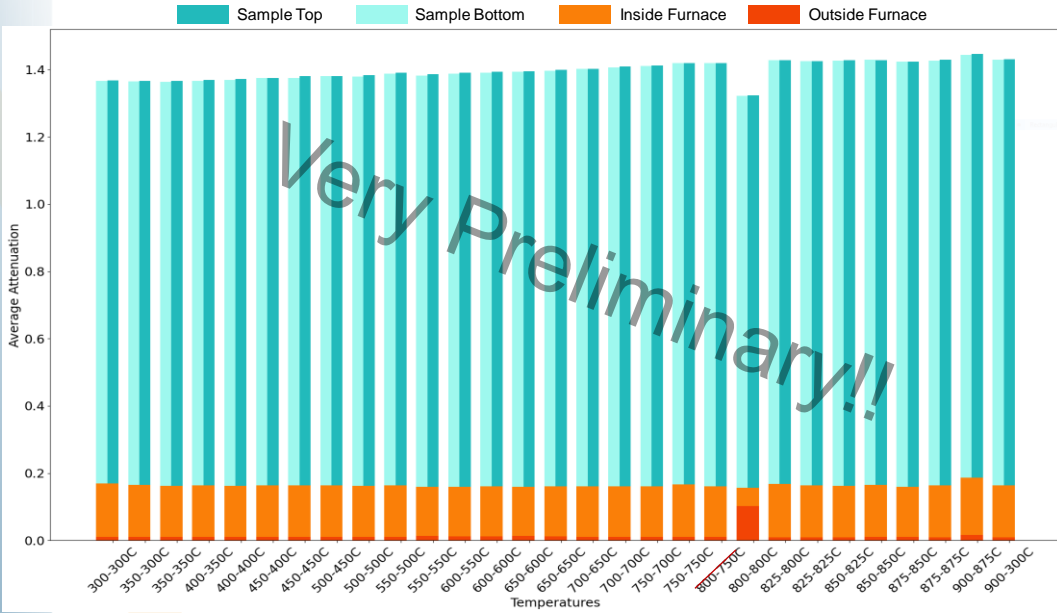
2021 in-Situ YH Measurements with Temp Gradient



Auxiliary Diagnostics



Average Neutron Attenuation in various ROIs



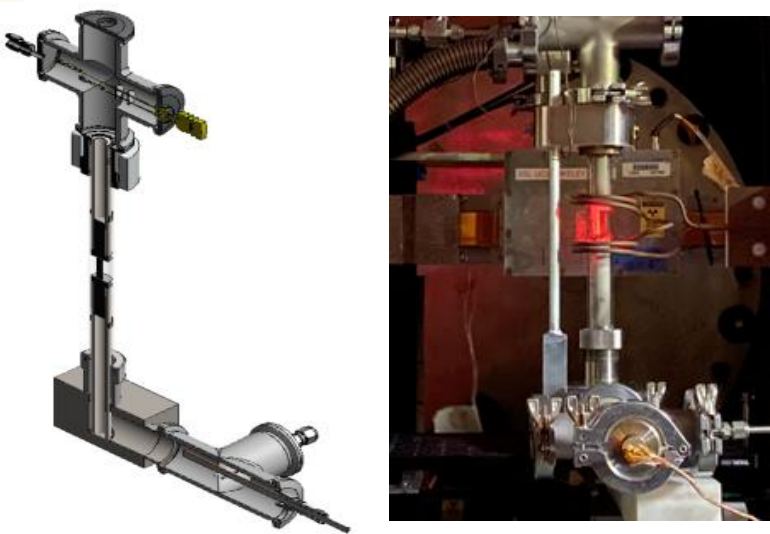
Initial observations and thoughts...

- Attenuation appear flat across sample and increasing as a function of temperature.
 - This might be due to oxidation of sample during heating.
- Oxygen monitor shows clear decrease in O₂ concentration as temps increase.
- The H2 monitor observes H leaving system starting at 650°C steps and ending around 800°C.
- Possibly look at attenuation ratio images, but difficult as sample moves due to thermal expansion of platens.

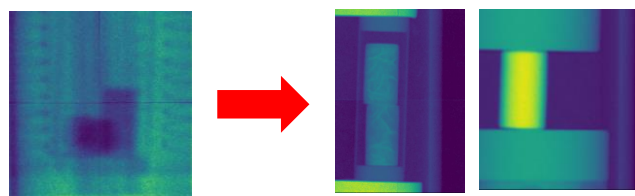
A more thorough analysis needs to be performed to investigate and interoperate results...

Looking forward...

1st Generation Compact Dual-Zone Furnace

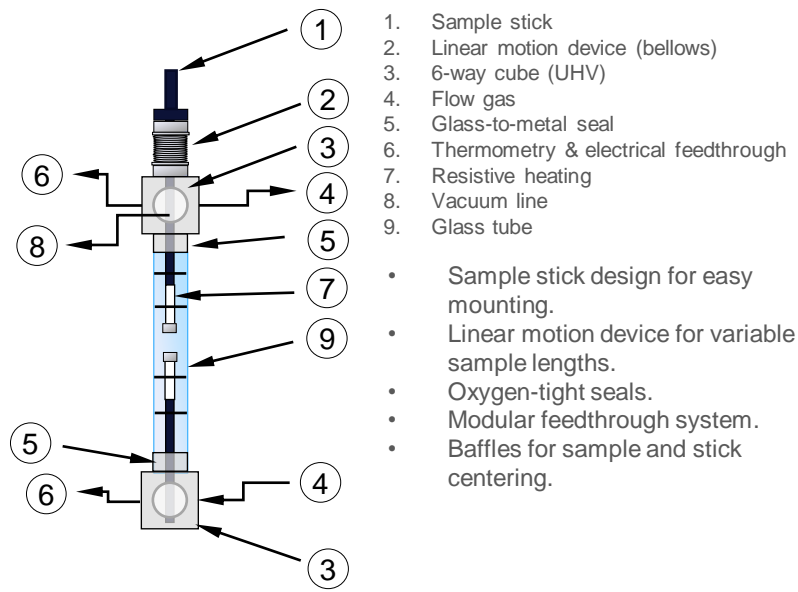


- Operated on FP5 in '20 and '21 run cycles.
- Suffered from delayed parts.
- Allowed for higher resolution imaging with screen to sample distances of ~2-3 inches.



- Could induce temperature gradients up to 100C across samples.
- Rubber O-rings on quick connectors seemed to allow some amount of oxygen into the Ar environment around sample during last run.
- Sample loading/unloading was difficult

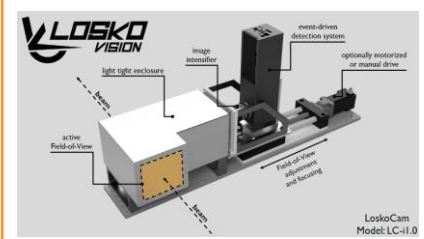
2nd Generation Compact Dual-Zone Furnace



- Sample stick design for easy mounting.
- Linear motion device for variable sample lengths.
- Oxygen-tight seals.
- Modular feedthrough system.
- Baffles for sample and stick centering.

Work done by James Torres and Travis Carver.
Expected to be up and running for 22 run cycle.

Better camera setups (BONUS)



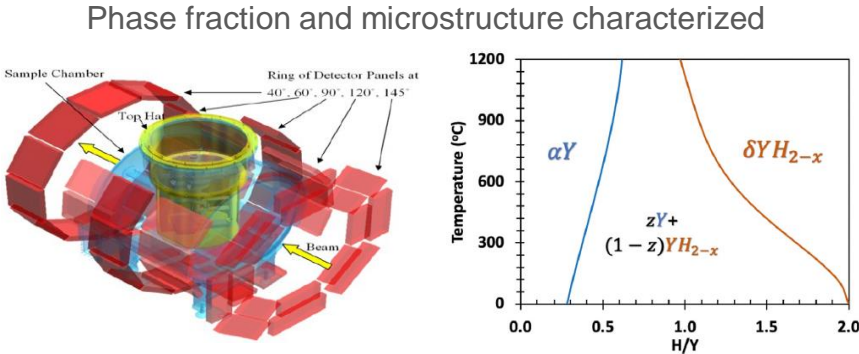
- Using hybrid camera setup, event-mode imaging with thick scintillator.
- Allow us to keep faster acquisitions and energy-resolved capabilities.
- From ASI and LoskoVision.

Multi-modal Pre- and Post-Hydride Characterization

Neutron Diffraction on FP4/HIPPO

Samples fabricated in house @ LANL

- Direct Hydriding
- Powder Met.
- Initial bulk stoichiometry measured.

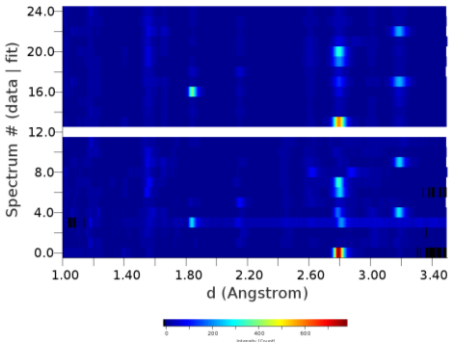


Neutron CT on FP5/ERNI

H-distribution characterized

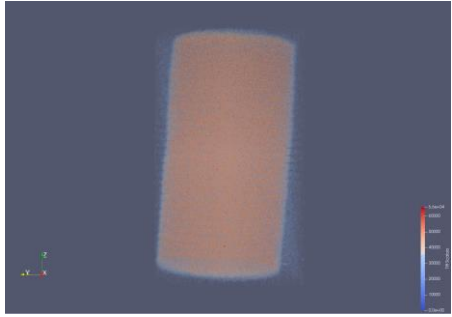


Sample 157-1

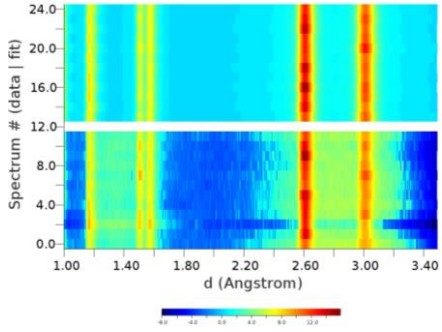


Diffraction Results:

- H/Y < 0.5
- mostly α -Y
- α -Y almost one single crystal
- Only a few grain boundaries.

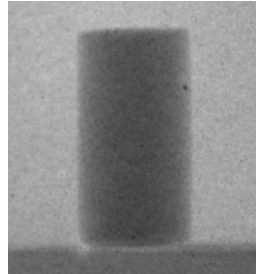


Sample 176-1

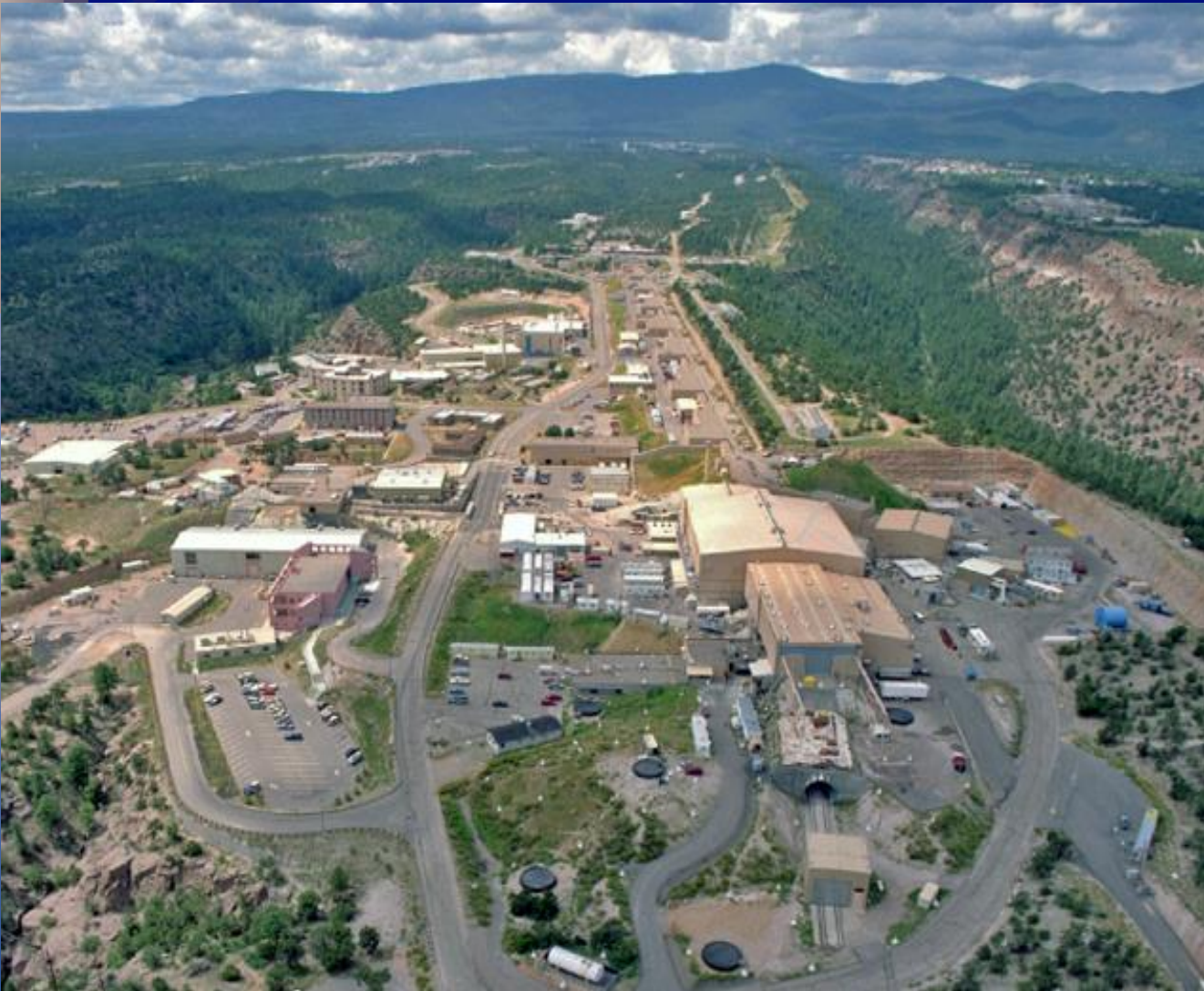


Diffraction Results:

- H/Y > 1.9
- No detectable preferred orientation in YH_2 phase
- Hydride process may have randomized texture



Analysis in progress



Thank you!

LANL Collaborators

- Holly Trelue (NEN-5)
- Travis Carver (MST-8)
- Alexander Long (MST-8)
- Erik Luther (SIGMA-2)
- Vedant Mehta (NEN-5)
- Caitlin Taylor (MST-8)
- James Torres (MST-8)
- Aditya Shivprasad (MST-8)
- and Sven Vogel (MST-8)

Please feel free to contact us if you have any additional questions!

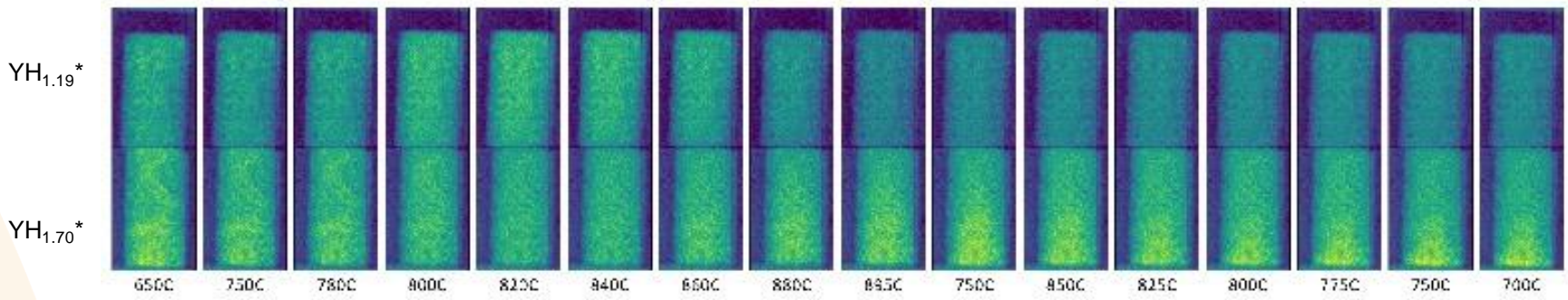
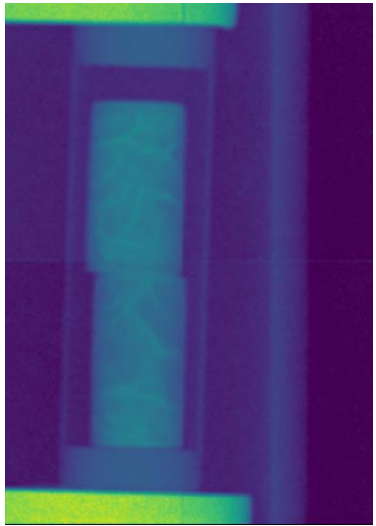
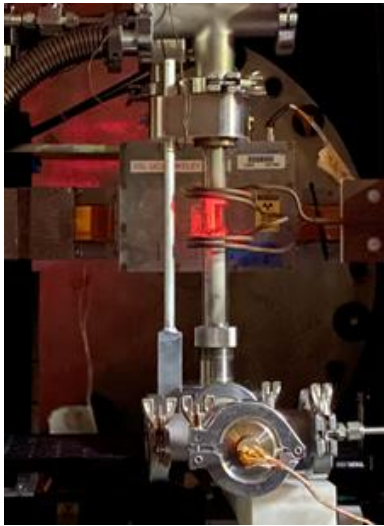
Holly Trelue	trellue@lanl.gov
Alexander Long	alexlong@lanl.gov
Sven Vogel	sven@lanl.gov



Backup: First in-situ YH Measurements at Elevated Temps

First measurements with new Compact Dual Zone (CDZ) furnace performed on FP5 in Dec 2020.

- ### Measuring YH_{1.2} and YH_{1.7} @ Elevated Temps
- Samples placement at ~ 1.5"
 - Original designed with two heating elements:
 - Each element can go up to 1000C
 - Capable of inducing 100 C temperature gradient.
 - Additional RF configuration.
 - Uses flowing Ar cover gas.
 - Thermocouples were attached to each steel platen (top and bottom)
 - Heating elements failed. Used RF config.
 - Two YH samples in a TZM can
 - No temp gradients with RF
 - Each temperature was held for ~3 hours during which roughly six 30 min exposures were taken.
 - All radiographs were integrated over thermal neutron energies



Demonstrated the capability to observe hydrogen redistribute in yttrium hydride over cm length scales in-situ at high temperatures. *“Effects of Hydrogen Redistribution at High Temperatures in Yttrium Hydride Moderator Material”*, H. Trellue et. al. JOM (2021)

Lower sample appears to accumulate H during cooling, though because of the TZM can and Ar gas flow temperature profiles were not spatially characterized.



Backups: A more sophisticated analysis

Working with the Initiative for Scientific Imaging (ISI) group at LANL to build better analysis techniques to overcome deficits in measurements and build confidence in results.

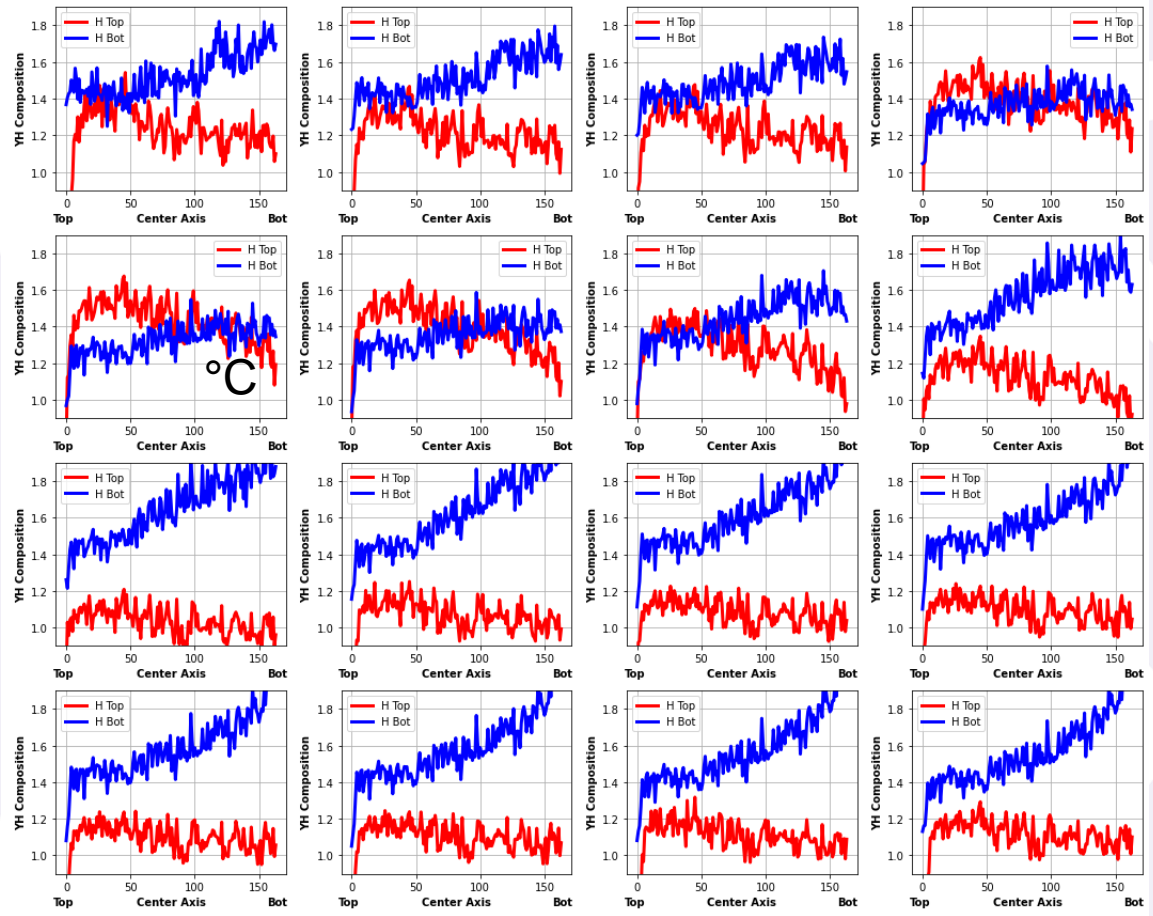
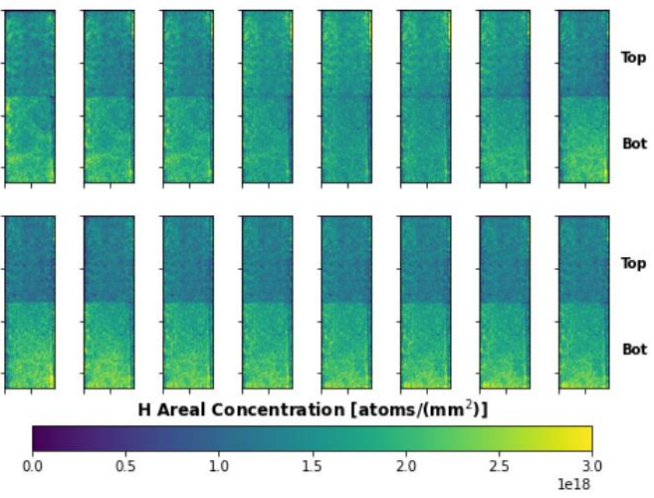
Sometimes there maybe no calibration samples that can be used or they are less than ideal...

Using solvers along with constraints, several unknowns can be determined.

$$h_{ij}H_{cs} + yY_{cs} = p_{ij}$$

$$\frac{\sum_{ij} h_{ij}}{yN} = C$$

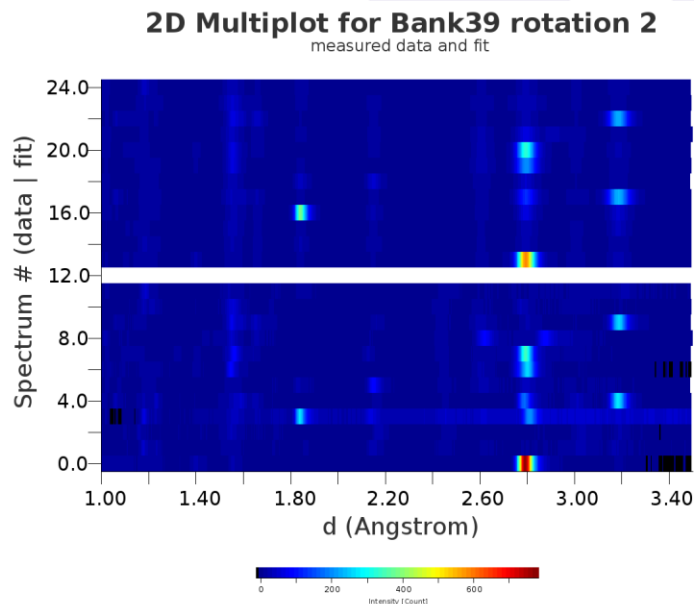
- h_{ij} : Hydrogen areal concentration (spatially heterogeneous) [atoms/(mm²)]
- y : Yttrium areal concentration (spatially constant) [atoms / (mm²)]
- H_{cs} : Hydrogen cross-section for neutrons (known constant) [82.3 barns \equiv 82.3 \times 10⁻²² mm² / atom]
- Y_{cs} : Yttrium cross-section for neutrons (known constant) [9 barns \equiv 9 \times 10⁻²² mm² / atom]
- p_{ij} : Pixel intensity (known measurement)
- C : Composition (known and constant)
- N : number of pixels per temperature measurement (known)
- M : number of temperature measurements (known)



*Will be verifying analysis with water plate samples.

Backups: Diffraction results on YH samples in High-Pressure Preferred Orientation (HIPPO instrument)

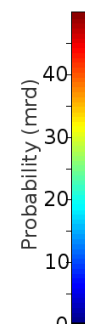
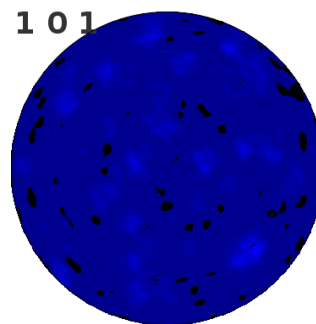
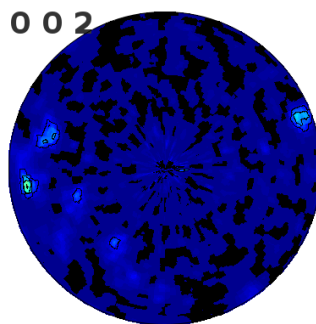
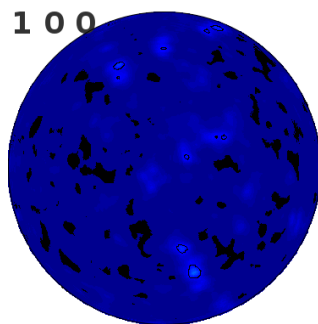
- YH was loaded in 6mm vanadium cans
 - 0, 67.5, 90 degree rotations on
 - HIPPO@20min/rot
 - E-WIMV representation of ODF, 7.5 degree resolution expect for α -Y in 157-1 which was 2.5 degree
- Very strong texture visible in raw data, peaks from both α -Y and δ -YH2



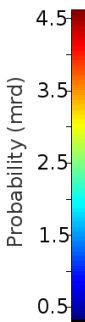
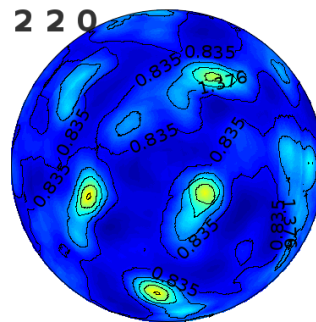
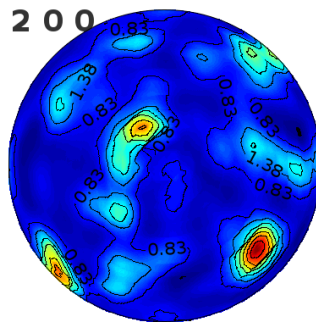
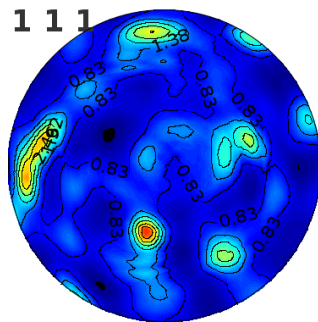
Backups: Diffraction results on YH samples in High-Pressure Preferred Orientation (HIPPO instrument)

157-1


- Alpha-Y
94.1 wt%
almost
sxtal



- YH2
5.9 wt.%



- Note different mrd scales



FY22 Microreactor Program (MRP) Review Instrumentation and Sensors

March 1, 2022

Chris Petrie, Oak Ridge National Laboratory

Troy Unruh, Idaho National Laboratory

David Mascarenas, Los Alamos National Laboratory

Objective

- Instrumentation and sensors research falls into three main categories:
 - primary instrumentation for nonnuclear testing,
 - embedded sensors for determining operating parameters, and
 - techniques for determining structural health.
- As part of nonnuclear test bed demonstrations, the program will research techniques for measuring parameters from heat pipes and/or other materials tested.
- Instrumentation technologies to monitor the structural integrity of microreactor structures operating at high temperatures (e.g., > 600°C) are also being developed.

Microreactor I&C needs

Today's light water reactors

- ~1000 MWe
- Large, onsite construction
- Regular, ~18 month refueling cycles
- ~Hundreds of onsite staff
- Large, expensive redundant safety systems
- Hesitant to adopt new I&C technology

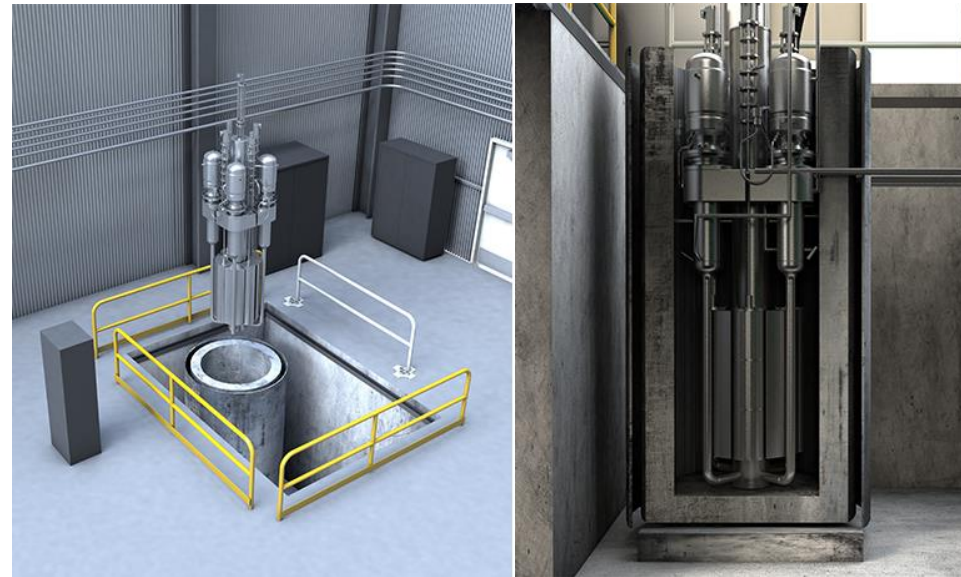


Westinghouse AP1000 plant

<https://www.westinghousenuclear.com/new-plants/ap1000-pwr>

Microreactor concepts

- ~kWe to tens of MWe
- Factory assembly, deployable
 - Instrumentation ideally integrated into factory assembly
- Some reactor concepts are never refueled
 - May enable increasing instrumentation without interfering with refueling operations
- ~Tens of onsite staff
 - Instrumentation must inform limited number of operators
 - Ideally passively safe, could support autonomous operation
- Small footprint limits space for instrumentation

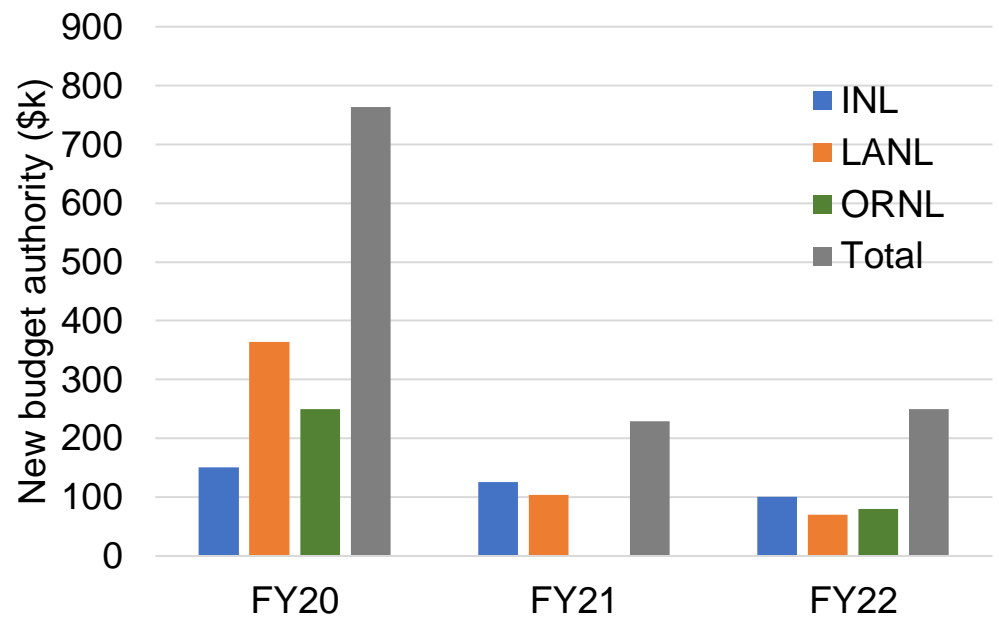


MARVEL microreactor

https://www.energy.gov/sites/default/files/styles/full_article_width/public/2021-04/MARVEL_TREAT_high-res.png?itok=w0WkRoYL

Scope

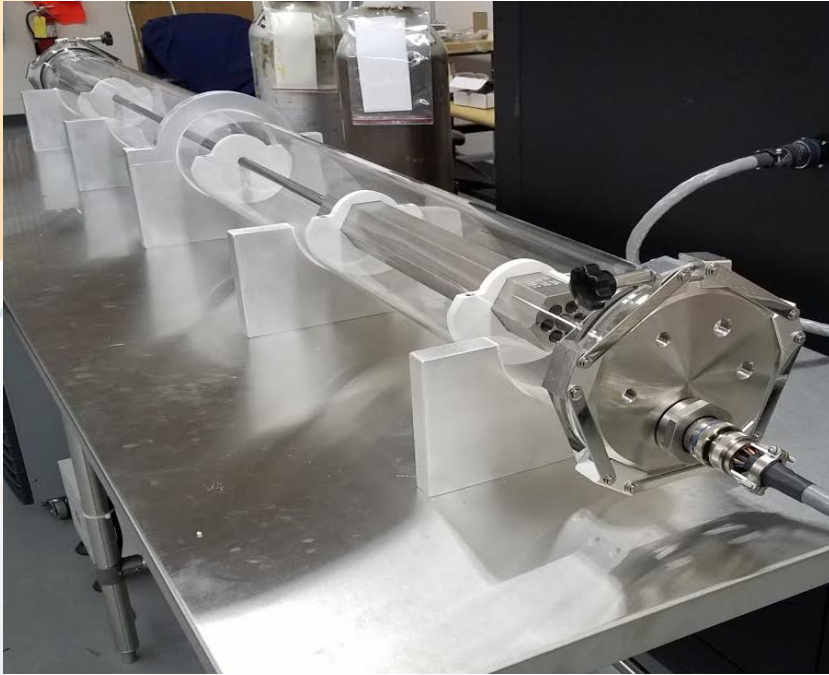
- Instrumentation and Sensors activities funded at levels that allow simple demonstrations that leverage other MRP-funded or NE-funded activities to maximize productivity



MRP instrumentation & sensors budget history

- MRP Capability Development: SPHERE, MAGNET testbeds
- Nuclear Energy Enabling Technologies Advanced Sensors and Instrumentation (NEET ASI) Program: Various sensor development activities
- Transformational Challenge Reactor (TCR) Program: AM-embedded sensors
- Programmatic focus
 - Health monitoring of microreactor components using embedded sensors, distributed sensors and other advanced sensing technologies during electrically-heated testing in SPHERE and MAGNET
 - Enhanced diagnostics to detect and mitigate issues and prevent unplanned shutdowns for maintenance
 - Advanced control strategies to support semi-autonomous operation

MRP: SPHERE and MAGNET testbeds (INL)



SPHERE - Single Primary Heat Extraction and Removal Emulator

- Single heat pipe coupled to forced convection cooling, surrounded by 6 electrical heaters
- Designed to quantify operational temperatures and heat rejection from of a single heat pipe
- Highly instrumented to measure temperature and strain distributions in a miniature monolithic core block



MAGNET - AGile Non-nuclear Experimental Test Bed

- Engineering scale test bed for testing large sections of a monolithic core block with an array (e.g., 37) of heat pipes and electrical heaters
- Capable of testing advanced heat rejection systems or integral effects such as the potential for cascading failures of multiple heat pipes

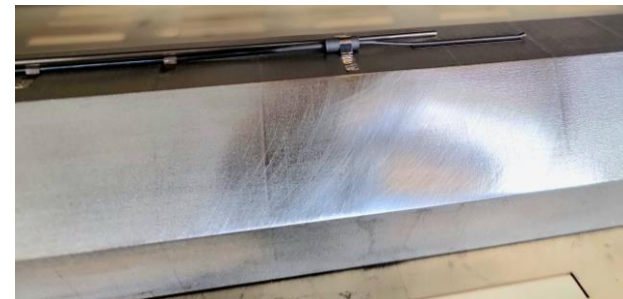
Increasing complexity

Leveraging sensor development activities under NEET ASI (INL)

- New website - <https://asi.inl.gov/>
- Fiber optic multi-point and distributed temperature sensor
 - Quantifying sensor performance and use under specific conditions
- Thermocouples
 - Performance assessment of commercial thermocouples
- Ultrasound thermometers
 - Fabrication optimization for high temperature/radiation environments
- Mechanical Properties
 - Deploy commercial high temperature strain gauges in SPHERE/MAGNET with ORNL developed embedded fiber strain gauge
 - Support Consolidated Innovative Nuclear Research call CT-5 for structural health monitoring of advanced reactors
- More input to Nuclear Energy Sensors Database, <https://nes.energy.gov/>



Thermocouple installed in SPHERE

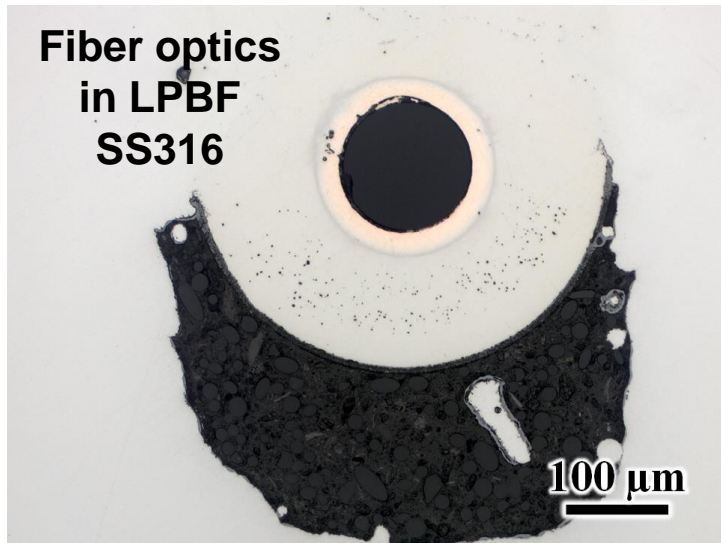
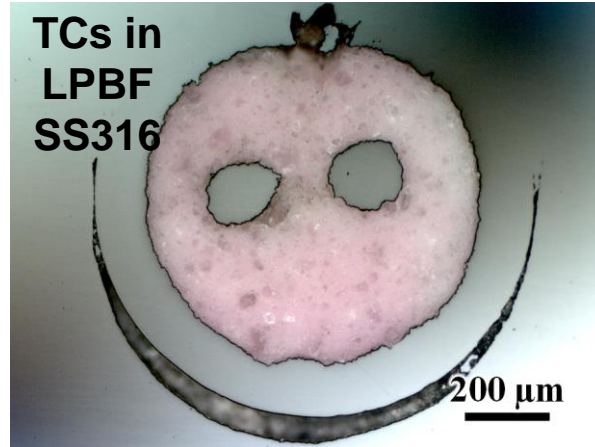
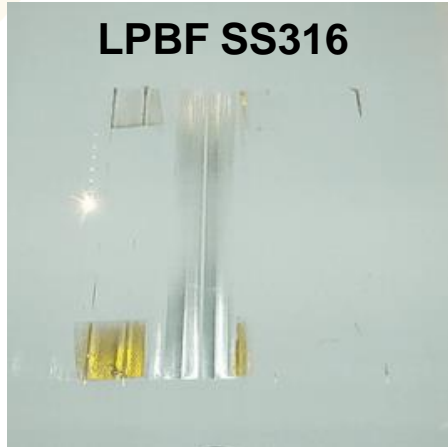


Welded strain gauge on a hexagonal test article for heat pipe-based microreactors

CT-5: ADVANCED SENSORS AND INSTRUMENTATION
FEDERAL POC – DANIEL NICHOLS & TECHNICAL POC – PATRICK CALDERONI
(ELIGIBLE TO LEAD: UNIVERSITIES ONLY)
(UP TO 3 YEARS AND \$800,000)

The Advanced Sensors and Instrumentation (ASI) program seeks applications to develop dynamic measurement systems for **structural health monitoring of advanced reactors**. Advanced reactors of interest are those defined in section A.2.2 Reactor Concepts Research, Development and Demonstration (RC RD&D) Program and related items in Appendix A. The proposal should demonstrate an adequate level of knowledge of the targeted application.

Leveraging AM and sensor embedding under TCR (ORNL)



BJ +
CVI
SiC

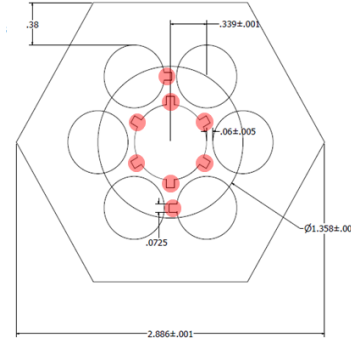


Embedding of fiber optics and thermocouples in stainless steel using ultrasonic additive manufacturing (UAM) and laser powder bed fusion (LPBF)

Embedding of thermocouples in binder jet (BJ) 3D printed SiC + chemical vapor infiltration (CVI)

INL accomplishments: Distributed temperature sensing in SPHERE

- Core block modified to include additional instrumentation
- New SPHERE test stands (horizontal/vertical) allow more room for sensor leads
- Thermocouples: Ordered, vendor delays
- Fiber-optic temperature sensors: Part in-house, under fabrication
- Ultrasound temperature sensor: Fabricated, undergoing heat treatment and calibration
- *Vendor delays caused delay of INL - M4 SPHERE deployment milestone into April*



Modified core block with extra channels for instrumentation

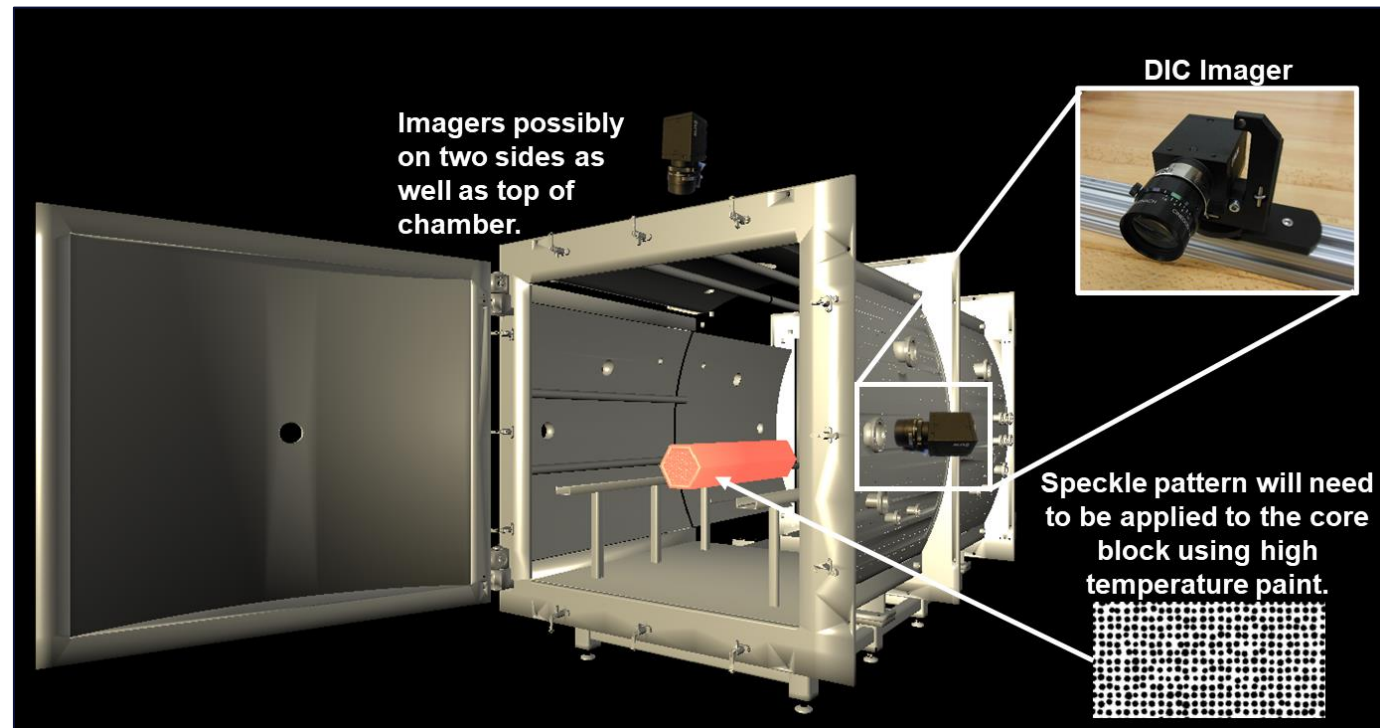


Horizontal and vertical test stands at SPHERE

LANL accomplishments: Non-contact digital image correlation (DIC) for MAGNET testing

- Simulated the lighting and potential distortion effects due to high temperatures on DIC measurements
- Determined optimum speckle size, focal length, and camera locations in MAGNET
- Currently performing high-temperature tests on 316 SS coupons

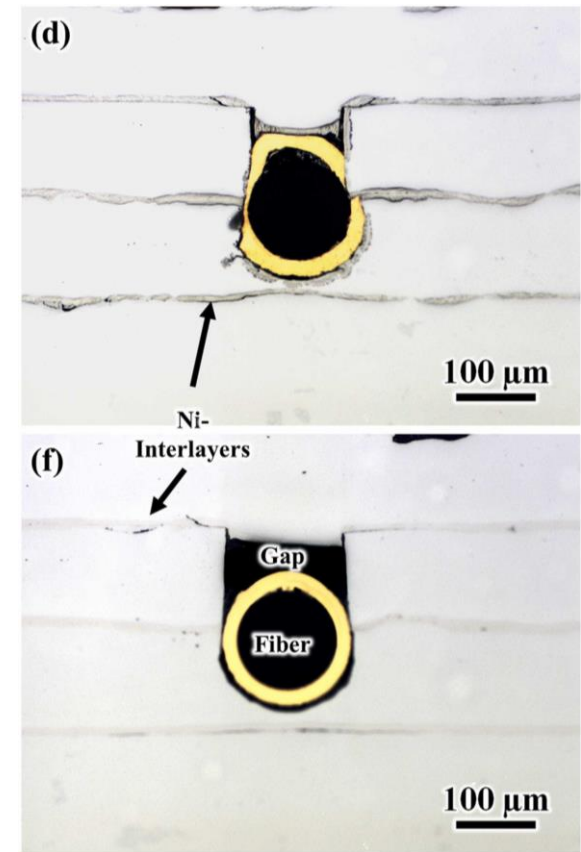
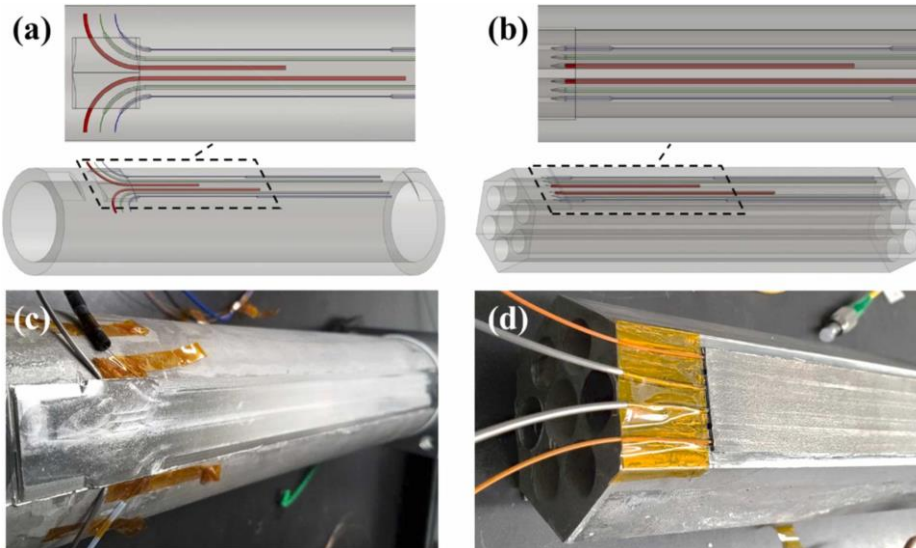
MAGNET DIC configuration



ORNL accomplishments: Demonstration of functional sensors embedded in microreactor components

- FY20–FY21 focused on expanding UAM process to embed thermocouples and fiber optic sensors in pipes and microreactor core block test articles
- Journal manuscript in FY22 on sensor embedding, thermal gradient testing, and characterization of sensor/component interfaces¹
- Sent test article with embedded thermocouples and fiber optics to INL for testing in SPHERE
- SPHERE testing planned for spring of 2022

Test
articles
with
embedded
sensors



**Process parameters optimized to
achieve fiber optic strain coupling
without damaging sensors**

¹ H.C. Hyer, D.C. Sweeney, and C.M. Petrie, “Functional fiber-optic sensors embedded in stainless steel components using ultrasonic additive manufacturing for distributed temperature and strain measurements,” *Additive Manufacturing* **52** (2022) 102681. <https://doi.org/10.1016/j.addma.2022.102681>

Milestone status

- **On schedule**

- **INL, M4AT-22IN0804027:** Test distributed temperature sensors in MAGNET deployment (due 7/28/22)
- **INL, M3AT-IN0804028:** Prepare report to document sensors and instrumentation (due 8/31/22)
- **ORNL, M3AT-22OR0804011:** Deliver test article with embedded sensors to INL and test performance (due 7/29/22)
- **LANL, M4AT-22LA0804031:** Report on proposed structural health measurements at MAGNET (due 9/30/22)

- **Delayed**

- **INL, M4AT-22IN0804026:** Test distributed temperature sensors in SPHERE deployment (originally due 12/31/21)
 - Delayed until 4/26/22 due to vendor delays in delivering thermocouples

Conclusions

- This work packages supports a wide range of technology maturation activities centered around instrumentation and sensors
 - Improved monitoring capabilities during nuclear and non-nuclear testing of microreactor components and systems
 - Health monitoring of operating microreactors using advanced non-contact and embedding sensing technologies
- FY21 focused on fabrication and initial testing of sensor technologies and embedding techniques
- FY22 is focused on:
 - Demonstrating these technologies during non-nuclear testing of microreactor components
 - Evaluation of options for structural health monitoring of larger components in MAGNET
- Potential FY23 scope includes:
 - Health monitoring/damage detection in microreactor components
 - Deploying distributed sensing technologies in the MAGNET testbed
 - Automated control and/or acoustic sensing



Heat Transfer

Objective

- Heat transfer in a microreactor overcomes unique challenges due to the compact footprint, radiation field, transportability, and high temperatures present.
- High temperature operation preferred to give higher power production efficiencies.
- Novel concepts explored to transport heat and dampen transients affecting structural integrity and performance of core structures/components.
- Research/testing of nonnuclear components helps increase our understanding of system performance.
- Feasible heat pipe and gas-cooled components plus heat exchanger and power conversion units can be integrated for non-nuclear testing easier than in nuclear demonstrations.
- Techniques for fabricating test articles with these features will also be developed and demonstrated.



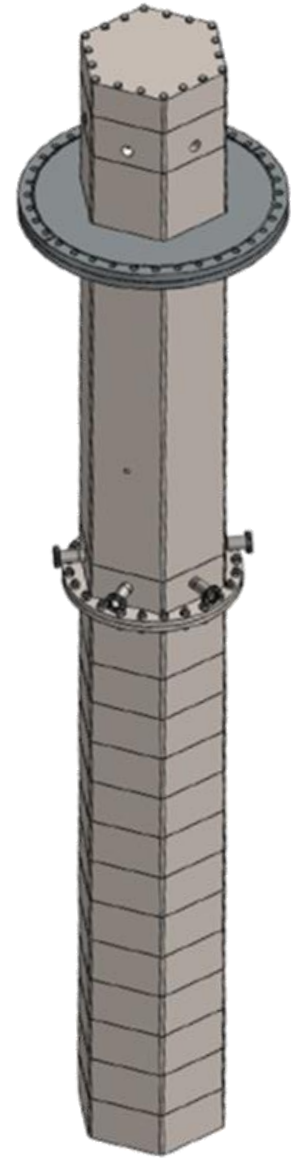
37 Heat Pipe Test Article

March 3, 2022

Bob Reid, Lindsey Gaspar, Michael Middlemas, and
Katrina Sweetland

Presentation Outline

- Overview
- eBlock37
- eXchanger37 Subassembly
- Core37 Subassembly
- eWick37
- eFill37 Subassembly
- eFill37 Charge Subassembly
- eFill37 Laser Weld Subassembly
- Facility Upgrades
- Ongoing and Future Work

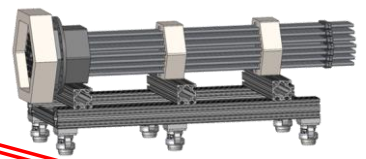


eBlock37 Build

gCart37



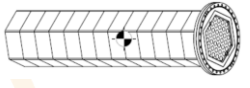
Handling Cart



Monolithic Reactor Core Block

Core37

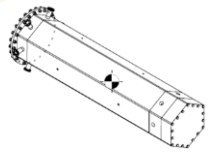
US DOE S133,464



Monolithic Heat Pipe to Gas Heat Exchanger

eXchanger37

US DOE S133,464



Mass Produced NQA-1 Quality High Capacity Heat Pipe Wicks

eWick37 (NQA-1)

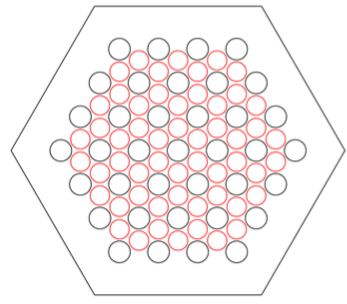
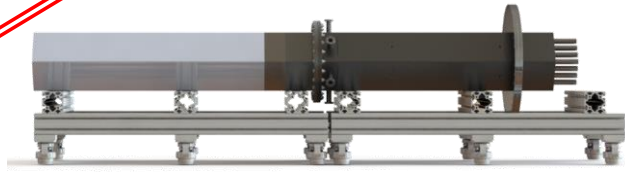
US DOE S133,680



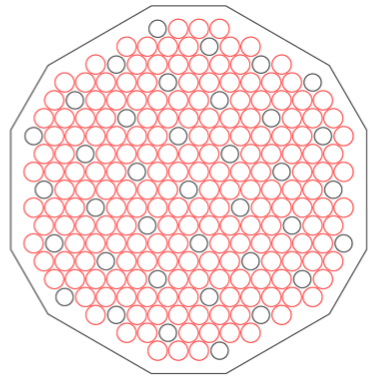
Mass Produced High Purity Heat Pipe Fill And Seal

eFill37

US DOE S133,662



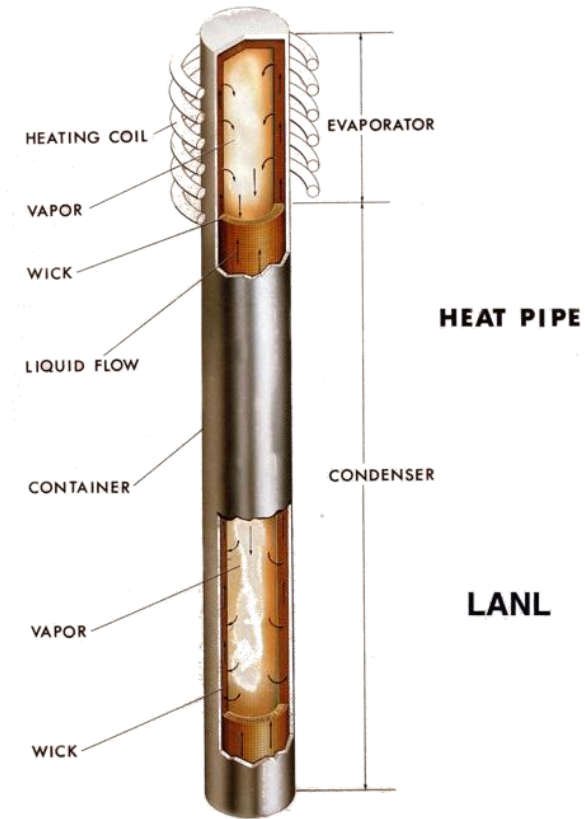
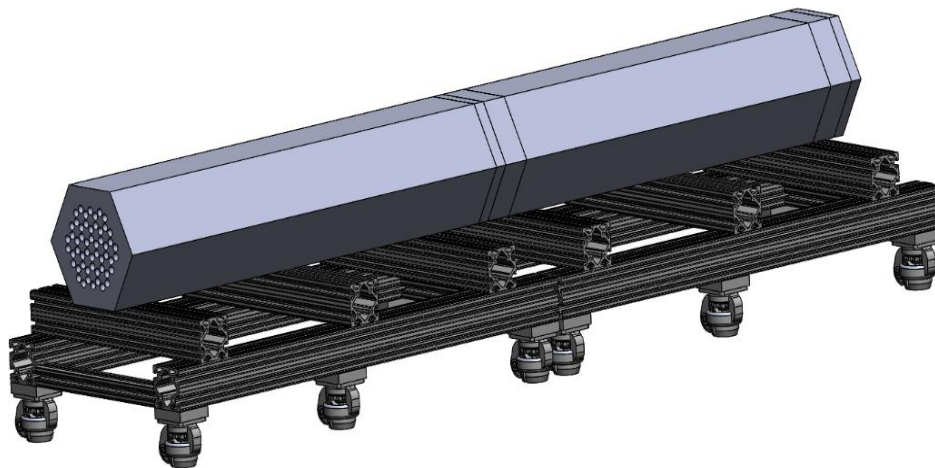
Thermal Hydraulic Similarity



Nuclear Similarity (criticality)

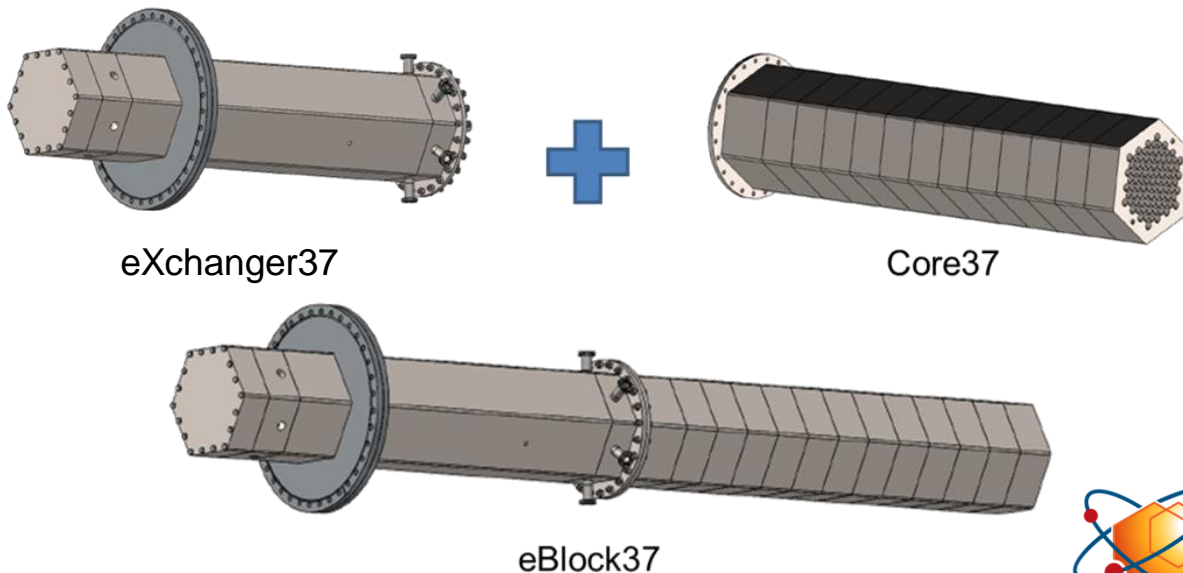
Overview

- Design and fabricate a sub-scale, electrically heated and heat-pipe-cooled prototype of a fast spectrum microreactor
- Testing will be conducted at Idaho National Laboratory MAGNET facility
- Fuel rods will be simulated with cartridge heaters and combined heat pipe/heat exchanger article



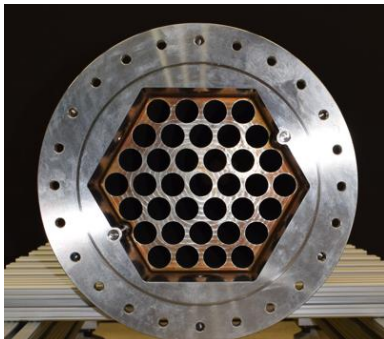
eBlock37

- The eBlock37 is a sub-scale, electrically heated and heat-pipe cooled prototype of a fast spectrum microreactor.
- Comprised of a gas-cooled heat exchanger (eXchanger37) and electrically-heated and heat-pipe cooled core (Core37),
- Subassemblies built from stainless steel 316L and thermally linked by an array of 37 sodium heat pipes
- Heat pipes transfer nominal 100 kW from the core at 700°C



eXchanger37 Subassembly

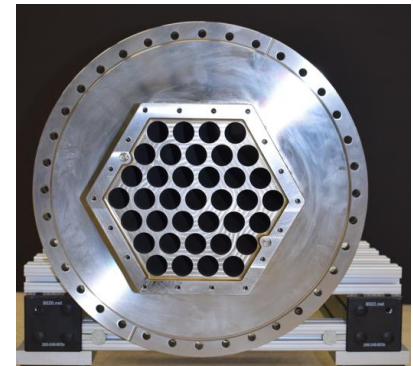
- Consists of a main body containing axial holes through which the heat-pipe array passes
- Flange on evaporator end links to Core37 Subassembly
- Flange on the condenser end links to the eFill37 and can be removed following heat-pipe fill operations
- Assembly completed CY21



Evaporator End



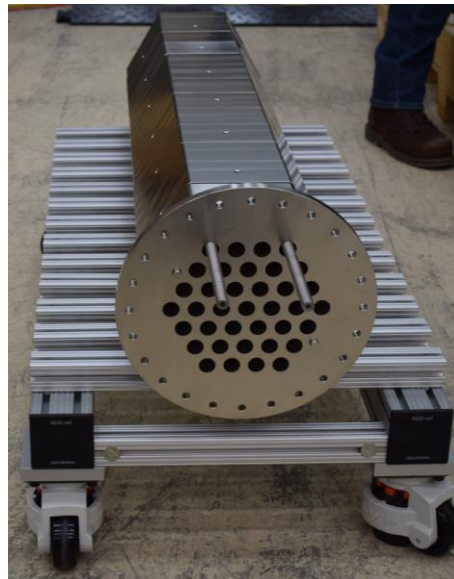
eXchanger on gCart



Condenser End

Core37 Subassembly

- Consists of 13 segments that will be diffusion bonded together
- Flange on the end links to the eXchanger37 Subassembly
- All 13 segments have been manufactured for full-scale core
- Alignment pins pressed into each segment to ensure alignment during bonding
- Segments packaged for shipment to Bodycote facility for diffusion bonding



Core37 Subassembly – Bonding Trials

- Diffusion bonding trials conducted on sub-scale, unit
 - Robust bond, but asperity closure incomplete due to pressure relaxation after initial asperity crush
 - Mismatch in Arrhenius diffusion rate and thermal diffusion rate believed to have resulted in uneven contact
 - Testing of alternate method currently being pursued
- Full-scale core bonding to be performed following assessment of new bonding parameter performance

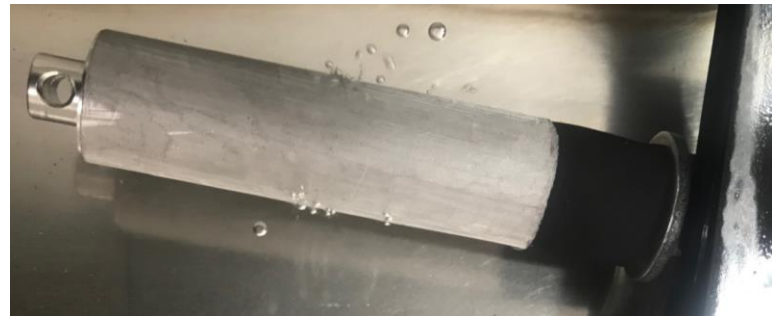
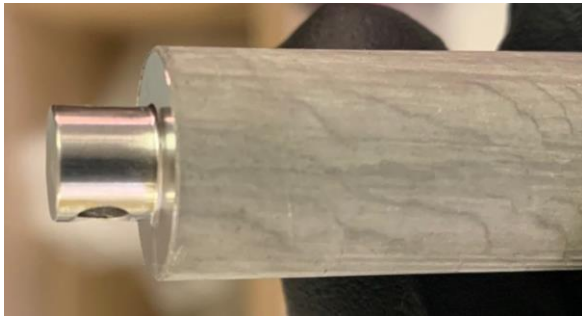
eWick37

- Ultimate Hydroforming, Inc. (UHI) is fabricating and completing a scaled-up production of LANL eWick37
 - Nadcap accredited
 - AS ISO 9001:2015 9100D registered
 - Fully validated and controlled process for wick manufacture consistent with NQA-1 quality standards
- A total of 54 stainless steel wicks are being produced
- Wicks required to be suitable for producing a minimum axial heat transfer rate of 2.7 kW at 1000 K



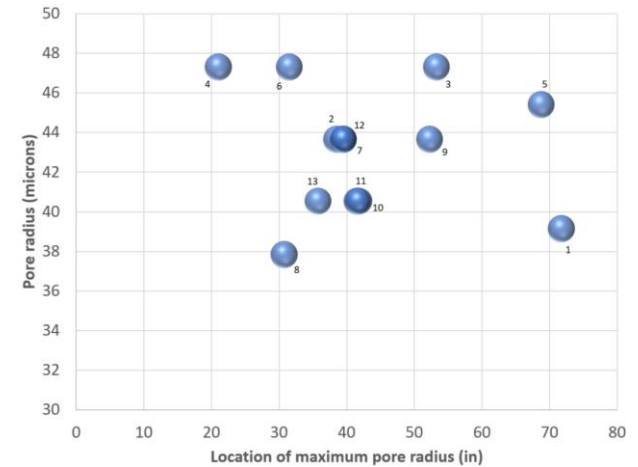
eWick – Fabrication Process

7. Bubble point testing used to determine pore distribution and size
8. Steel plug bonded to end of wick
9. Repeat bubble point test with plug installed



eWick37 – Status

- Wicks produced to date have consistently been manufactured with < 50 micron effective pore radius
 - Suitable for axial heat transfer rates of at least 8.0 kW at 1000 K with selected heat pipe design and materials (2.7 kW maximum test article requirement)
 - 13 assemblies completed through bubble point testing (1/22)
 - 22 assemblies in copper tubes and are being sized (1/22)
 - Remaining screen material will be cleaned and assembled once copper has been etched away from remaining assemblies



eFill37 Subassembly

- The eFill37 is a scalable heat pipe charging and sealing apparatus developed with the intent of easing and automating the manufacture of heat-pipe-cooled microreactors
- Interfaces directly with eBlock37 via vacuum flange, providing inert gas or vacuum conditions to mitigate hazards associated with alkali metal handling and prevent contamination
- Theta-theta stage manipulation enables access to every heat pipe in the array

eFill37 Subassembly

- eFill37 uses multiple configurations for completing distinct steps of the manufacturing process
 - Charging
 - Plug insertion
 - Sealing
- Fill system represents a significant departure from earlier approaches for alkali metal heat pipe fill methods that only allowed for fill of a limited number of heat pipes at a time

eFill37 Charge Subassembly

- eFill37 charge subassembly sits atop the eFill37 rotating stages, enabling transfer of high-purity sodium into each heat pipe
- Gate valves linking the eFill37 with the charge subassembly help maintain vacuum environment during filling operations and allow for changing out subassemblies for subsequent process steps
- A vertical lifting column and expandable bellows provides method of fill stem insertion

eFill37 Laser Weld Configuration

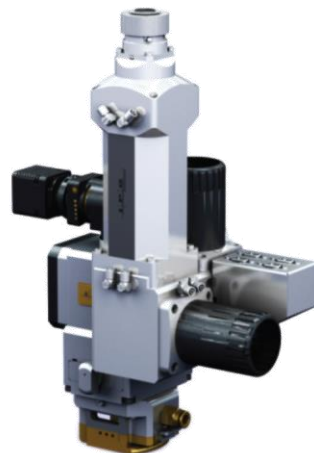
- eFill37 laser weld subassembly sits atop the eFill37 rotating stages, enabling sealing of the heat pipe array after fill
- Gate valves linking the eFill37 with the laser weld subassembly help maintain inert environment (0.1 mbar helium) during sealing operations



- Custom bellows attaches to the laser head on one end and chamber viewport window on the other, creating a light-tight environment through which the laser beam travels
- Full-beam enclosure allows system to be treated as Class 1 laser system

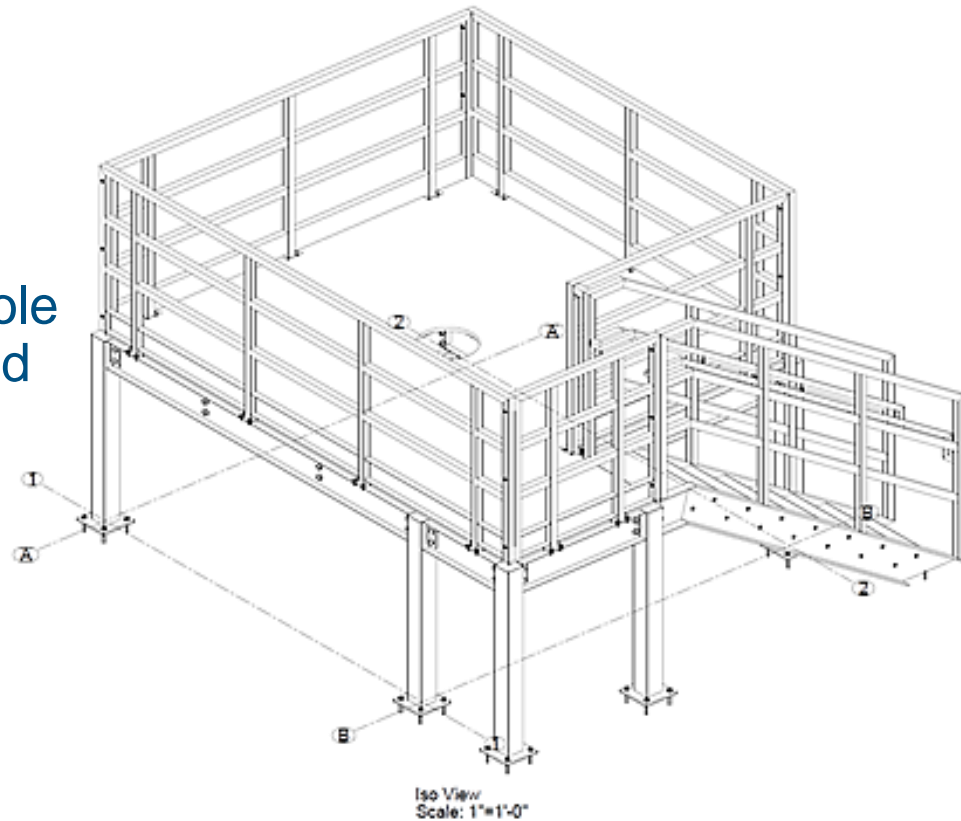
eFill37 Laser Weld Configuration

- Support stand allows for x and y-coordinate positioning, while linear motion stage enables more precise vertical positioning to account for design tolerances
- IPG Photonics YLS-4000 laser and D50 wobble head will be used for weld operations
- All necessary components have been purchased



Facility Upgrades

- A mezzanine has been designed to facilitate heat-pipe filling operations using the eFill37
- Penetrating radar has been used to survey floor of installation area for footings
- eBlock37 will be placed through a centrally located hole in the mezzanine and secured to the floor and



Ongoing and Future Work

- Core37
 - Diffusion bonding of sub-scale core to verify new bonding parameters
 - Diffusion bonding of full-scale Core37
 - Weld heat-pipe tubing to Core37
- eWick37
 - Complete wick fabrication
- eFill37
 - Assemble plug and laser weld configuration subassemblies
 - Laser installation
- Facility Upgrades
 - Procure and install mezzanine
- Insert wicks; fill article with sodium and weld shut.
- Ship to INL for non-nuclear demonstration.



Technology Maturation – Conclusions and Future Work Ideas

Holly Trelue
Technical Area Lead

March 3, 2022

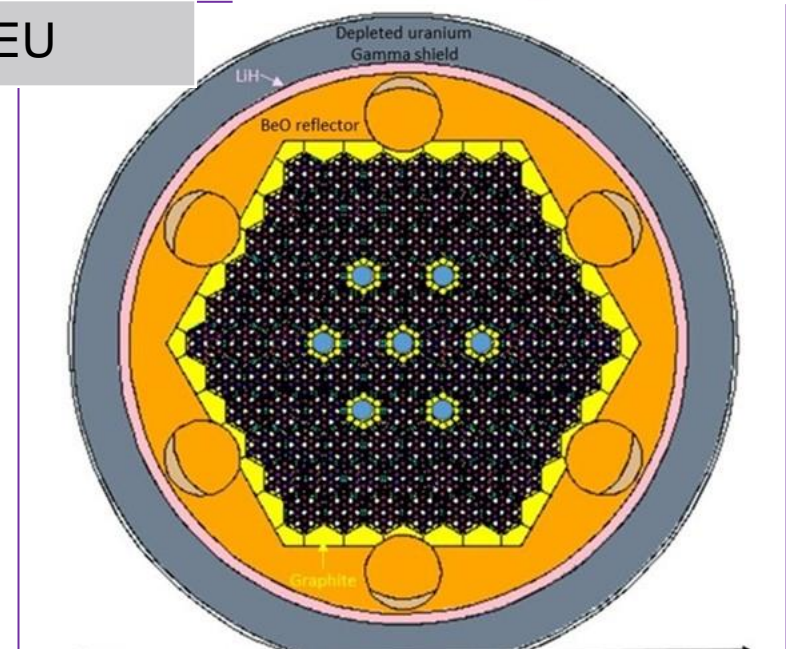
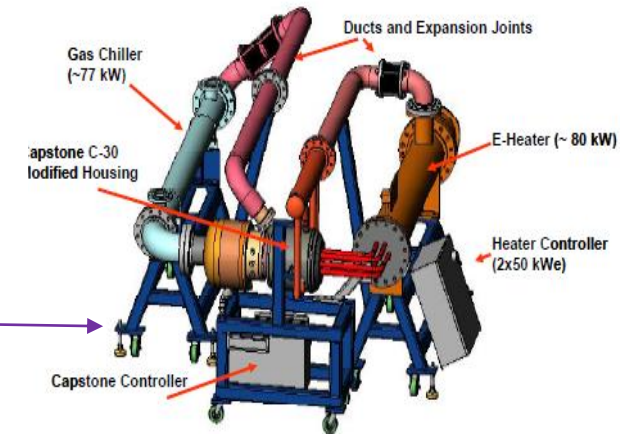
In summary

- Technology maturation is a vital part of the microreactor program to help numerous vendors achieve higher TRLs and successfully deploy microreactors.
- Work on 37 heat pipe test article and PIE of YH_x will yield valuable information for microreactors and are a focal point of FY22.
- Embedded sensors and other measurements at MAGNET are also important.
- More technology maturation is required for microreactor building and deployment though.
- Structural material, autonomous control, legacy fuel and other activities may be examined soon, but the list of needs does not end there.

Needs

Feature	Commercial Reactors	Microreactors
Cooling	Water	Heat pipes, gas
Control	Soluble boron	Control drums
Electricity Generation	Steam Generator /Turbine	Heat Exchanger/ Power Conversion
Moderator	Water	Hydrides/Graphite?
Enrichment	<5% UO ₂	<20% HALEU

- Shielding, reflectors, and control material such as drums or burnable poison need to be assessed along with safeguards and other topics in conjunction with other programs (i.e. NEAMS, MPACT, NEET).
- Power conversion unit (PCU) and other technology such as gas coolant are important in addition to enhanced measuring techniques at MAGNET.



Additional Workscope Planned for FY22 (assuming \$25M and end of CR)

High Temperature Moderator	<ul style="list-style-type: none"> - Encapsulation and containment of YH - Advanced Coatings
Instrumentation and Sensors	- Microreactor Autonomous Control System for graded response of critical systems
Fuel Qualification	Complete microreactor activities on legacy fuel qualification of metallic fuels.
Heat Transfer	<ul style="list-style-type: none"> - Support PCU integration - Fabricate gas-cooled test article
Instrumentation and Sensors	- Acoustic Sensors, Improve DIC
Structural Materials	Refractory metals: Perform initial investigations of advanced materials and manufacturing for microreactors such as TZM and gap analysis on code qualifying

Potential Future Work Scope

- Fabricate graphite/based heat pipe test article
- Integrate power conversion unit with test articles/heat exchanger for thermal energy conversion
- Complete PIE and other analyses of YH_x samples irradiated in ATR
- Fabricate and test encapsulated sample of YH_x for hydrogen permeation for long lifetime operation
- Examine other types of moderator material (Be, graphite, ZrD_2)
- Complete evaluation of burnable poisons, reflectors, control drums, and/or shielding material options for microreactors
- Evaluate results of instrumentation and sensor measurements of test articles at MAGNET
- Develop acoustic or other structural health monitoring techniques for microreactors (embedded fiber optic sensors, piezoelectric sensors, traditional bonded strain gauges, DC potential drop, or non-contact techniques)
- Extend distributed temperature and strain sensing capabilities from SPHERE to MAGNET test articles
- Fabricate metal refractory test articles to examine structural material integrity
- Test safeguards instrumentation at MAGNET or MARVEL



Determining the Effects of Neutron Irradiation on the Structural Integrity of Additively Manufactured Heat Exchangers for Very Small Modular Reactor Applications

*John Gahl¹, Scott Thompson², **Bart Prorok³**, Valentina O'Donnell¹,
Mohanish Andurkar², Tahmina Keya³, Ashley Romans³, Greyson Harvill³*

¹University of Missouri Research Reactor (MURR), University of Missouri

²Alan Levin Department of Mechanical and Nuclear Engineering, Kansas State University

³Department of Materials Engineering, Auburn University

MICROREACTOR PROGRAM REVIEW, MARCH 2022



MURR[®]
Matters...

KANSAS STATE
UNIVERSITY

AU AUBURN
UNIVERSITY

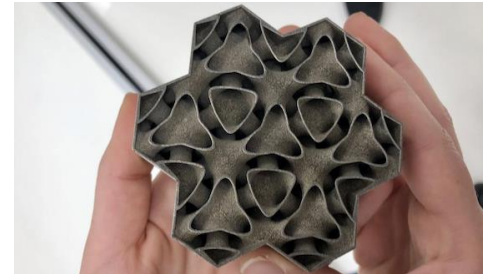
 **MRP** Microreactor
Program

overview

- Nuclear applications
- Project Objectives
- Materials and Production Method
- Radiation Experiments
- Experimental Results
- Summary, Conclusions, and Continuing Work

Additive manufacturing – complex hExs

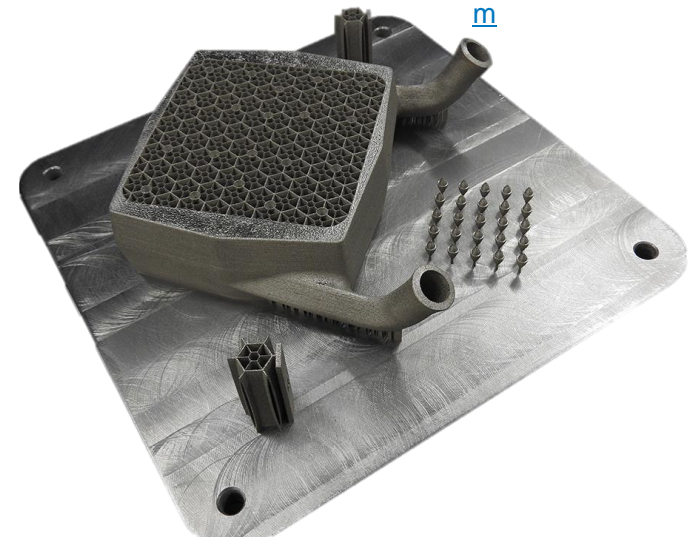
- Additive Manufacturing enables novel geometries and performance
 - part/joint consolidation
 - non-uniform cross-sectioned channels,
 - asymmetric core architecture,
 - fully-circular channels
- Effects of neutron irradiation on AM not well studied yet
 - Nuclear Attenuation
 - AM Processing Characteristics
 - Microstructure / mechanical / corrosion properties
- AM Microstructures differ from wrought microstructures
 - AM microstructures are anisotropic
 - Limited to no thermal-mechanical processing



<https://www.metal-am.com/>



www.renishaw.com



<https://design-engineering.polimi.it/portfolio/additive-manufacturing-and-heat-exchangers/>

Project Objectives

Determine effects of thermal and fast neutron irradiation on additively manufactured (AM) 625 and 718 nickel-based super alloys

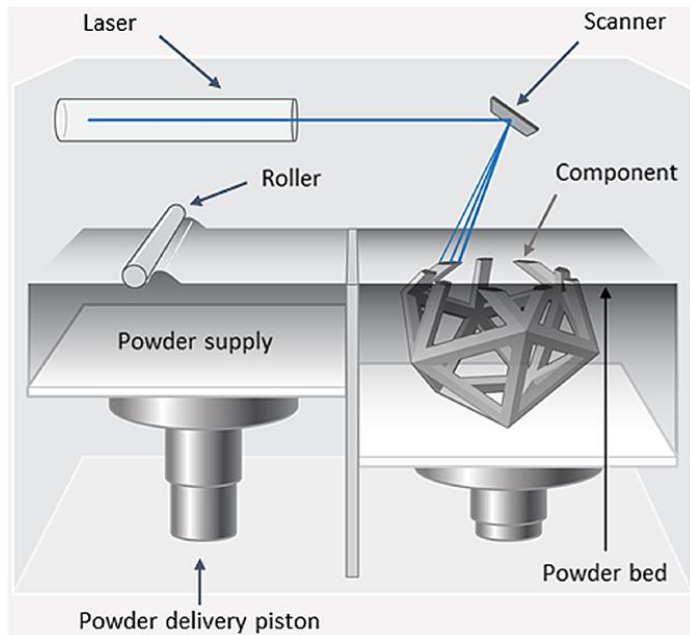
- **Neutron Irradiation Effects**

- Swelling
- Voids
- Frenkel pairs
- Dislocations
- Hardening & Embrittlement
- Impurity formation (hydrogen, helium)

- **Microstructure/mechanical properties**

- Micro/nano hardness
- As-printed microstructure
- Heat-treatment effects
- AM built angle effects

Laser Powder bed fusion (L-PBF)



O'Brien, *Optical Engineering* **58**(1), 010801 (2019)



Heat-treatment schedules

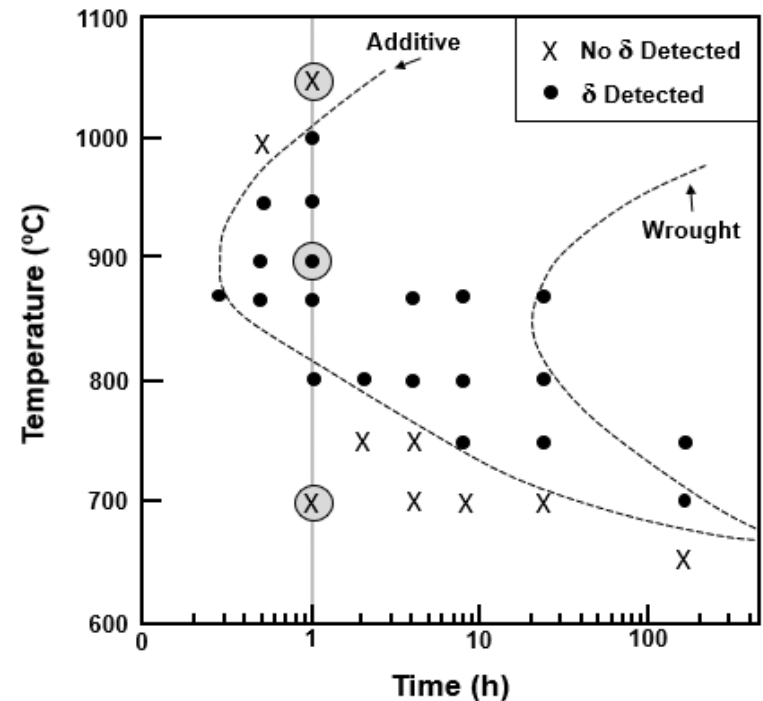
Heat treatment schedules for this study

- As-built (no heat treatment)
- 700 °C - 1 hour
- 900 °C - 1 hour
- 1050 °C - 1 hour

Precipitates formed

- γ'' - contributes to hardening effect in microstructure
- δ - Needle and plate shaped precipitate (deleterious)- makes part brittle
- Both precipitates are rich in Niobium
- 1050 °C -1h was carried out to dissolve all precipitates back in Ni-Cr matrix.
- Final microstructure resembled wrought IN625 microstructure.

Heat treatments were performed on samples of both build orientations



<https://doi.org/10.1007/s11661-018-4643-y>

Radiation Experiments

MURR

Full-Spectrum Neutron

- 10 MW reactor at MURR
- 310 hours
- Neutron flux = 6.61×10^{13} neutrons/cm²/s
- Neutron fluence = 7.37×10^{19} neutrons/cm²

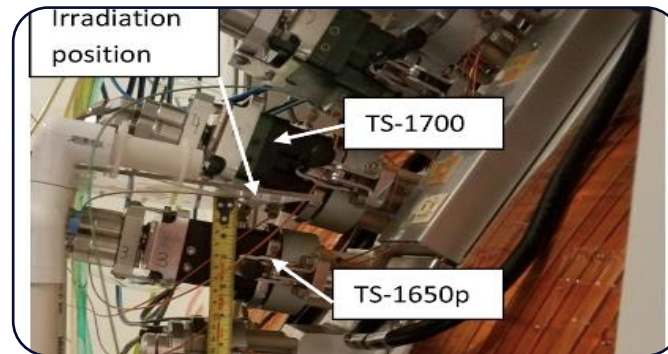
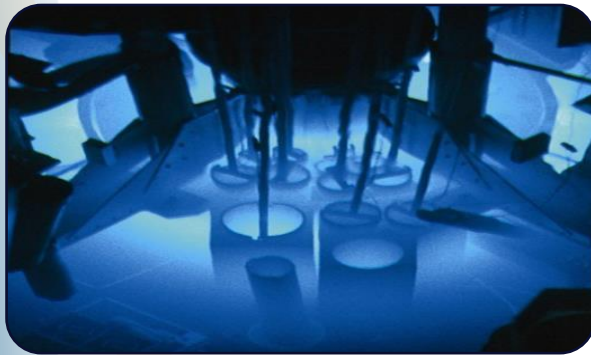
16 MeV Cyclotron

(Fast) Neutron

- Neutrons from PET isotope production $^{18}\text{O}(p, n)^{18}\text{F}$ reaction
- 25-week experiment
- Neutron fluence = 9.08×10^{15} neutrons/cm²
- Low fluence, but low activity

Proton

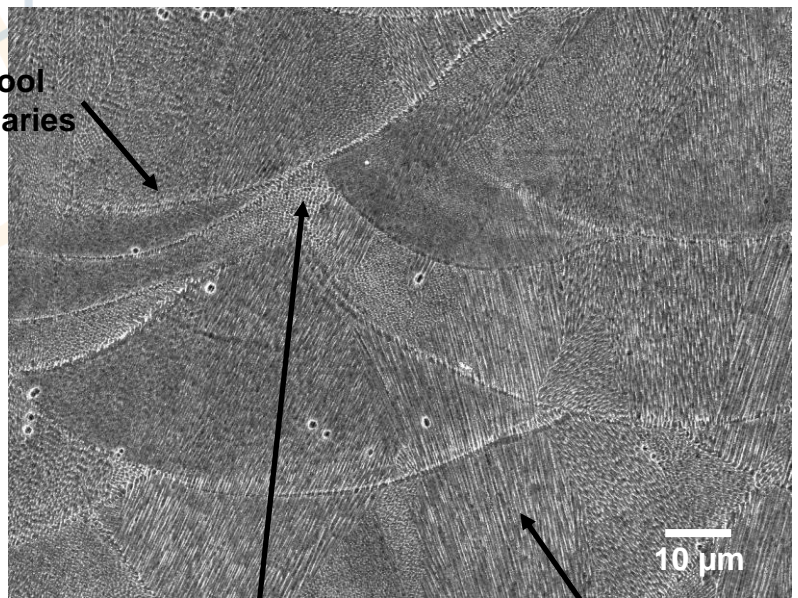
- 80 μA BEAM
- Currently investigating the methodology



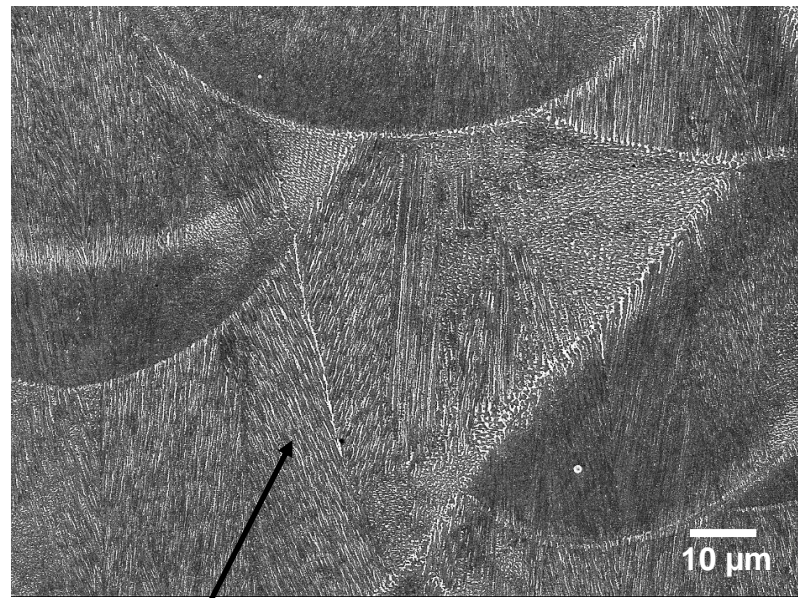
MICROSTRUCTURE

As-Built Microstructure

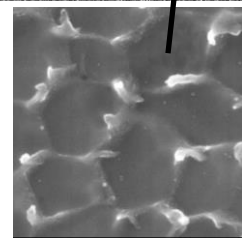
Melt-Pool
Boundaries



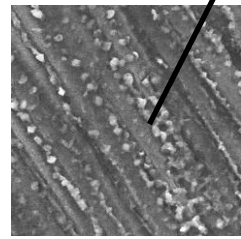
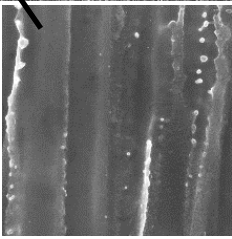
700°C Microstructure



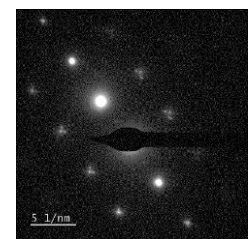
↑ Build
Direction



Dendritic
Solidification
+
Interdendritic
Chemical
Separation

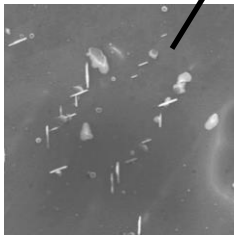
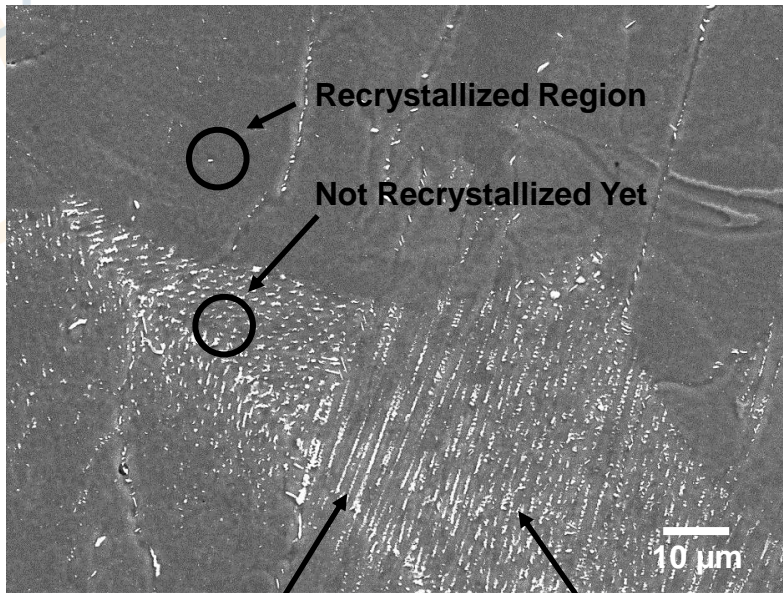


γ'' ppt
Formation in
Interdendritic
Region

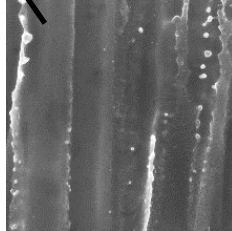


MICROSTRUCTURE

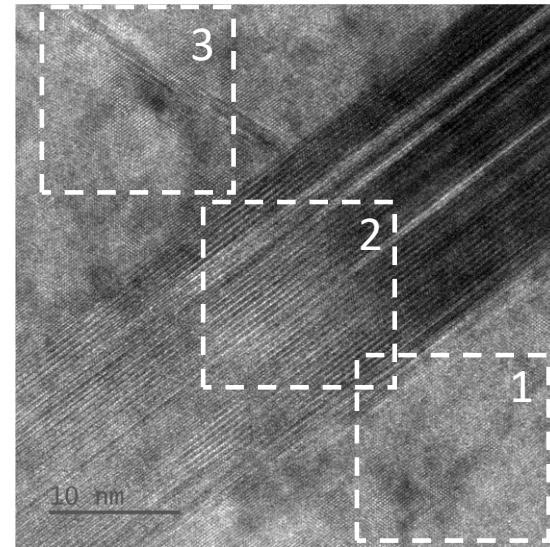
900°C Microstructure



δ ppt
Formation in
Interdendriti
c Region



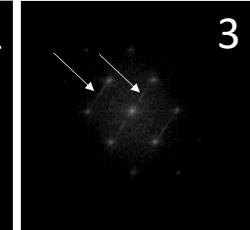
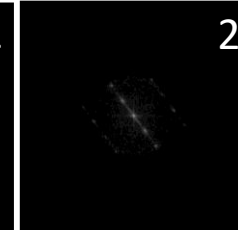
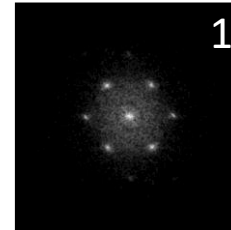
↑ Build
Direction



Matrix $\langle 110 \rangle$

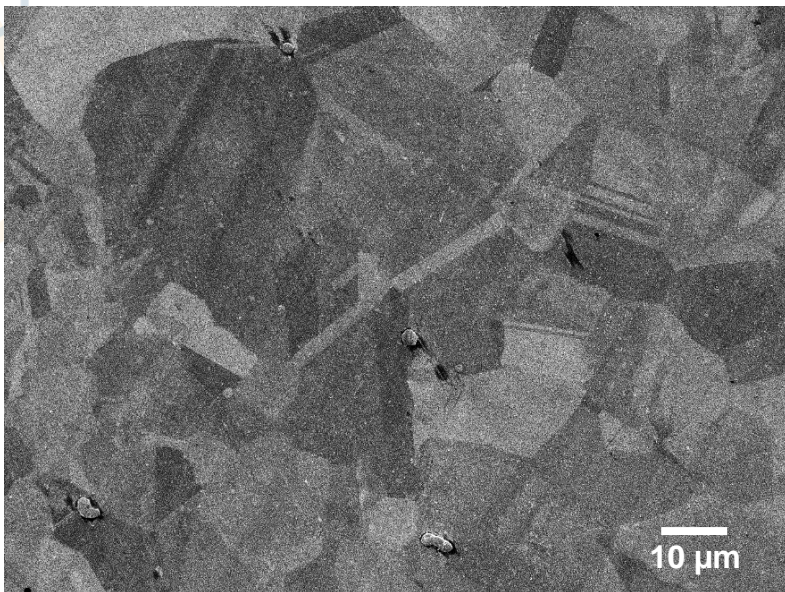
δ ppt

Dislocation

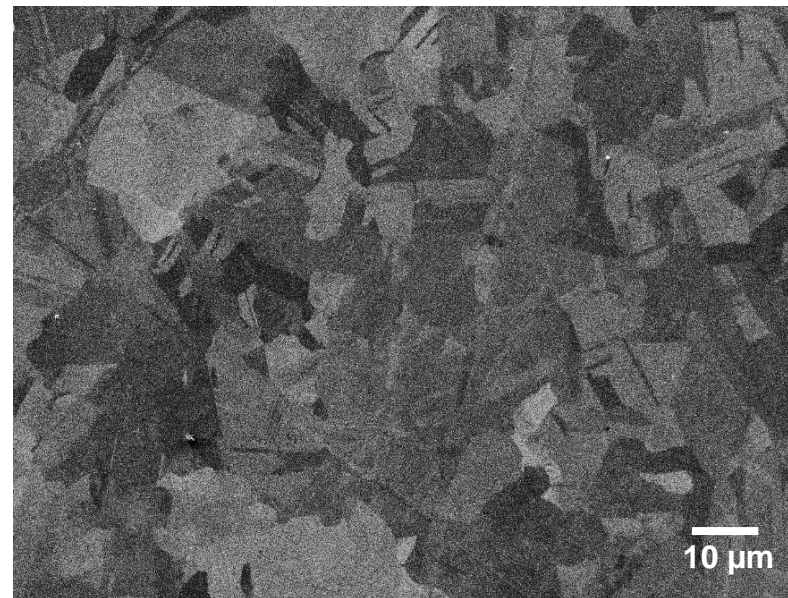


MICROSTRUCTURE

As-Built Microstructure



700°C Microstructure



Completely
Recrystallized

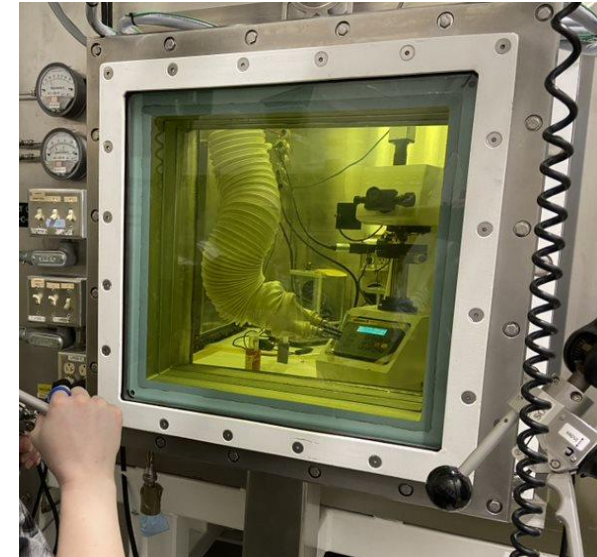
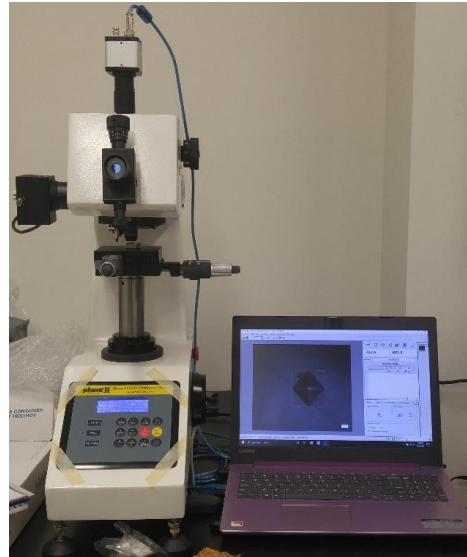
ppts
Dissolved

↑ Build
Direction

Microhardness measurements

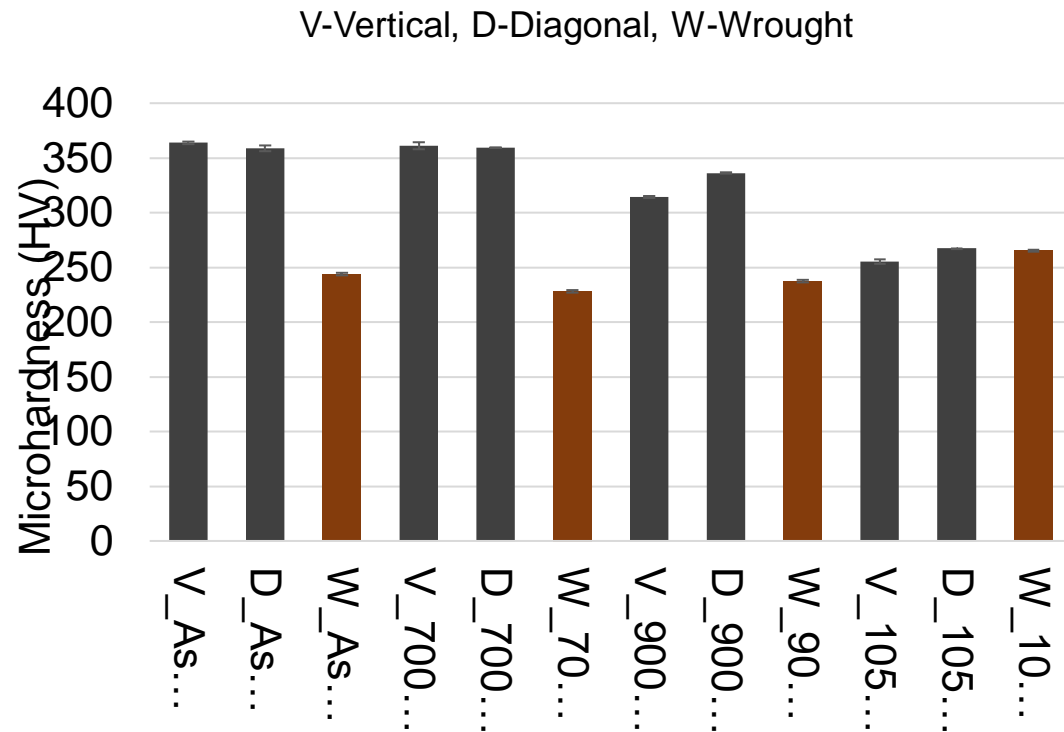
Vickers Microhardness

- Phase II 900-391D
- Load = 1 kgf (9.8 N)
- Dwell time = 15 secs
- Hot cell and manipulator arms for radioactive samples
- Hardness measurements pre- and post- irradiation to track radiation-induced changes



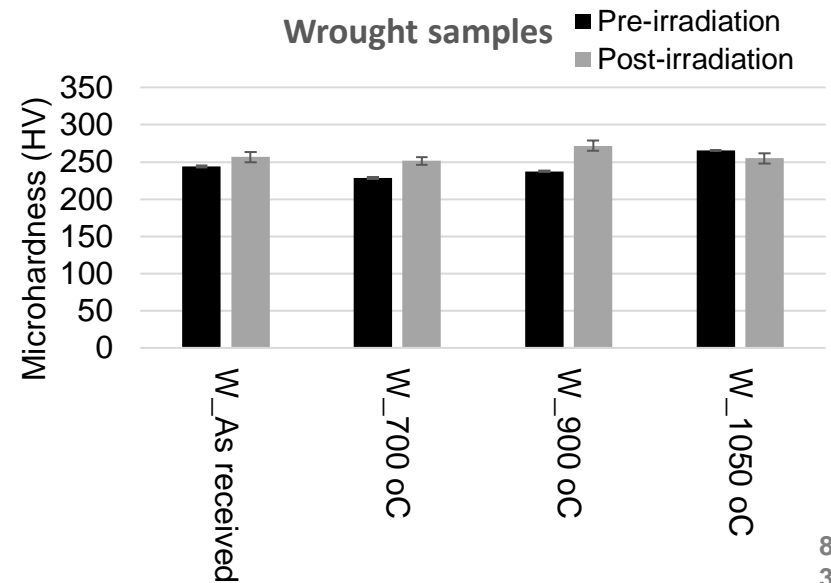
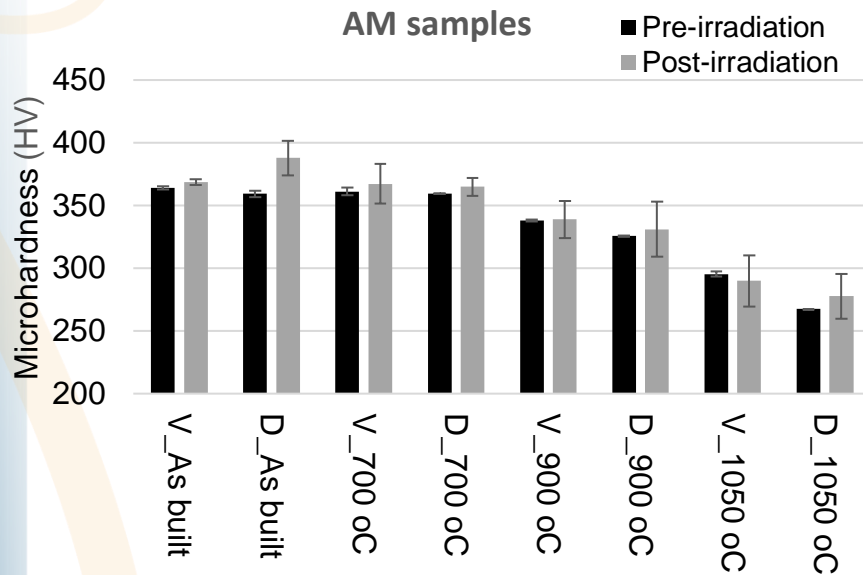
Microhardness of L-PBF and wrought in625

- As-built Vert and Diag showed minimal variation in microhardness.
 - This shows built directional independence.
- Microhardness decreased as heat treatment temperature increased
- 1050 °C AM samples display similar microhardness to wrought Inconel 625
 - This indicates the microstructures are similar



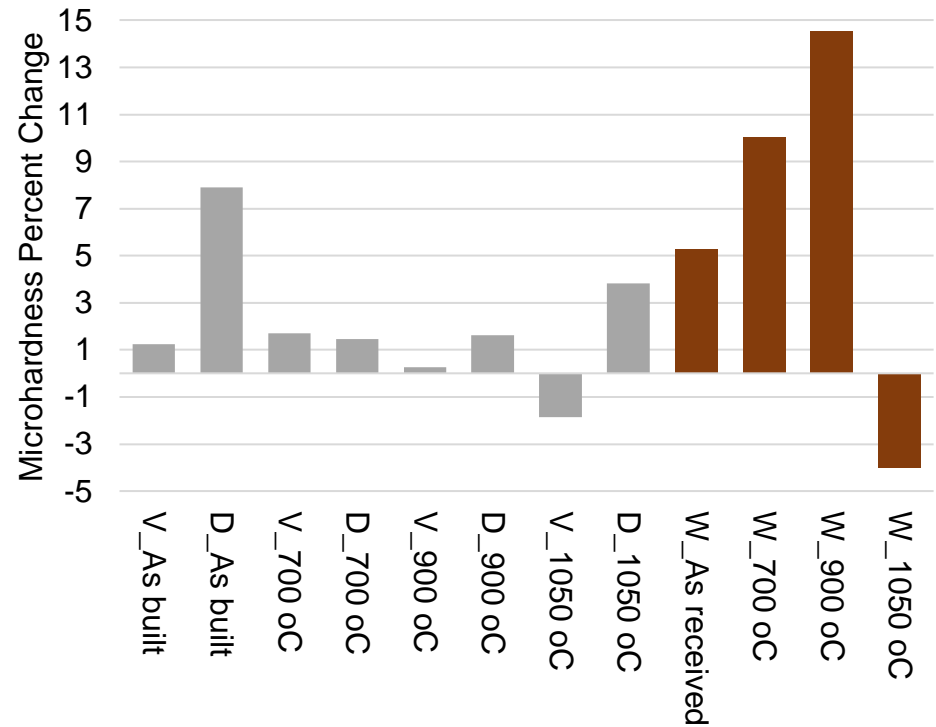
Full-spectrum neutron irradiation

- Thermal neutron irradiation induced embrittlement/hardening in AM and wrought IN625
- 1050 °C AM vertical and wrought showed slight radiation softening phenomenon
- Preliminary results show AM IN625 to be more resistant to radiation hardening than wrought IN625



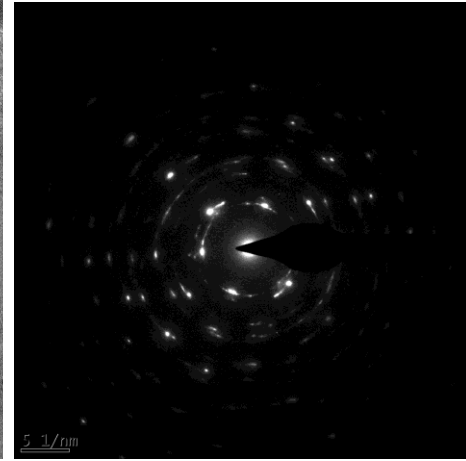
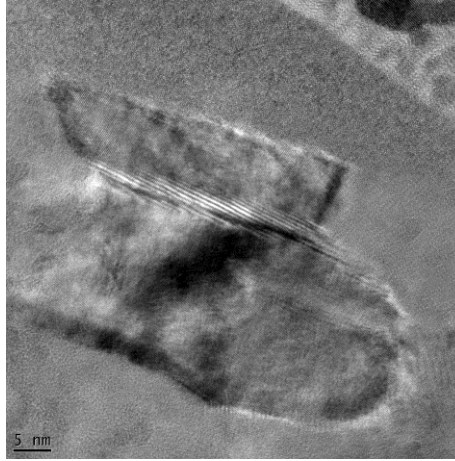
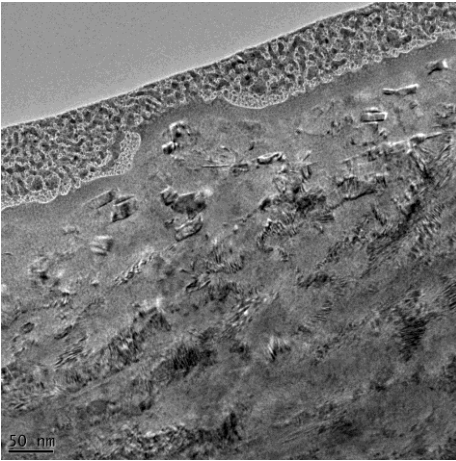
Full spectrum neutron irradiation

- Vertically printed AM samples hardened 0.4% on average
- Diagonally printed AM samples hardened 3.8% on average
- Conventionally wrought samples hardened 6.1% on average

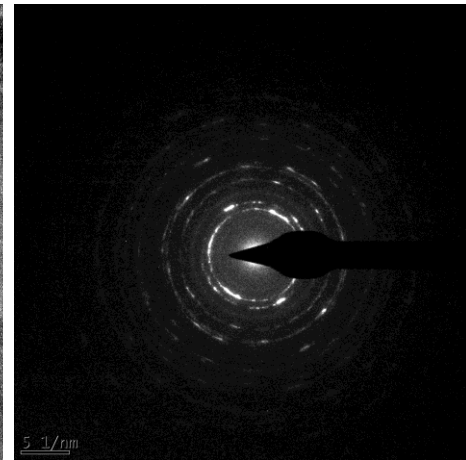
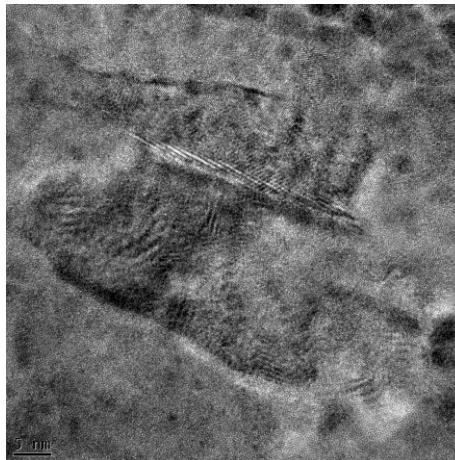
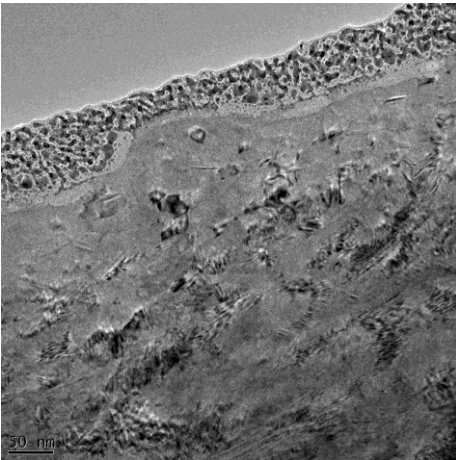


FAST NEUTRON IRRADIATION – LAMELLA TECHNIQUE

Pre-irradiation

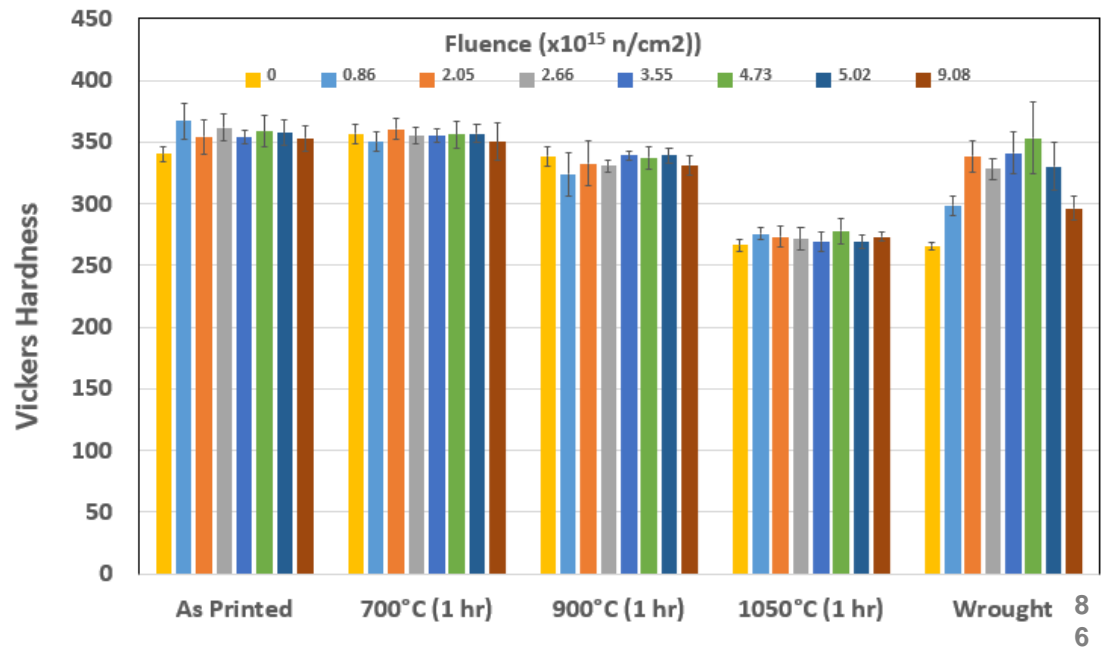


Post-irradiation



FAST NEUTRON IRRADIATION

- Microhardness was measured at different neutron fluences
- Less variation seen in the microhardness values of AM Inconel 625 compared to wrought Inconel 625
- Lower overall fluence compared to thermal neutron irradiation meaning lower DPA
- No thermal neutrons meaning lower activity



SUMMARY AND CONCLUSIONS

- Several L-PBF AM IN625 and wrought IN625 samples were irradiated using thermal and fast neutrons.
 - Results showed that L-PBF IN625 samples were more resistant to radiation hardening compared to wrought IN625.
 - Wrought IN625 samples were most prone to radiation hardening with average of 6.1%.
 - Diagonal AM IN625 samples experienced slightly more radiation hardening than vertical AM samples
- L-PBF AM IN625 and wrought IN625 samples were irradiated using fast neutrons
 - Results showed that wrought IN625 hardness values had more variation over the course of the experiment than the AM IN625 samples

CONTINUING WORK

- Detailed microstructure investigation to thoroughly understand the radiation damage mechanism in L-PBF AM and wrought samples
 - SEM and TEM imaging
 - Investigation of phase contributions, build orientation effects
- L-PBF AM Inconel 718 samples currently undergoing irradiation trials.
- Proton beam experiments are being conducted to supplement full-spectrum neutron irradiation experiments.

THANKS

Contact Information

- **John Gahl**
 - Nuclear physics/engineering
 - gahlj@missouri.edu
- **Bart Prorok**
 - Additive manufacturing, materials science
 - prorobc@auburn.edu
- **Scott Thompson**
 - Additive manufacturing, heat transfer
 - smthompson@ksu.edu



(NEUP Project 19-17416)
Experiments and computations to address the
safety case of heat pipe
failures in Special Purpose Reactors

Victor Petrov, Annalisa Manera, Pei-Hsun Huang, Taehwan Ahn

DOE-NE Microreactor Program

Winter Review Meeting

3.3.2022

Two papers for ANS – ATH22: Data analysis for the experimental campaign of vertical orientated HP#1 (FR = 50%) and HP#13 (FR = 25%)

The characteristic plot of HP operation conditions

- The sodium vapor temperature is defined as the average temperature at the adiabatic section; the upper and lower bound of the error bar were referred to the max. and min. heat pipe surface temperature
- The heat transfer rate on the y-axis represents the heat removal rate in the condenser

❖ The cooling conditions and heater input power effects on two HPs with different filling ratios (FR)

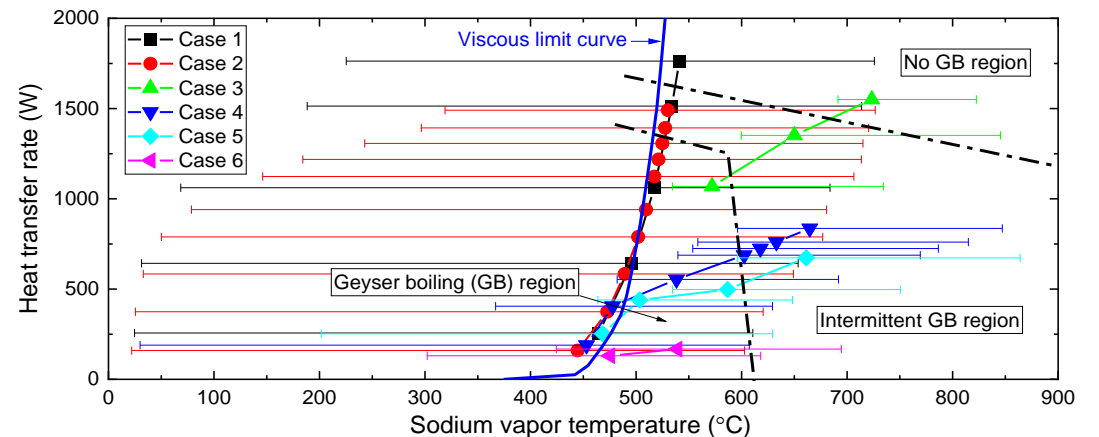
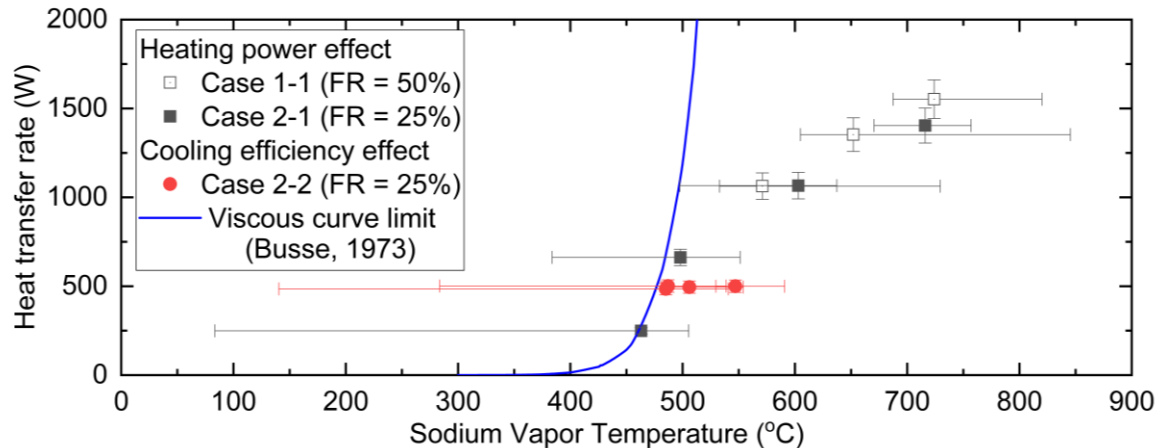
- The operation condition of heat pipe is confined by the theoretical viscous curve limitation
- Significant end-to-end temperature differences of heat pipe as the operation condition approach to the viscous curve limitation
- Temperature oscillated in the case of HP with 50% FR unless the power increased above 1500 W

❖ The cooling conditions and heater input power effects on geyser boiling phenomenon of heat pipe with 50% FR

- As the cooling efficiency decreases, the vapor temperature tends to increase under the given heat transfer condition, facilitating the isothermal operation of the heat pipe.
- The geyser boiling usually occurred in the region near the viscosity limit, and completely disappeared under high heat transfer rate and sodium vapor temperature.
- In between, there is a transition region where intermittent geyser boiling occurs

Tests	Filler material	Cooling fluids	Flow rates (g/s)	Cooling efficiency	Heater power range (kW)
Case 1	SiC powder	Water	27 – 28	Highest	500 – 2.25
Case 2	Copper wire	Water	27 – 29	Very high	500 – 2.1
Case 3	SiC powder	Air	6.1 – 6.7	High	1500 – 2.25
Case 4	Copper wire (coarse)	Water	25	Medium	0.5 – 1.5
Case 5	Copper wire	Air	2.2 – 2.9	Low	0.5 – 1.5
Case 6	Copper wire (oxidized)	Air	1.2	Very low	0.5 – 0.75

Test	Filling ratios (%)	Filler materials	Water flow rates (g/s)	Air flow rates (g/s)	Heating power (W)
Case 1-1	50	SiC powder	0	6.4	1,500 – 2,250
Case 2-1	25	SiC powder	10	4	500 – 2,000
Case 2-2	25	SiC powder	10	0.48 - 7	800



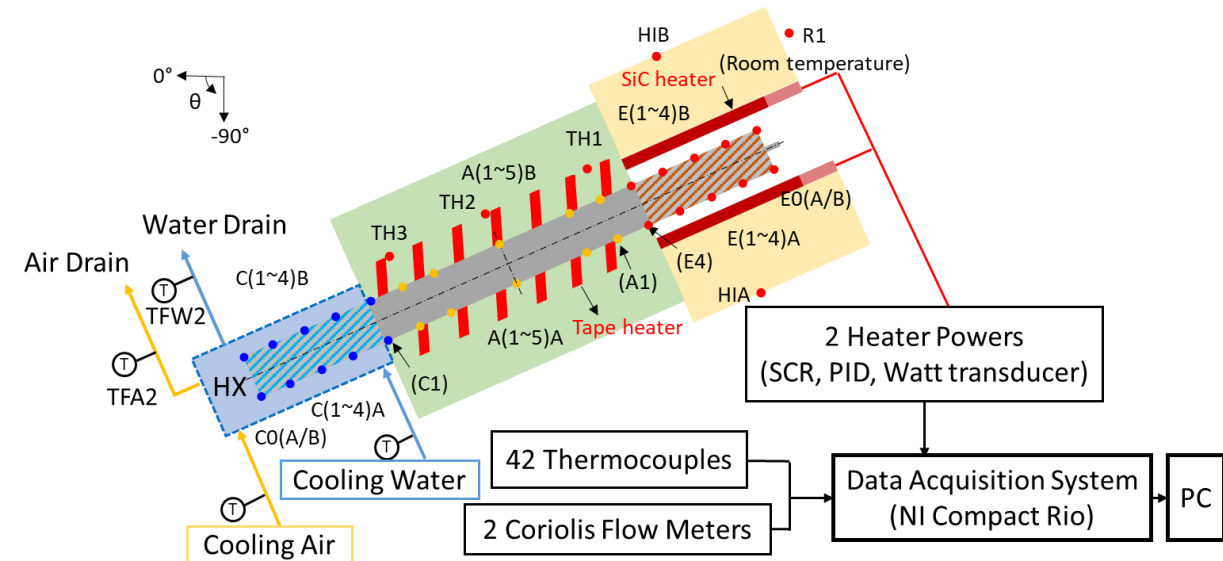
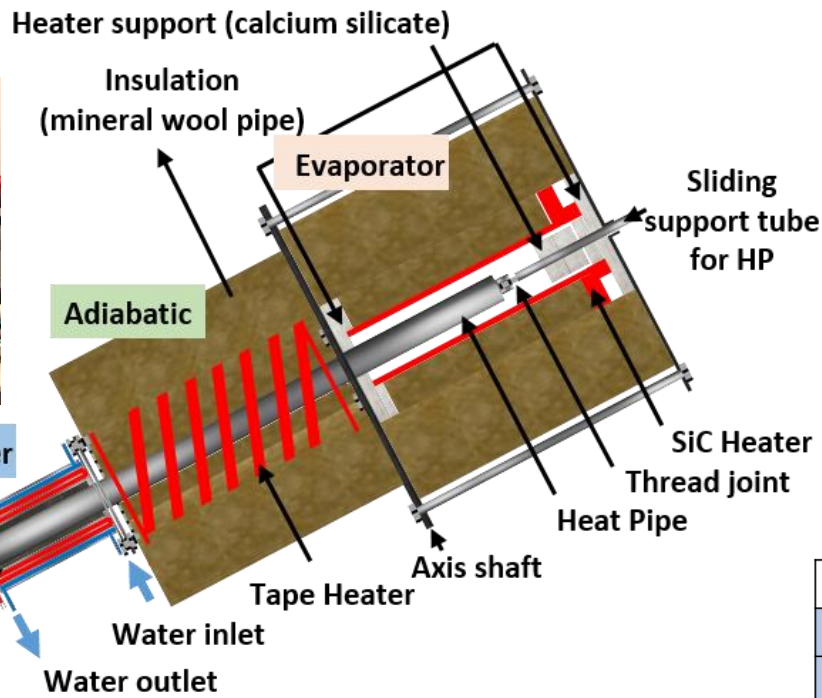
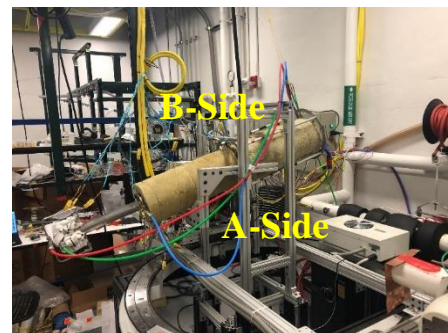
The startup process and performance of a negative orientated heat pipe

❖ Experimental Apparatus

- B-side was arranged at the top side, which is against the gravity more than A-side
- Trace heater was installed in the adiabatic section and controlled by PID with the setting temperature slightly lower than the minimum temperature in the adiabatic section
- SiC powder was applied between the heat pipe and heat exchanger to enhance the cooling efficiency in the condenser



<Trace heater>

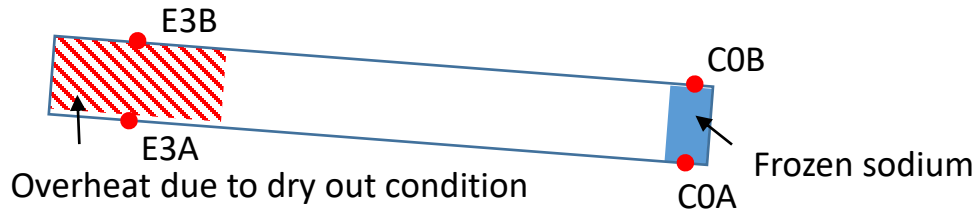
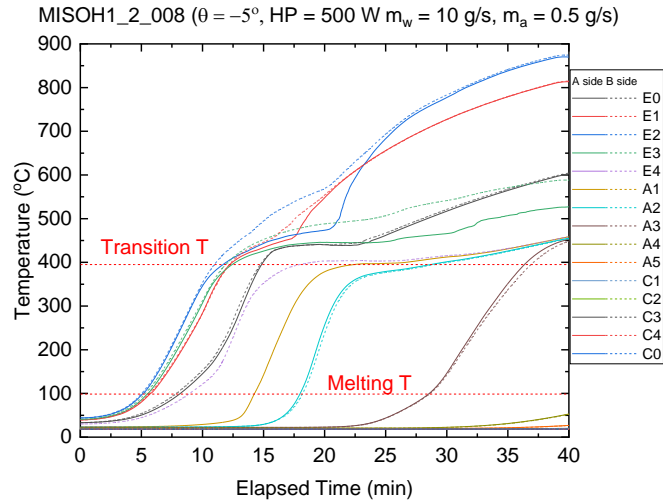


30 TC locations on the heat pipe (mm)

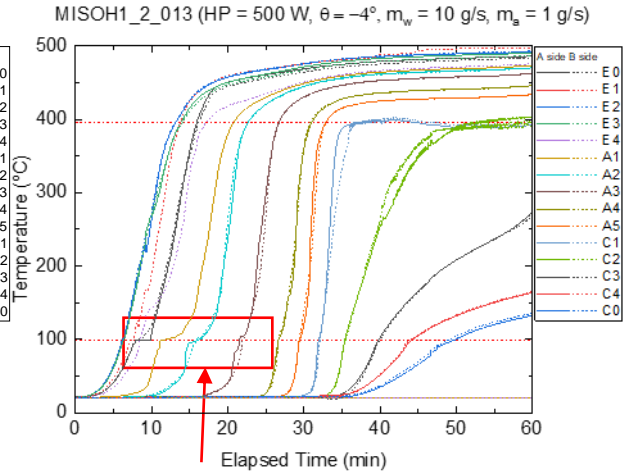
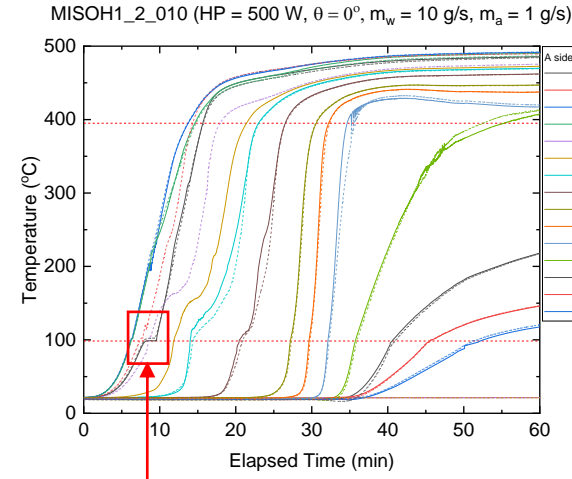
$T_{w,C}$					$T_{w,A}$					$T_{w,E}$				
C0	C4	C3	C2	C1	A5	A4	A3	A2	A1	E4	E3	E2	E1	E0
1016	952.5	889	825.5	762	698.5	635	508	381	317.5	254	190.5	127	63.5	0

The startup process and performance of a negative orientated heat pipe with 25% filling ratio

❖ The effect of initial sodium location in the heat pipe

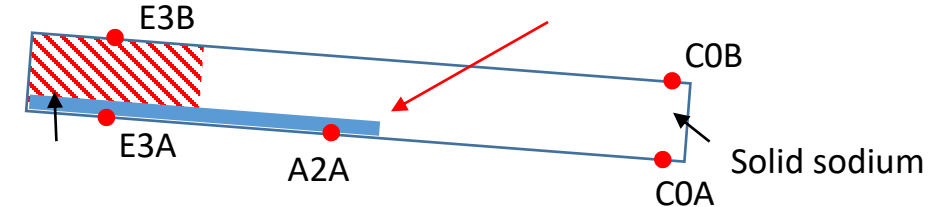


❖ The effect of inclination angle on the startup process of the heat pipe



<melting at the evaporator end>

<melting and solidifying process along the heat pipe>

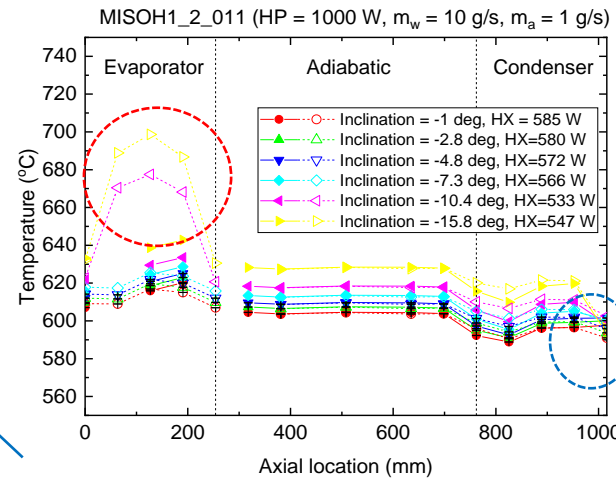
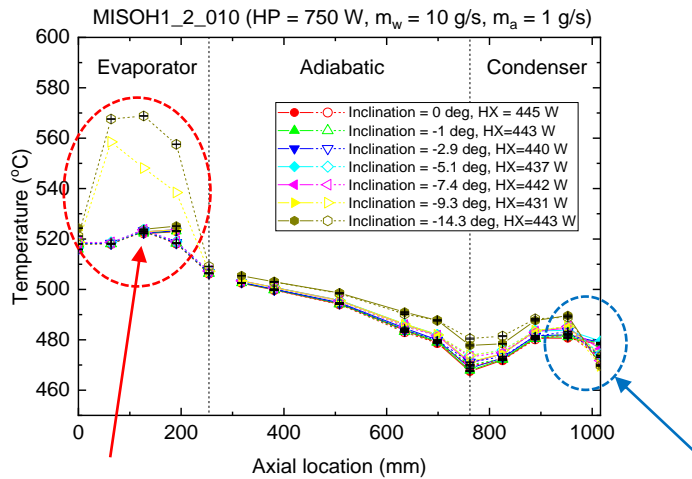
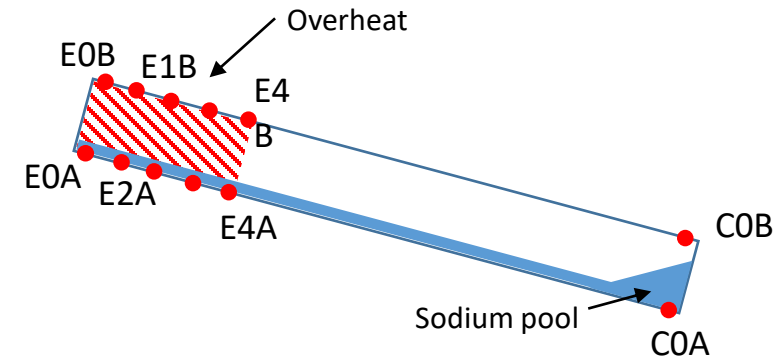
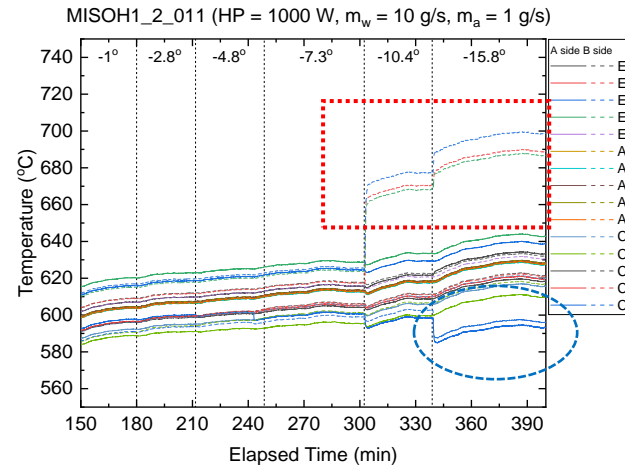
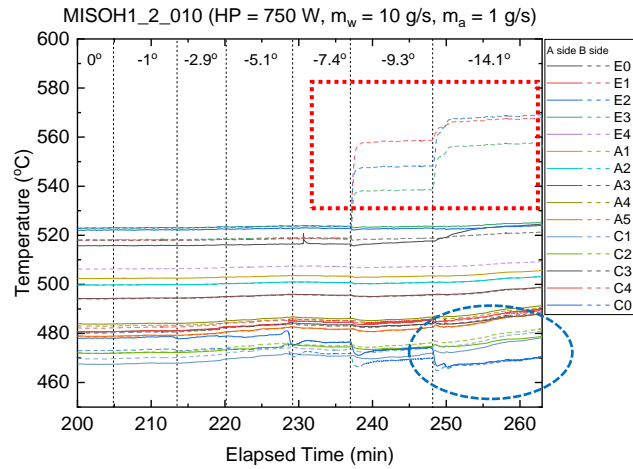


Summaries

- The initial location of sodium in the heat pipe is crucial for the successful startup of the heat pipe, when solid sodium was initially located at the condenser under slightly negative inclination, fail startup was presented severe overheat in the evaporator region.
- When the solid sodium was initially located in the evaporator, the melting and solidifying process along the heat pipe during startup under negative inclination angles.

The startup process and performance of a negative orientated heat pipe with 25% filling ratio

❖ The change of inclination during operation of heat pipe



Summaries

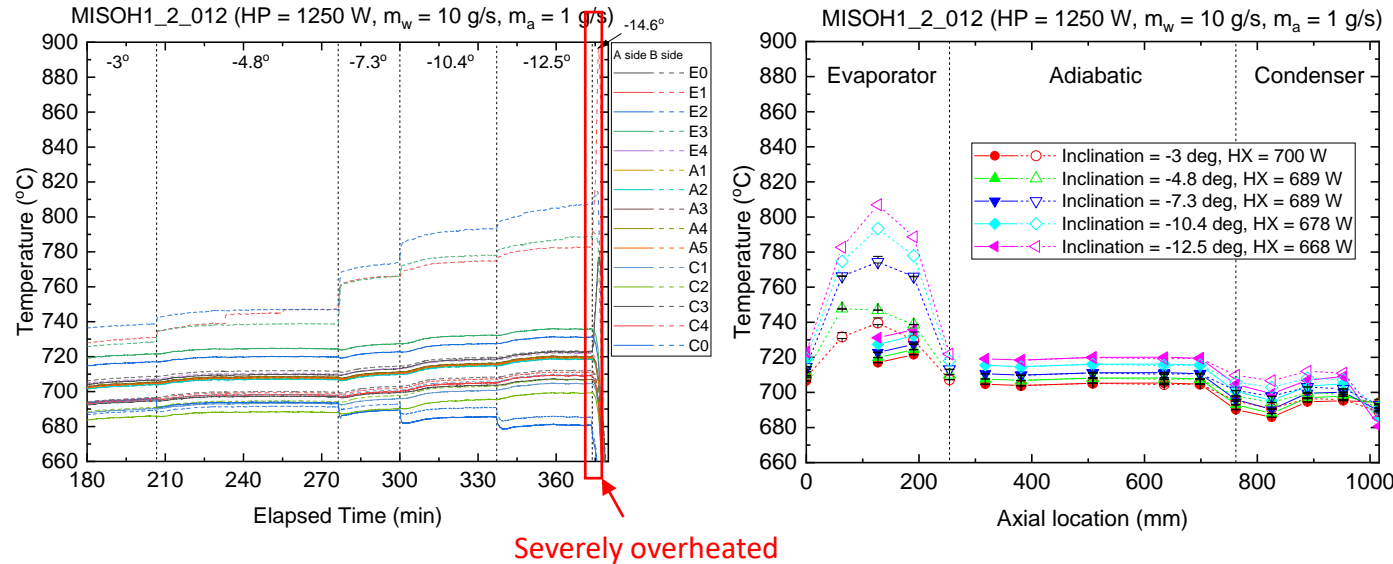
- Liquid reservoir formed in the condenser end under the heating power of 750 W with -7.4 deg and heating power of 1000 W with -10.4 deg.
- B-side at the evaporator was overheated under the heating power of 750 W with -9.3 deg and heating power of 1000 W with -10.4 deg.

Overheat at the B-side of evaporator

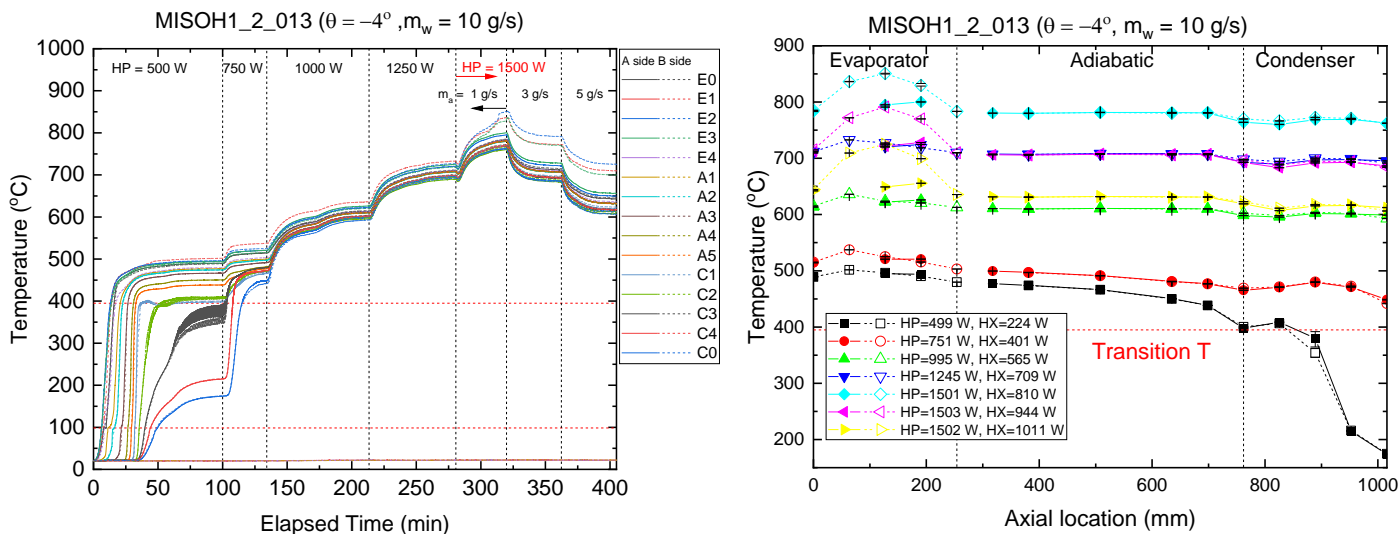
Formation of liquid pool at the A-side of condenser end

The startup process and performance of a negative orientated heat pipe with 25% filling ratio

❖ The change of inclination and cooling condition during operation of heat pipe



MISOH1_2_012: As the input power ≤ 1000 W, the heat pipe can be operated under -15 deg, but the temperature becomes not isothermal (overheated at the B side of the evaporator and subcooled at the A side of condenser end). On the other hand, severe overheat occurred as the input power approaches 1250 W under -14.6 deg



MISOH1_2_013: Comparing the steady-state temperature profile between pink and dark blue and between yellow and green. B side at evaporator was overheated under high heat transport rate with the same sodium vapor temperature. It is because more sodium is needed to support such a high heat transport rate so insufficient liquid sodium at B side lead to overheat

X-ray radiography measurement of a vertical orientated heat pipe with 25% FR

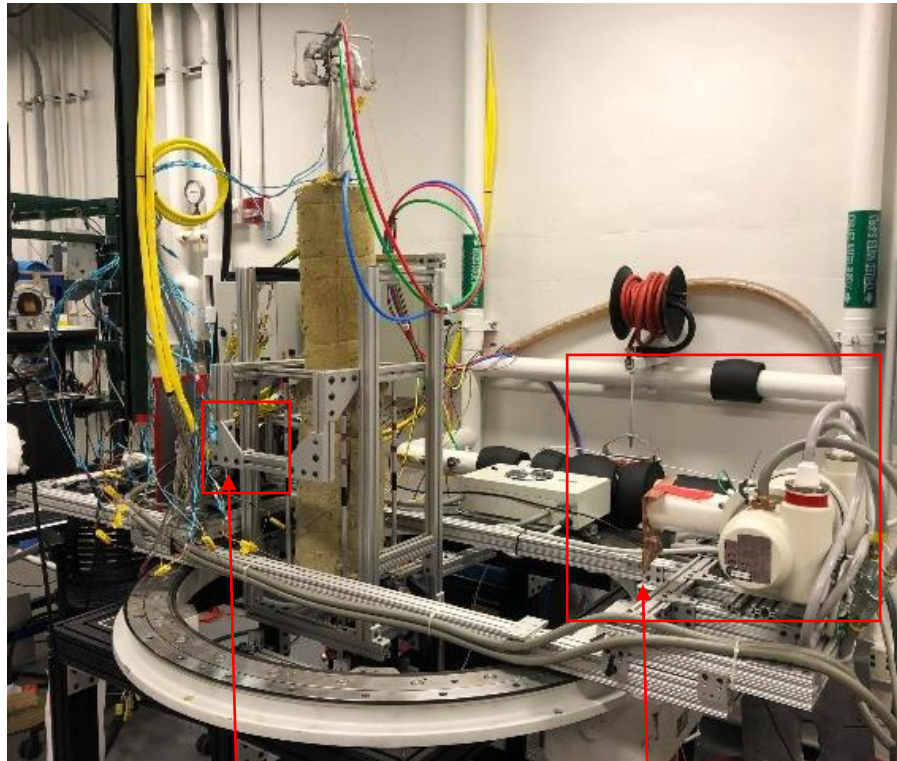
❖ Experimental Apparatus

❑ Test section (MISOH1)

- Vertical HP (90 deg)
- $m_a = 4 \text{ g/s}$
- $m_w = 10 \text{ g/s}$

❑ X-ray radiography system

- X-ray tube - 150 kV, 80 mA, 500 ms
- Detector settings - 360 frms, 300 Hz



Detector

X-ray tube

❖ Measurement preparation

- ❑ Magnification factor was estimated based on the known dimension of injection tube on the heat pipe

Digitalization: 8.11 mm
(Real: 8 mm)

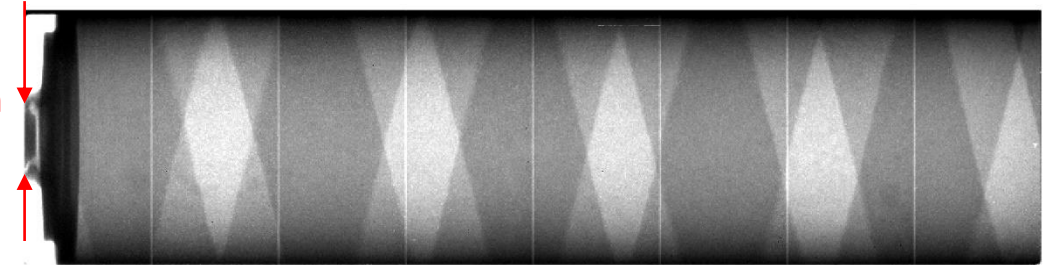


Magnification factor (MF) = 1.01315

- ❑ Calibration image was acquired by measuring a dummy tube with the same dimension of the heat pipe container



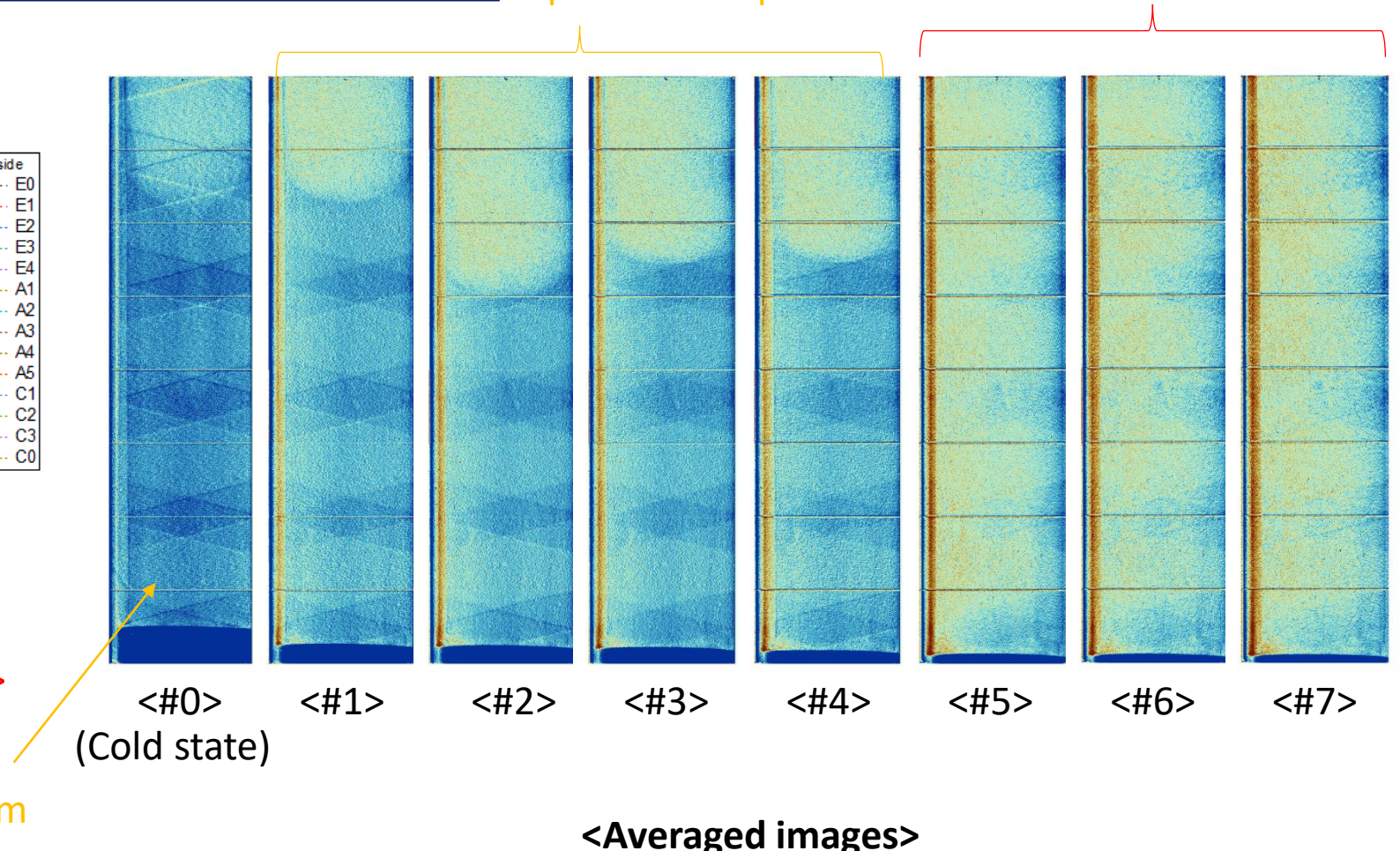
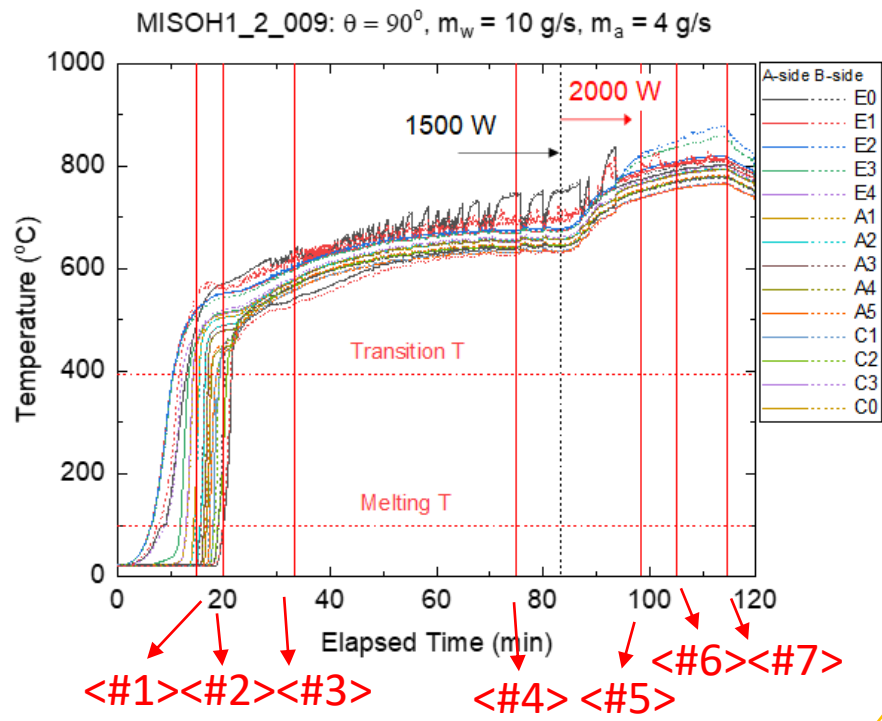
Dummy tube



X-ray radiography measurement of a vertical orientated heat pipe with 25% FR

Liquid sodium pool

Transient 2 phase flow!



Solid sodium

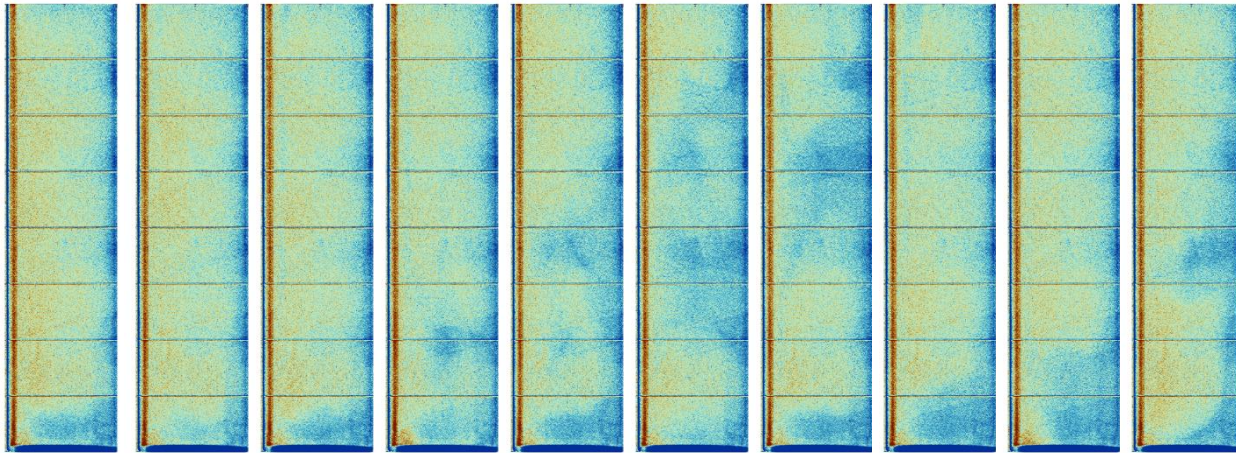
Summaries

- No two-phase flow was observed under the heating power of 1500 W (only liquid pool presented)
- Intense two-phase flow was captured as the heating power proceeded to 2000 W

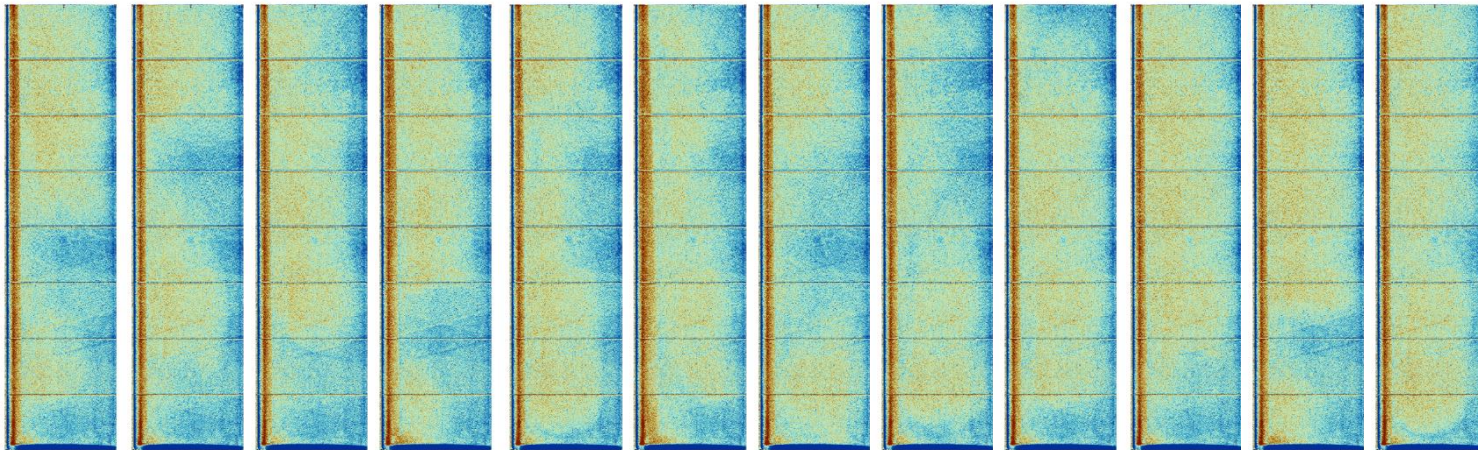
X-ray radiography measurement of a vertical orientated heat pipe with 25% FR

❖ Transient flow images

<#5>

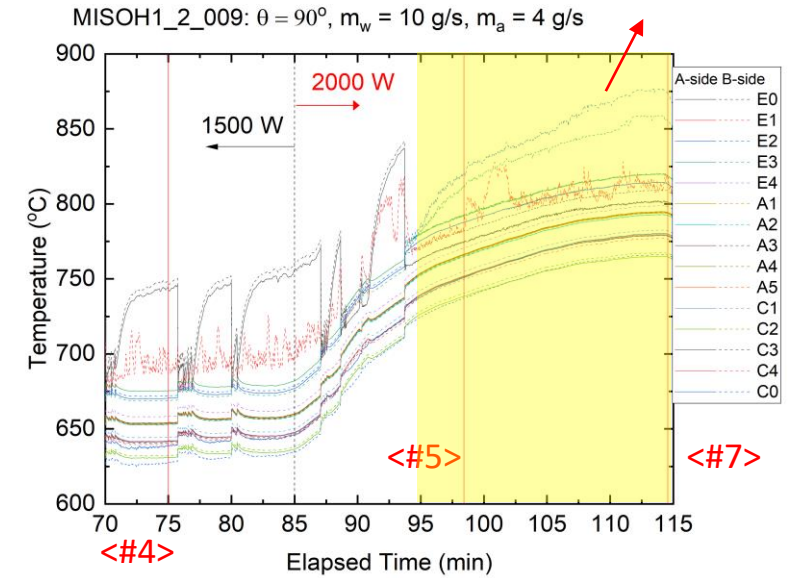


<#7>

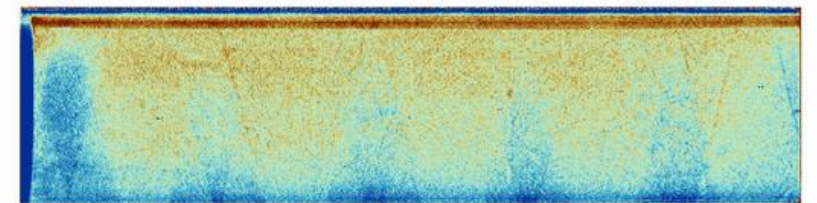


The sodium vapor was mostly generated from the B-side during the transient process, which matches with the temperature readings (B side temperature was higher than A side in the evaporator)

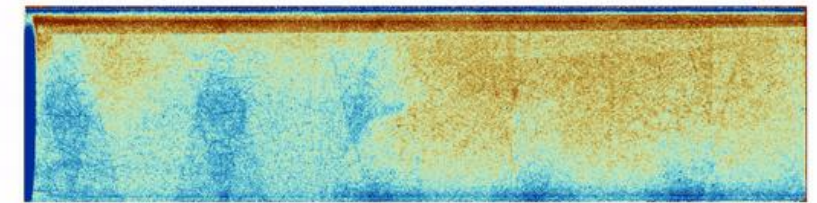
<Around 50°C overheating at B side (left side on the images) under 2000 W where intense two-phase slug flow observed>



<#5>



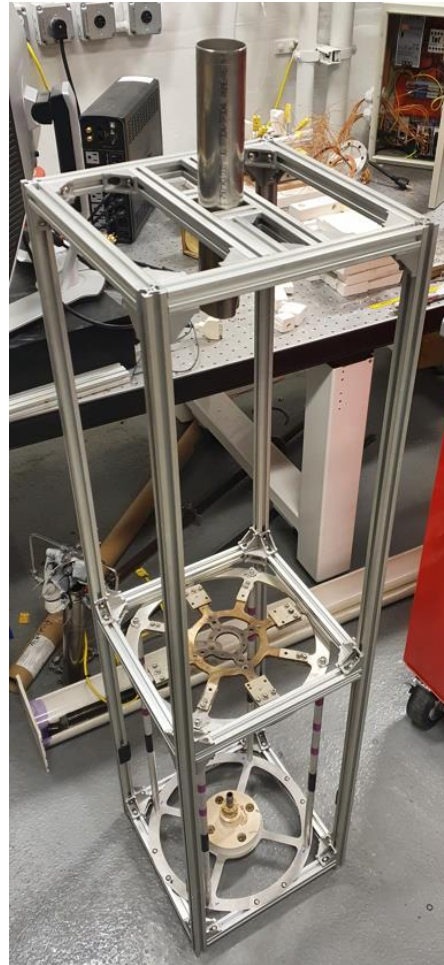
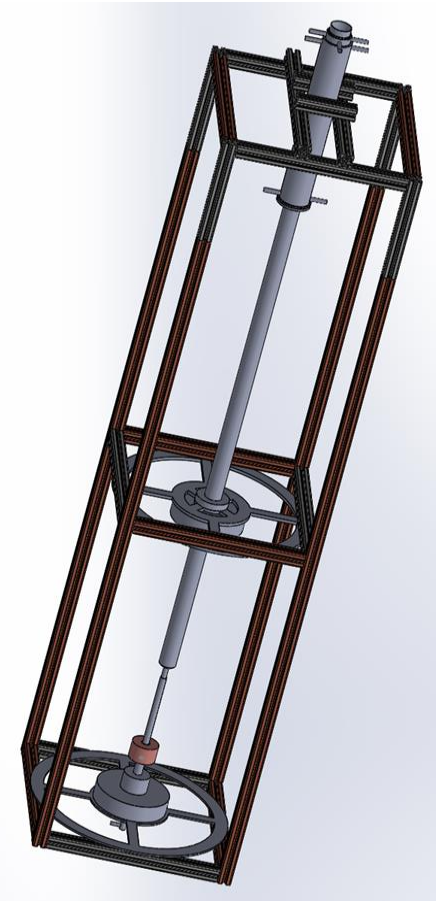
<#7>



Test section upgrade

❖ Structural upgrade

- Additional Aluminum profiles were installed on the test section to enhance the integrity of the structure and prevent the heat pipe from touching the heater during operation



❖ New split (UX type) SiC heater for X-ray radiography measurement

- Although the heater strip artifacts presented on the X-ray images had been mitigated upmost by the developed image morphing tool in the Matlab environment, the heater with uniform surface is desirable because it makes the analysis of void fraction becomes possible



For that, a DC power supply is required for controlling because of the difference of resistance range.

The new heaters had arrived, and the DC power supply had been ordered.

New experimental campaign (In progress)

❖ Experimental Apparatus

- Trace heater was installed in the adiabatic section and controlled by PID with the setting temperature slightly lower than the minimum temperature in the adiabatic section
- SiC powder was applied between the heat pipe and heat exchanger to enhance the cooling efficiency in the condenser

❖ Experimental purpose

- Investigate the heat pipe performance under highest cooling efficiency with upgraded test section

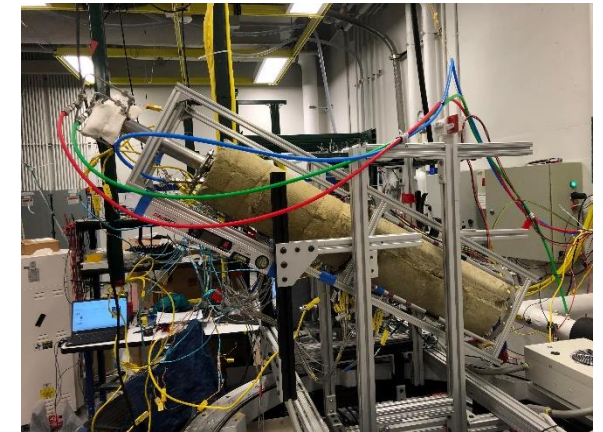
❖ Boundary conditions:

- Air mass flow rate = 7.5 g/s, Water mass flow rate = 10 g/s, HP inclination angle = 90, 30, 15, 0 deg with HP#31 (similar filling ratio as HP#13)

<Upgraded test section>



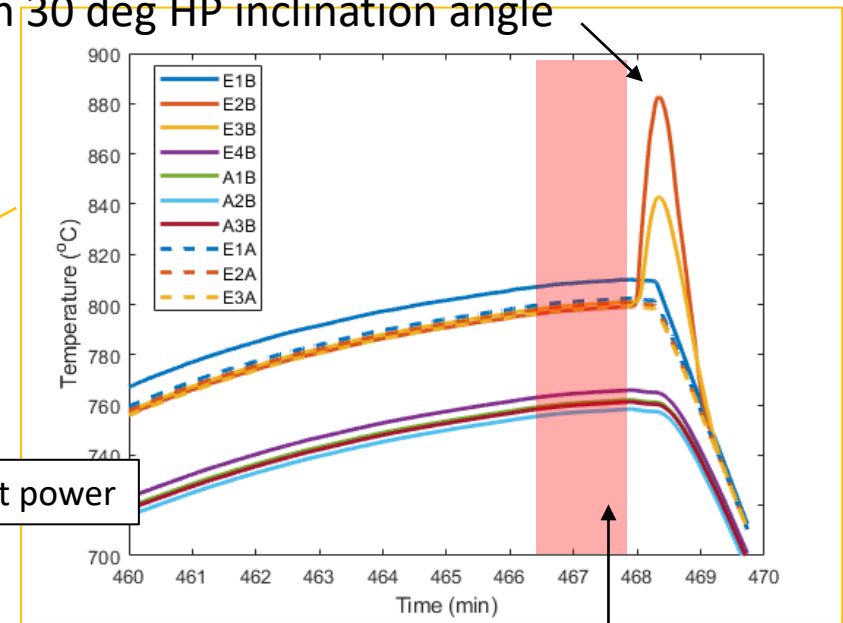
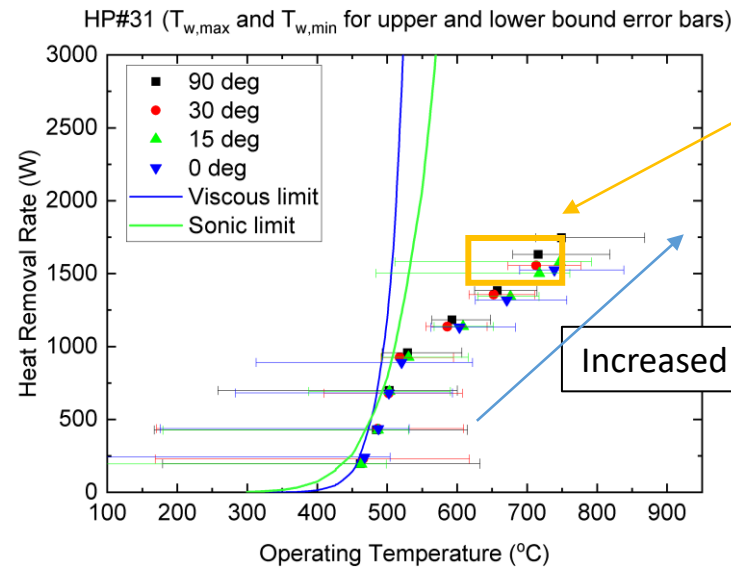
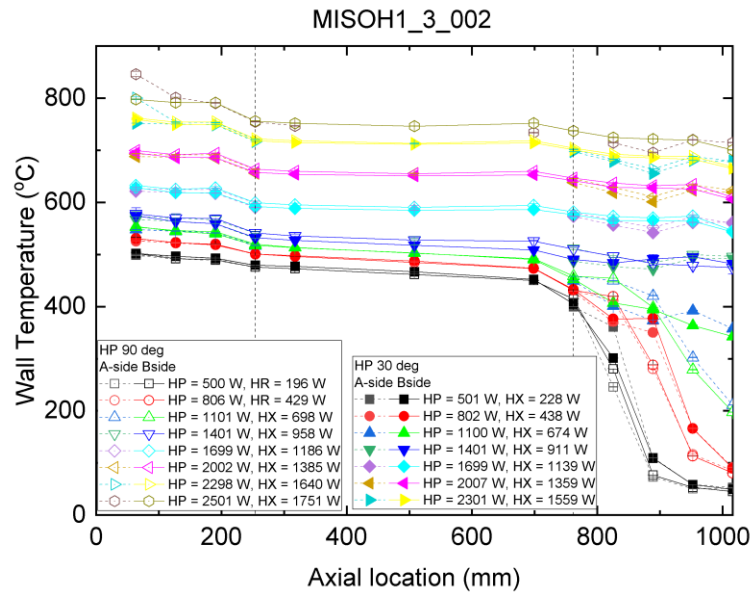
<90 deg>



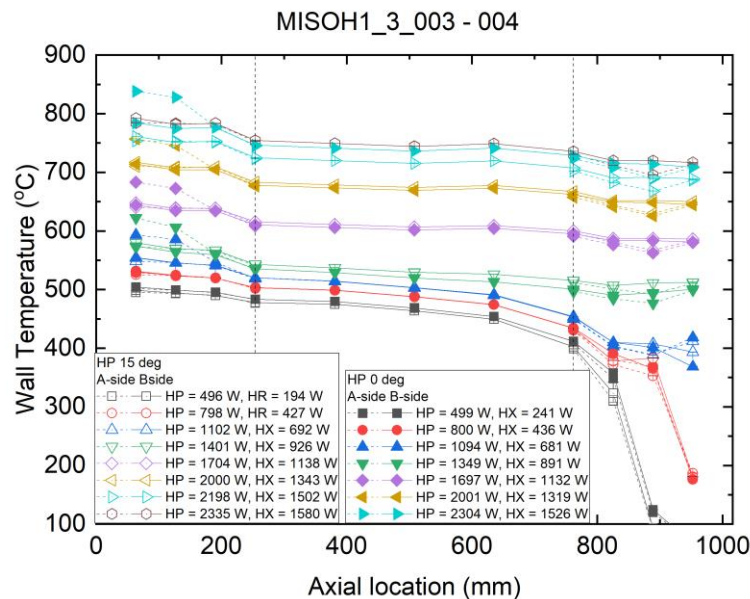
<30 deg>

Results

sudden temperature peak under high heat transfer rate with 30 deg HP inclination angle



Increased input power

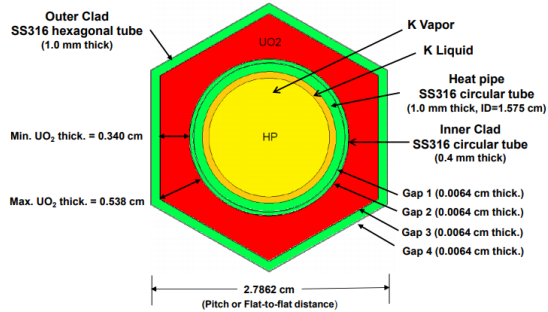


Summaries

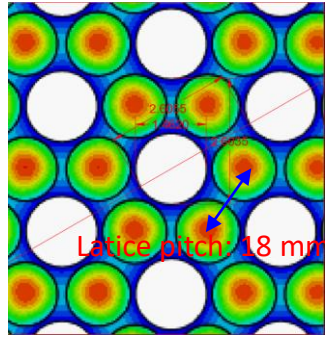
- The operating temperature of the heat pipe follows similar operation curve regardless of the inclination angle
- Large end-to-end temperature differences of the heat pipe as operating near viscous curve
- A sudden temperature surge at B-side of heat pipe (top side) under high heat transfer rate with 30 deg of hp inclination angle, which is possibly resulting from the CHF or local dry-out

Heat pipe mini-core design

❖ Design of the evaporator



<Design A>
P/D = 1.570



<Design B>
P/D = 1.756
(Sterbentz et al. 2018)

<Heating element>



MoSi2 Heating element
(3 mm OD (HZ) x 6 mm OD (CZ))

Potential issues and solutions

Contact resistance between the blocks

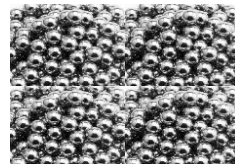
- Using larger blocks (2" or more), but the machining will be somehow challenging and not precise (enlarged error as the depth gets larger)
- Applying high temperature thermal paste between slabs



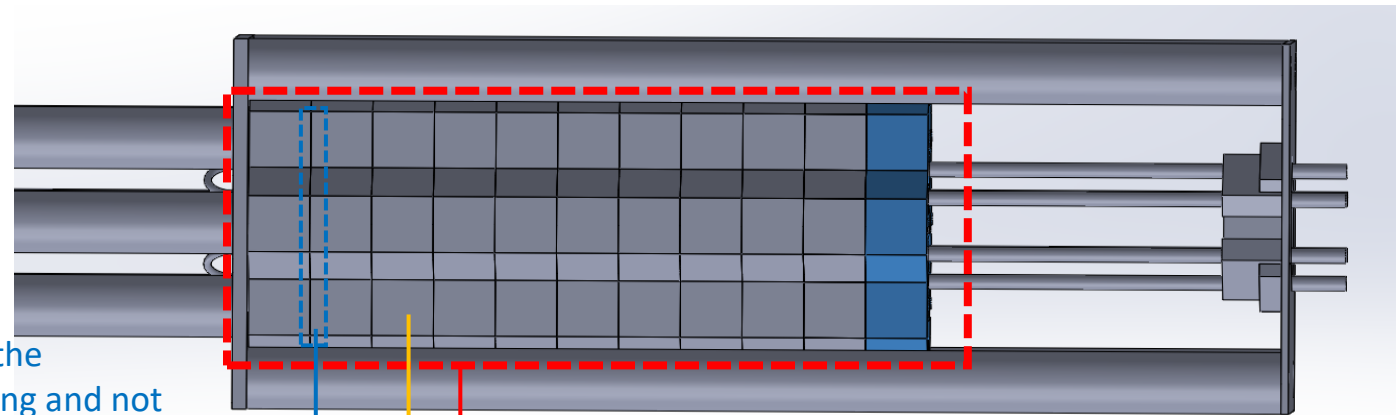
<Conductive powder>



<Alternative: coarse pebble or beads>



<Side View>



Weight of the hex block

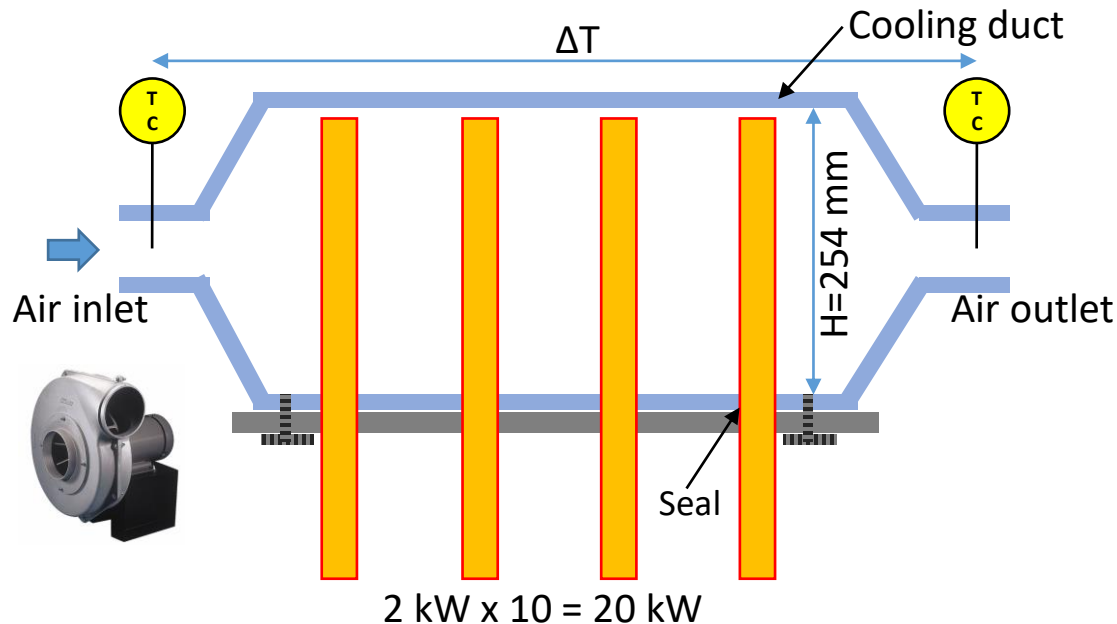
- Strong bottom insulation support
- Angle adjustment by two different height support at the condenser and evaporator sections

Thermal stress of the hex block and HPs

- Sliding support at the right side for HPs to allow thermal expansion

Heat pipe mini-core design (1st design for the condenser)

❖ Design of the condenser



Geometry specifications:

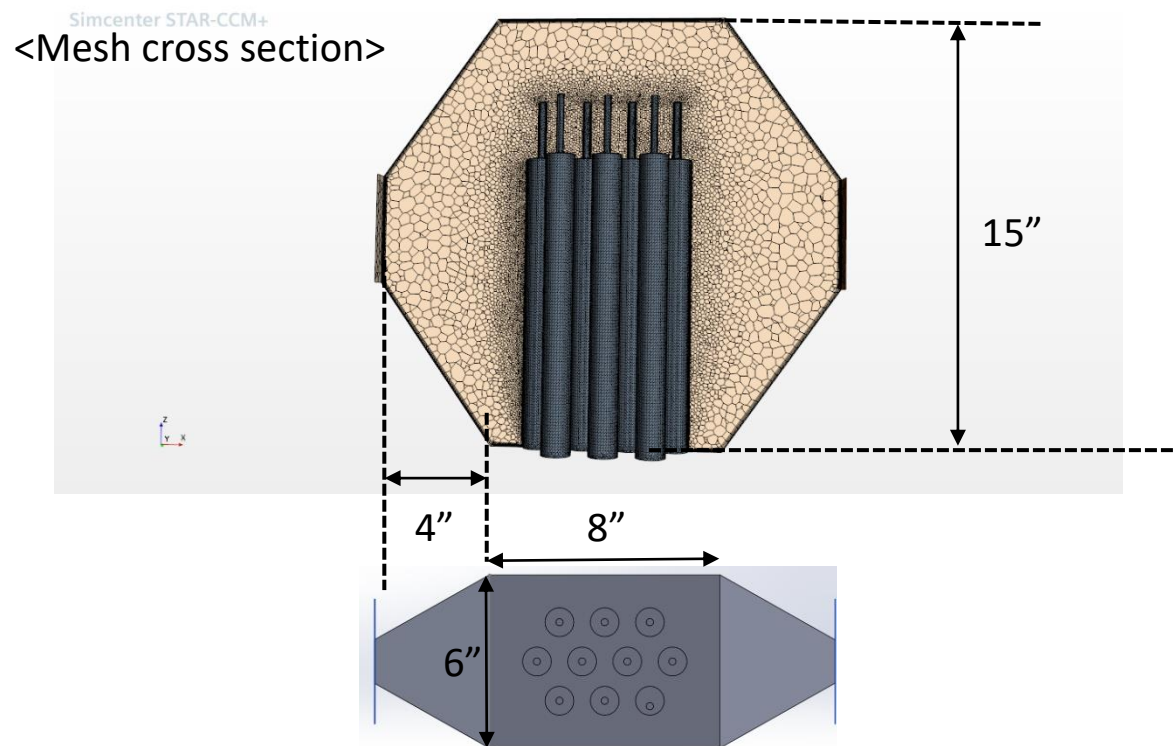
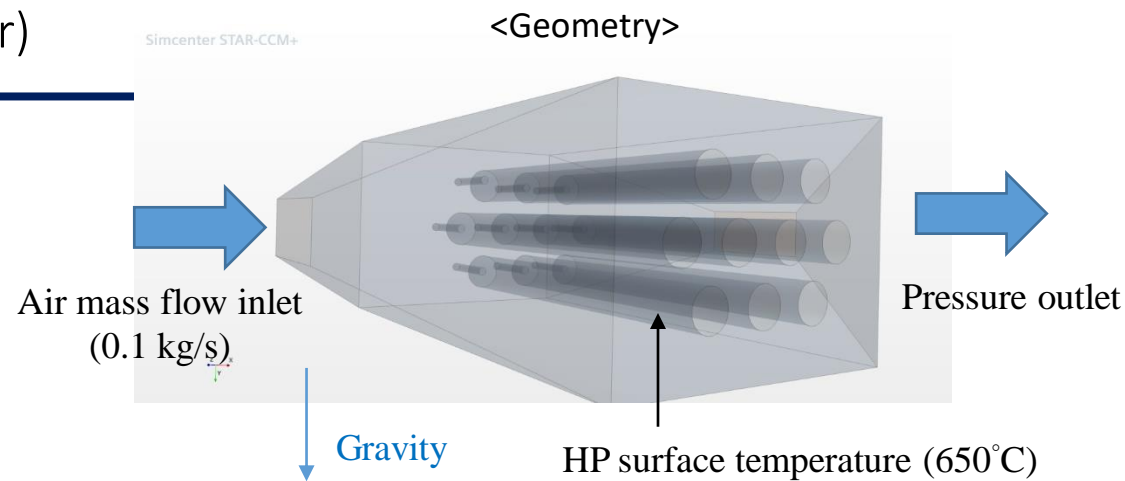
- HP-HP pitch = 1.57"
- Inlet & Outlet: 1.5" x 3.75" rectangular channel
- Wind tunnel: 8" x 6" x 15"

Assumptions:

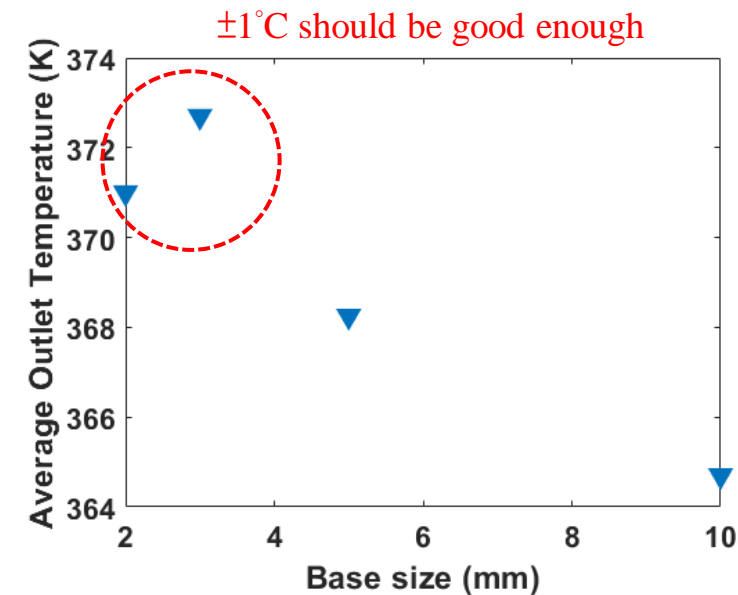
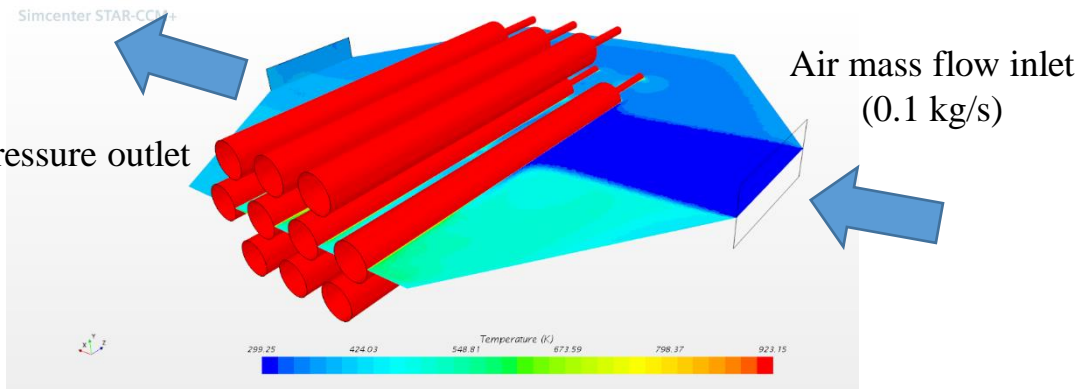
- Ignore radiation heat

Mesh conditions:

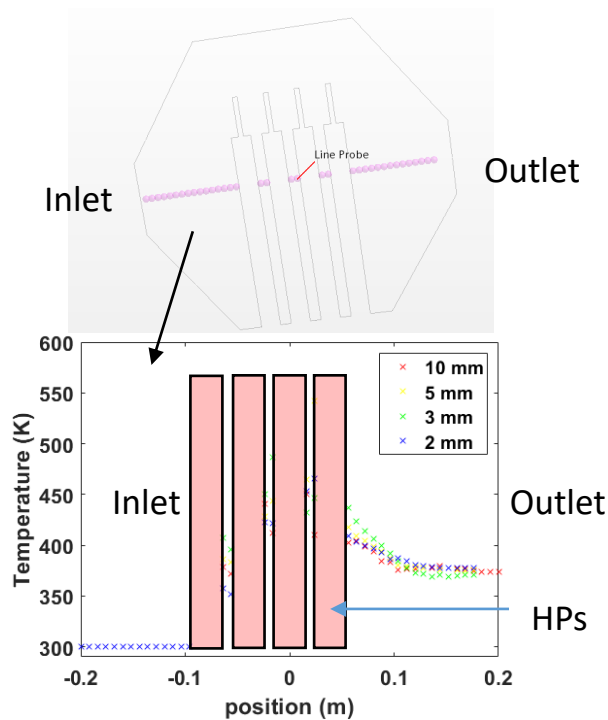
- 5 prism layers with total thickness of 1 mm is applied near boundaries
- 4 different base sizes were tested



Heat pipe mini-core design



<Mesh sensitivity study>



<Temperature profile at the central line>

Summaries

- Although it was not converged very well from the central line temperature profile, especially near the gaps between the HPs, the average outlet temperature is not sensitive to the mesh base sizes
- The average outlet temperature is estimated to be around 372 K, based on the energy balance equation, the heat removal rate is calculated as follows:

$$\dot{Q} = \dot{m}C_p\Delta T = 0.1 \left(\frac{kg}{s}\right) * 1006 \left(\frac{J}{kgK}\right) * (372 - 300)(K) = 7243.2(W)$$

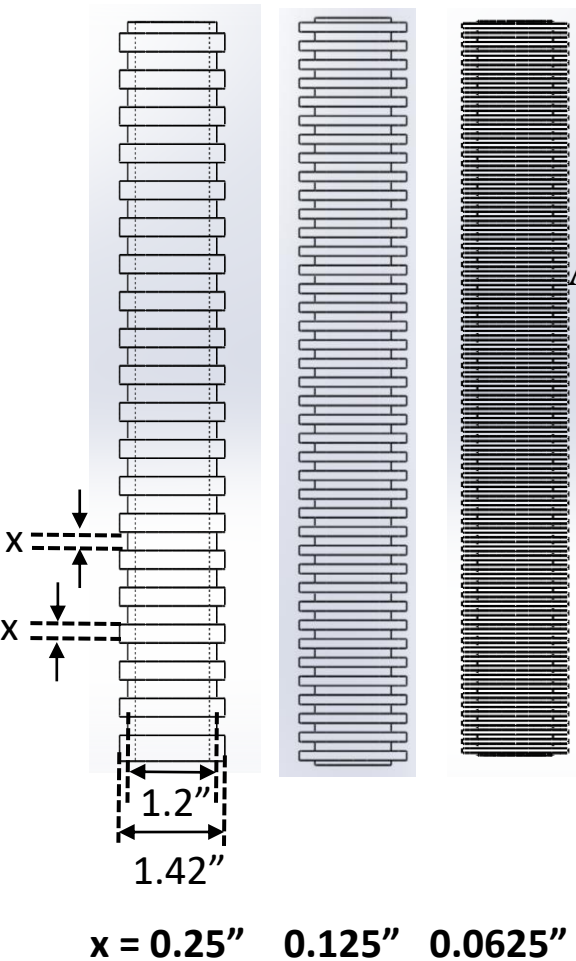
- The maximum required heat removal rate under horizontal HP is around 800 (W)*10 (HPs) = 8000 W, the result shows slightly insufficient heat transport capacity
- Another issue is the HP where directly facing the air inlet may be too cold for successful startup

Heat pipe mini-core design (2nd design for the condenser)

❖ 2nd design of the condenser

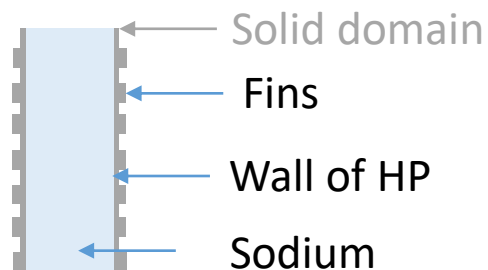
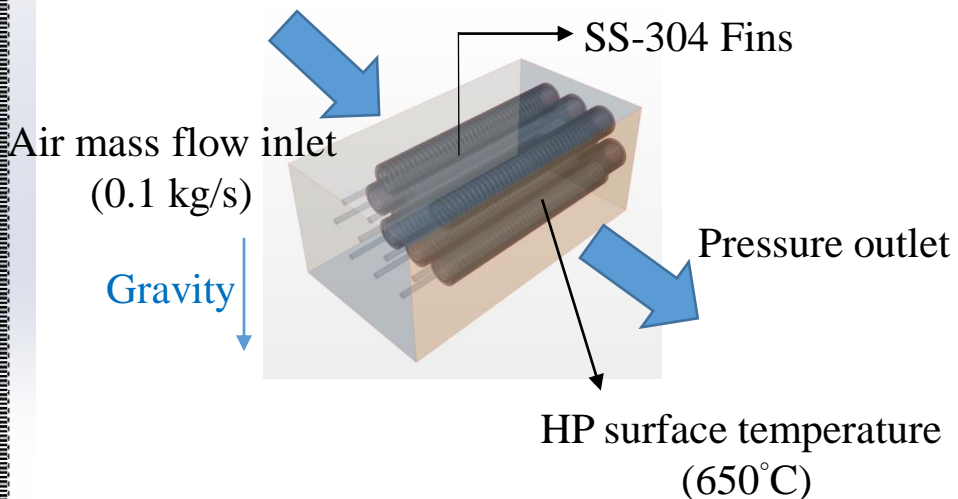
- Apply fins on the surface of the heat pipe to enhance the heat transfer rate

<Fin geometry>



<Geometry condition>

The size of wind tunnel was reduced for efficiency



<fin on HP>

Mesh conditions:

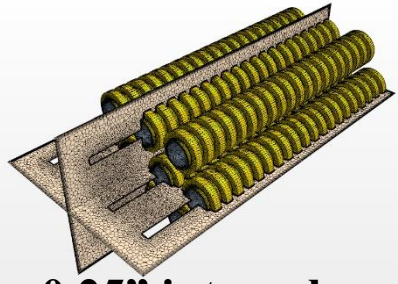
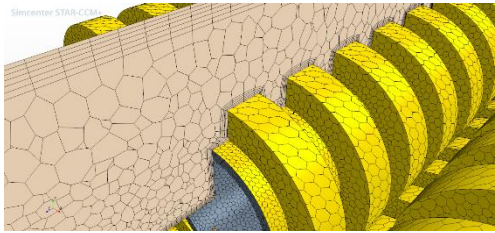
2-3 mm base size for solid fins, prism layers were applied in the solid-fluid interface, the mesh information of fluid domain are as follows:

	Base size	Cell #	Faces #	Vertices #
0.25" interval	10 mm	746321	3169672	1913267
	5 mm	1132014	4944705	3078931
	3 mm	1572237	7589406	5151847
0.125" interval	10 mm	4347786	19549956	13195943
	5 mm	5811361	26079798	17450696
	4 mm	5949960	26865336	18053038
0.0625" interval	3 mm	6344471	29239130	19927031
	10 mm	2099786	9221106	5831188
	7.5 mm	3462920	15584816	10105716
	5 mm	6219812	28248596	18482155
	4 mm	19487903	87808358	58642545

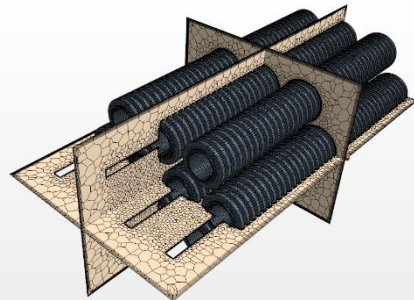
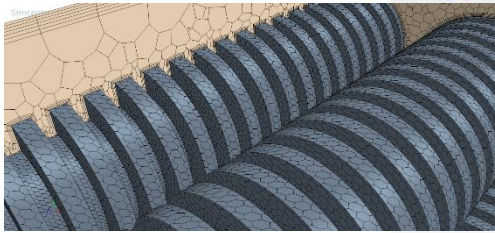
<Large cost to make fine enough mesh>

Unit: inches

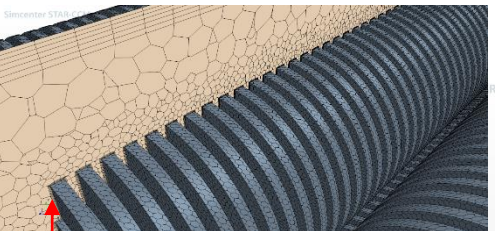
Heat pipe mini-core design (2nd design for the condenser)



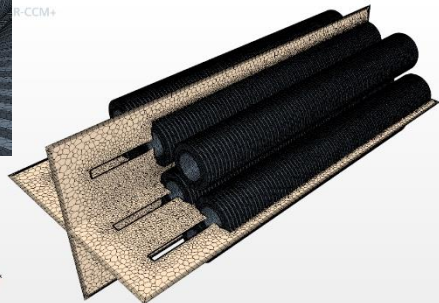
0.25" interval



0.125" interval



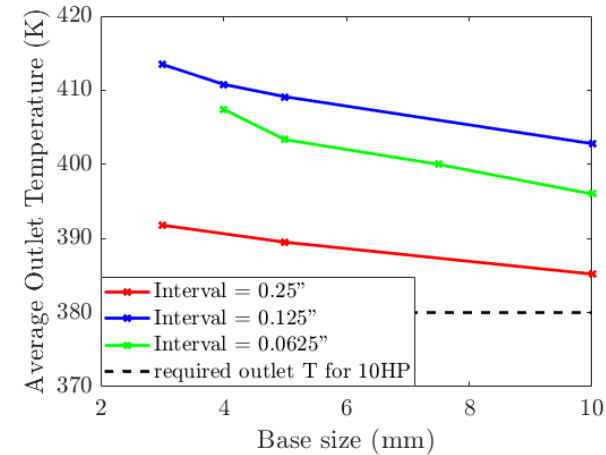
Large cost to make fine enough mesh



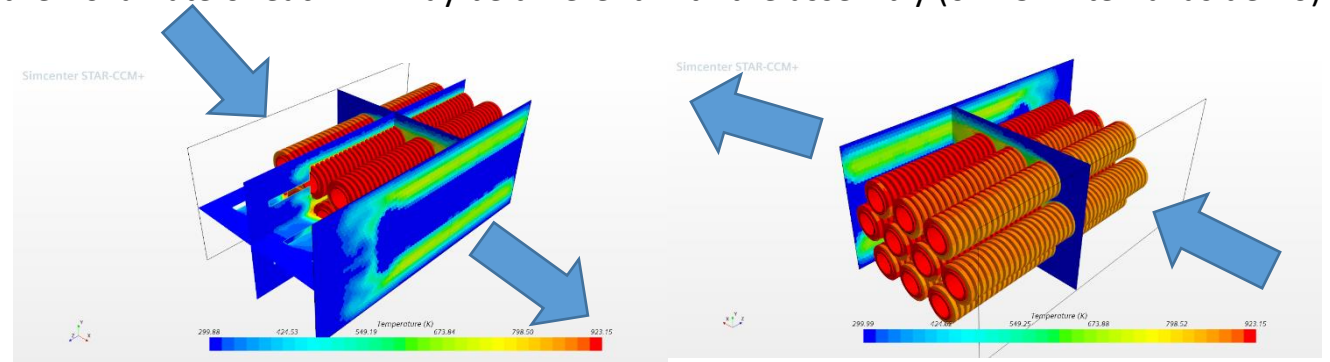
0.0625" interval

Results:

- The mesh average outlet temperature versus the mesh base size of fluid domain along with these three fin geometries shows:
 - More mesh is needed for interval = 0.0625" because of the complex geometry
 - The heat removal rate increases a lot as the interval of fins reduce from 0.25" to 0.125", but the effect become not significant as the interval from 0.125" to 0.0625"
 - Anyway, the required heat transfer rate can be achieved with the applied fins on HPs



- The heat removal rate of each HP may be different with the assembly (0.125" interval as demo)



Conclusion

- ❖ The data analysis for the experimental campaign of HP#1 (FR = 50%) and HP#13 (FR = 25%) indicates:
 1. the isothermal behavior of heat pipe is sensitive to the cooling efficiency as the operation condition approached the viscous limit curve
 2. Geyser boiling induced temperature oscillation increased the end-to-end temperature of the heat pipe. The geyser boiling, intermittent geyser boiling, and ideal regions were classified on the heat pipe performance characteristic plot
- ❖ The study of the startup process and performance of heat pipe under negative orientation shows:
 1. When the solid sodium was initially located in the condenser, the heat pipe failed startup as the inclination angles are close to horizontal
 2. When the inclination angle of the heat pipe decreased up to around -10 deg during isothermal operation, the B-side at the evaporator overheated and the liquid pool at the condenser end formed, heat pipe completely failed under -15 deg of inclination angle with the heating power of 1250 W
- ❖ The intense two-phase (slug) flow was observed in a vertical orientated heat pipe under 2000 W heating power through X-ray radiography measurement
- ❖ Aluminum profiles were utilized to enhance the structural integrity of the test section, new (UX type) split heater is going to be used for future X-ray radiography measurement to reduce the image artifact
- ❖ The MoSi₂ heaters are planned to be used for the heat pipe mini-core facility (MISOH2), the concept of the design had been performed, in the design 10 heat pipes are arranged under horizontal orientation. The condenser capacity analysis was conducted, showing the required heat transfer rate of the system (8000 W) can be realized

Cost Reduction for Advanced Integration Heat Exchanger Technology for Microreactors

DOE-NE Microreactor Program

NEUP Project 21-24226

University of Wisconsin

Greg Nellis and Mark Anderson, Professors

Ian Jentz and Jun Wang, Scientists

Erik Tillman, Graduate Student

Justin Apresa, Andrii Hopanchuk, and Madeline Morrell, Undergraduate Students

Idaho National Lab

Andrew Foss and Rami Saeed

Nuclear Energy Markets, Economics and Systems Analysis

Westinghouse Electric Company

Patrick Kopfle and Timothy Norton

Advanced Reactor Modeling and Simulation

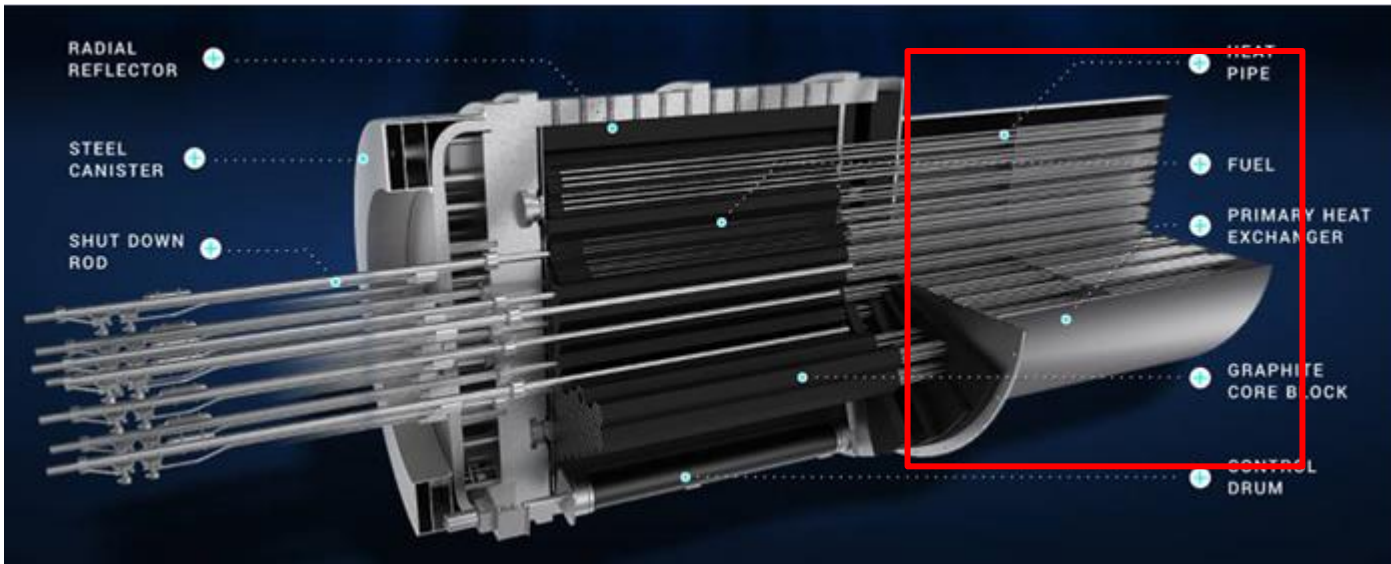
Overview

- Introduction to project and organization
- Work on Tasks 1 and 2 – development of simulation capability
 - Microreactor
 - Heat pipes
 - Cycle
 - PCHE interface heat exchanger
- Progress towards year 1 milestones
- Future work and conclusions

Interface Heat Exchanger

Objectives

- Development and validation of microreactor integration heat exchanger design tools
- Demonstrate potential cost-reduction/performance improvements in the context of an eVinci-like microreactor
- Obtain benchmark and validation data
- Obtain data for ASME boiler pressure vessel code case for PCHE HX in nuclear applications
- Demonstrate sub-size PCHE-based integration HX for sCO₂ and air working fluids
- Train several students for nuclear industry



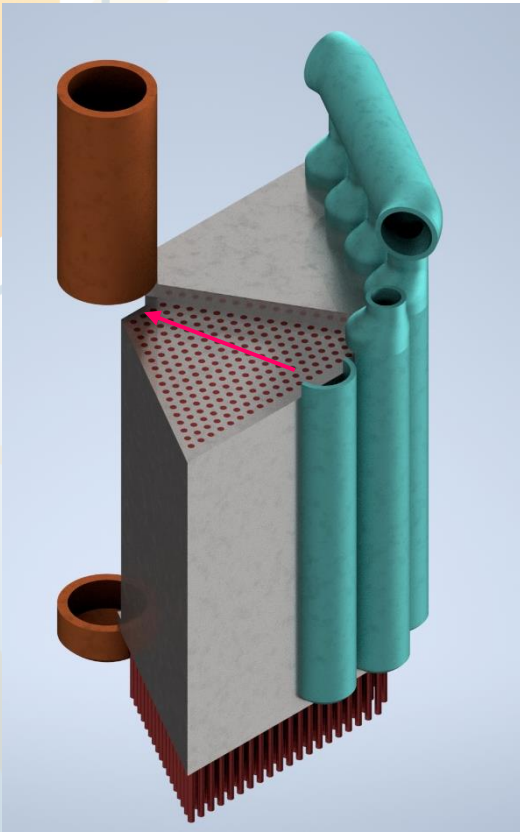
eVinci™ Micro-Reactor, Courtesy of Westinghouse Electric Company LLC

eVinci is a trademark or registered trademark of Westinghouse Electric Company LLC, its affiliates and/or its subsidiaries in the United States of America and may be registered in other countries throughout the world. All rights reserved. Unauthorized use is strictly prohibited. Other names may be trademarks of their respective owners.

© 2022 Westinghouse Electric Company LLC

All Rights Reserved

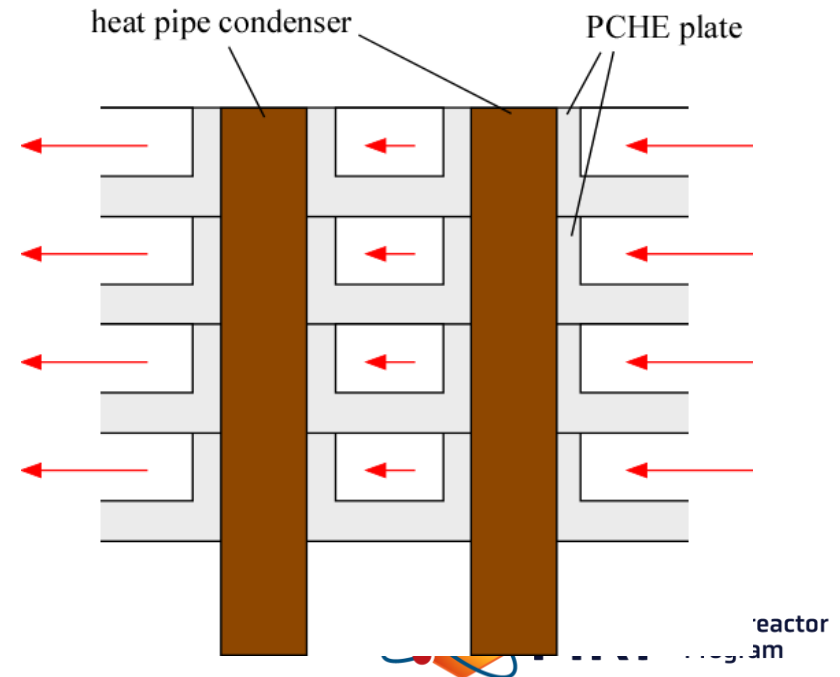
PCHE-Based Interface Heat Exchanger



Concept of a PCHE-based integration heat exchanger

Potential advantages (Morton, 2020 [6])

- Mature technology.
- Additional geometric degrees of freedom.
- Plates provide additional surface area
- Low susceptibility to single channel blockage.
- Reduced axial temperature gradient.
- Uniform condenser temperature (per heat pipe) takes advantage of the entire condenser section.
- High pressure capability of PCHE geometry.



Project Organization

Task 1: Develop balance of system models (Q1-Q4)

- Develop low-level models of the components affected by the integration heat exchanger
- Microreactor: fuel and monolith in order to predict limiting reactor hot spots and coupling between heat pipes
- Heat pipe: sodium heat pipe in order to predict thermal resistance and performance limits
- Cycle: end-use application in order to provide insight into the value of improved interface heat exchanger performance

Task 2: Develop model of PCHE-based integration heat exchanger (Q1-Q5)

- High fidelity model of the heat exchanger capable of carrying out design studies.
- Used to optimize heat exchanger subject to constraints related to loading and operating conditions.
- Develop detailed design for heat exchangers for air- and sCO₂-Brayton applications.

Task 3: Techno-economic optimization of integration heat exchanger (Q2 – Q6)

- Assess the value of PCHE-based integration heat exchanger in the context of two end-uses: air-Brayton and sCO₂-Brayton power cycles.
- Compare with alternative integration heat exchanger.
- Extension of the Economics-by-Design approach discussed in INL/EXT-21-63067 [1]

Project Organization

Task 4: Procure test articles (Q6-Q8)

- Obtain sub-size test articles corresponding to the two designs (air and sCO₂) developed in Task 2.

Task 5: Demonstrate performance using sCO₂ at UW (Q8-Q12)

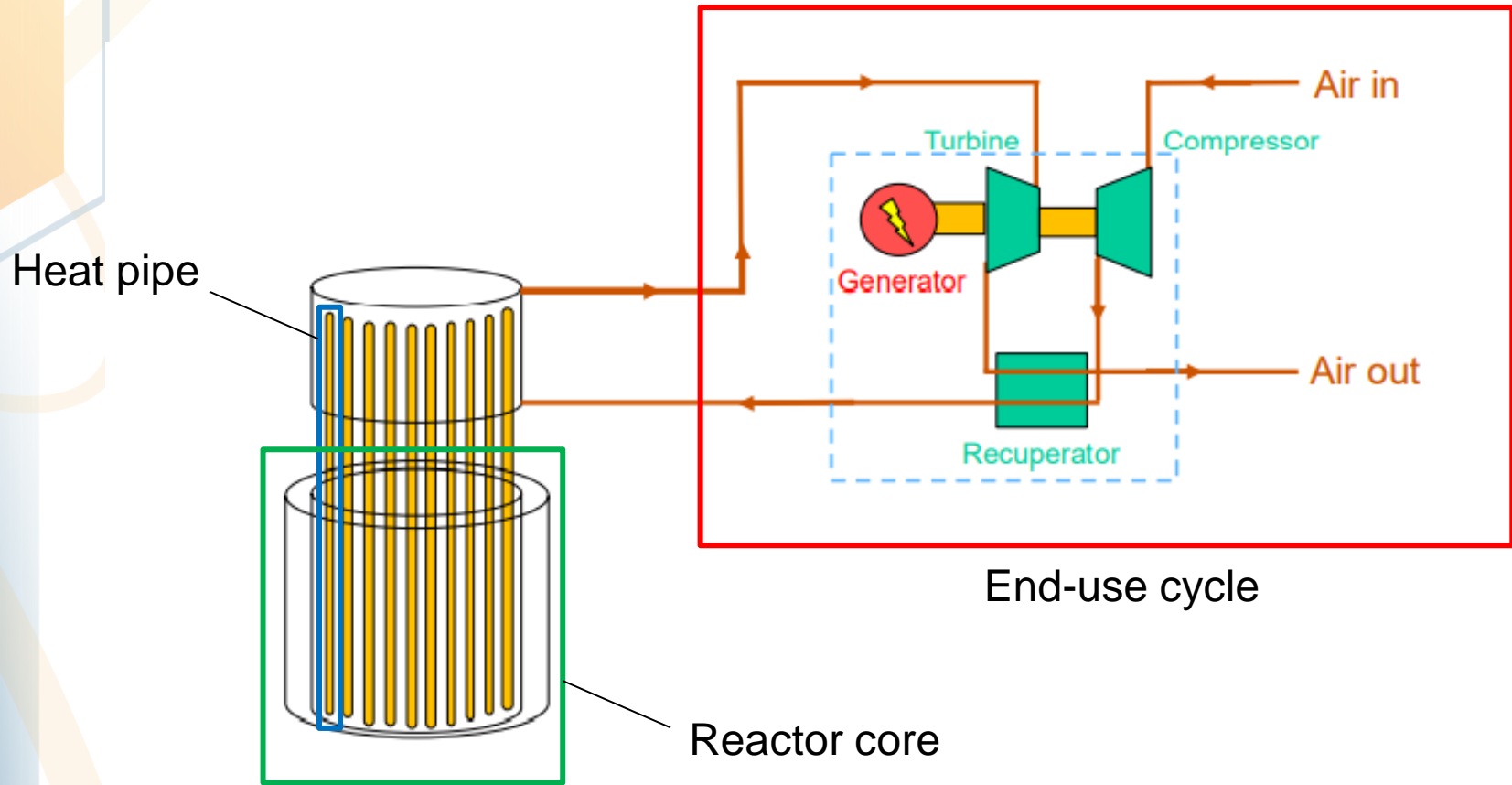
- Instrument sCO₂ test article in order to characterize thermal-hydraulic performance.
- Optical sensors will be used to obtain details regarding temperature distribution along plates.
- Install in sCO₂ loop at UW.

Task 6: Demonstrate performance using N₂ in MAGNET facility (Q9 – Q12)

- Instrument air test article at UW and deliver to MAGNET facility for integration and test.

	Quarter (relative to start of project)											
	1	2	3	4	5	6	7	8	9	10	11	12
Task 1: Develop micro-reactor model	■	■										
Task 2: Develop integration HX model	■	■								■	■	■
Task 3: Techno-economic optimization		■										
Task 4: Procure test articles		■				■	■	■				
Task 5: Demonstrate perf. w/sCO ₂ at UW		■						■	■	■	■	■
Task 6: Demonstrate perf. w/N ₂ at MAGNET		■							■	■	■	■

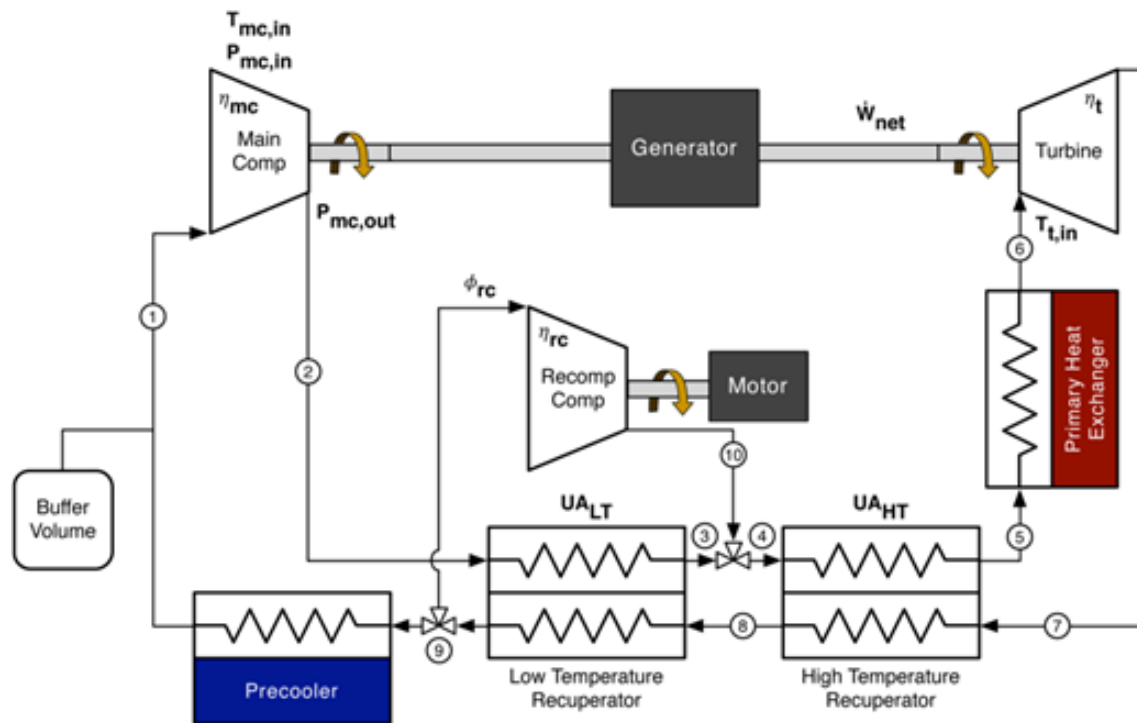
Task 1: Develop Balance of System Models



Conceptual schematic of microreactor interfaced with air-Brayton cycle, from Abou-Jaoude et al., (2021) [1]

End-use cycle

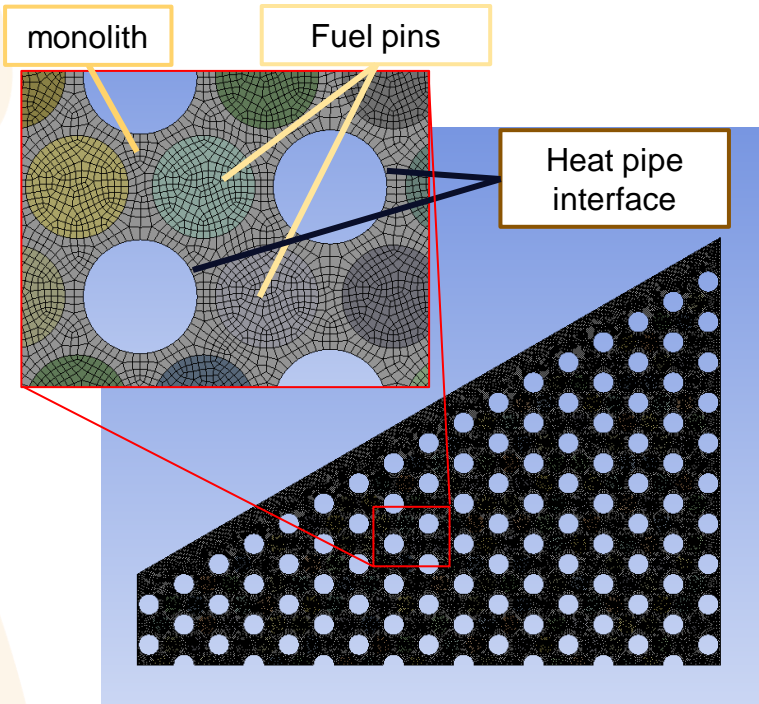
- Implemented in Engineering Equation Solver (EES) [2]
- Recompression $s\text{CO}_2$ cycle and recuperated air-Brayton cycle
- Integration heat exchanger performance included as pressure drop and approach temperature difference
- Still under development



Schematic of recompression $s\text{CO}_2$ cycle, from Dyreby et al., (2014) [3]

Microreactor

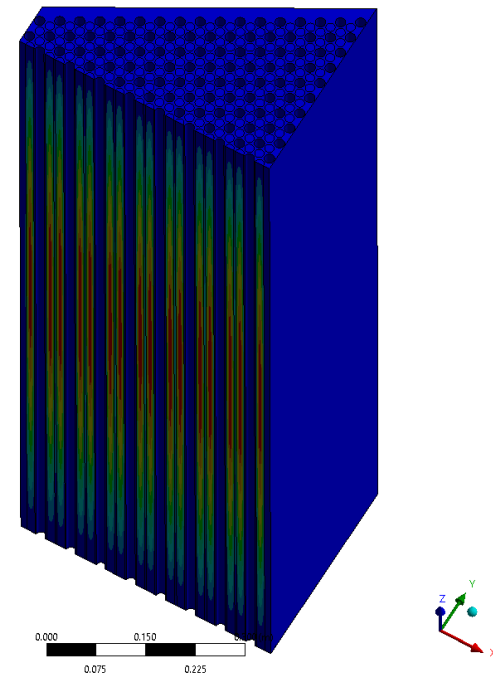
- Developed 1/12th symmetry model of microreactor core in both MOOSE and ANSYS
- ANSYS model runs more quickly and provides the necessary information for this project
 - Thermal resistances from evaporator to fuel center
 - Interaction between fuel rods based on non-uniform evaporator temperature



1/12th symmetry mesh of 316L stainless steel monolith and UO₂ fuel pins (2D face swept into 150 sections over 1.5 m core height)

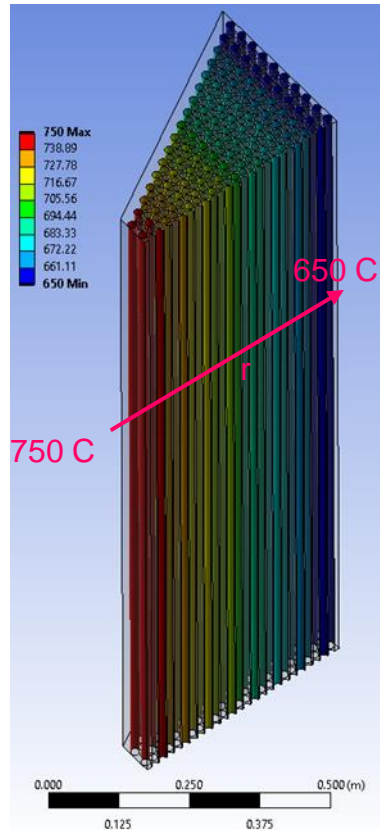
C: Steady-State Thermal
Temperature
Type: Temperature
Units: °C
Time: 1 s
1/19/2022 4:34 PM

772.2 Max
764.16
756.15
748.13
740.11
732.09
724.07
716.04
708.02
700 Min

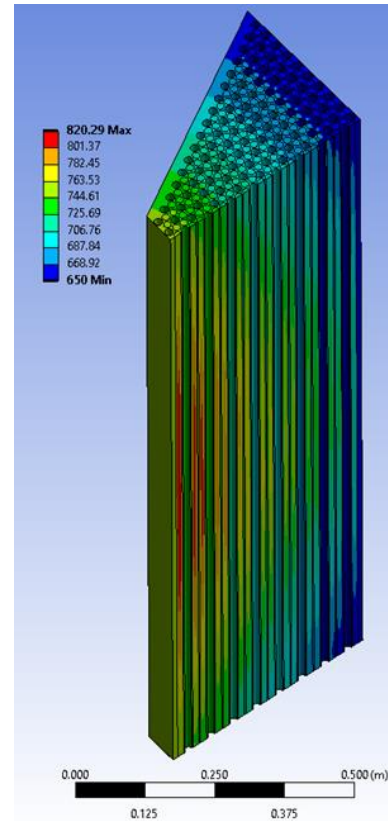


Fuel centerline temperatures peak 72.2 K above uniform 700°C Na heat pipe evaporators

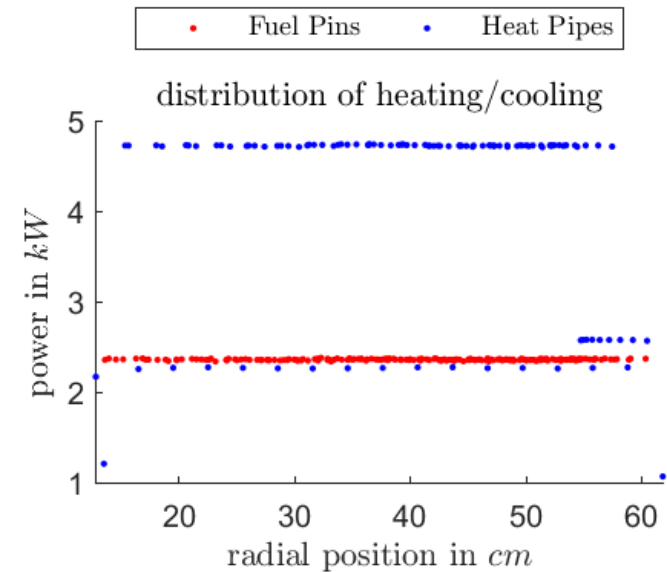
Microreactor: 5 MW removed by heat pipes



Heat pipe evaporator temperature decreases radially from 750 C to 650 C



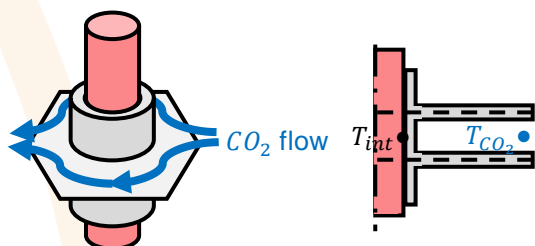
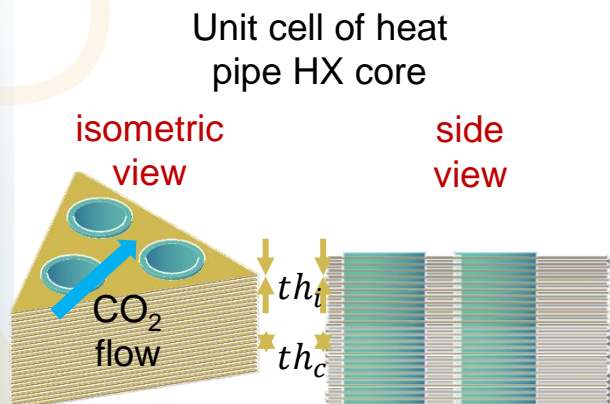
Monolith and fuel temperatures under radially decreasing heat pipe temperature (fuel centerline is max temp due to cosine power profile)



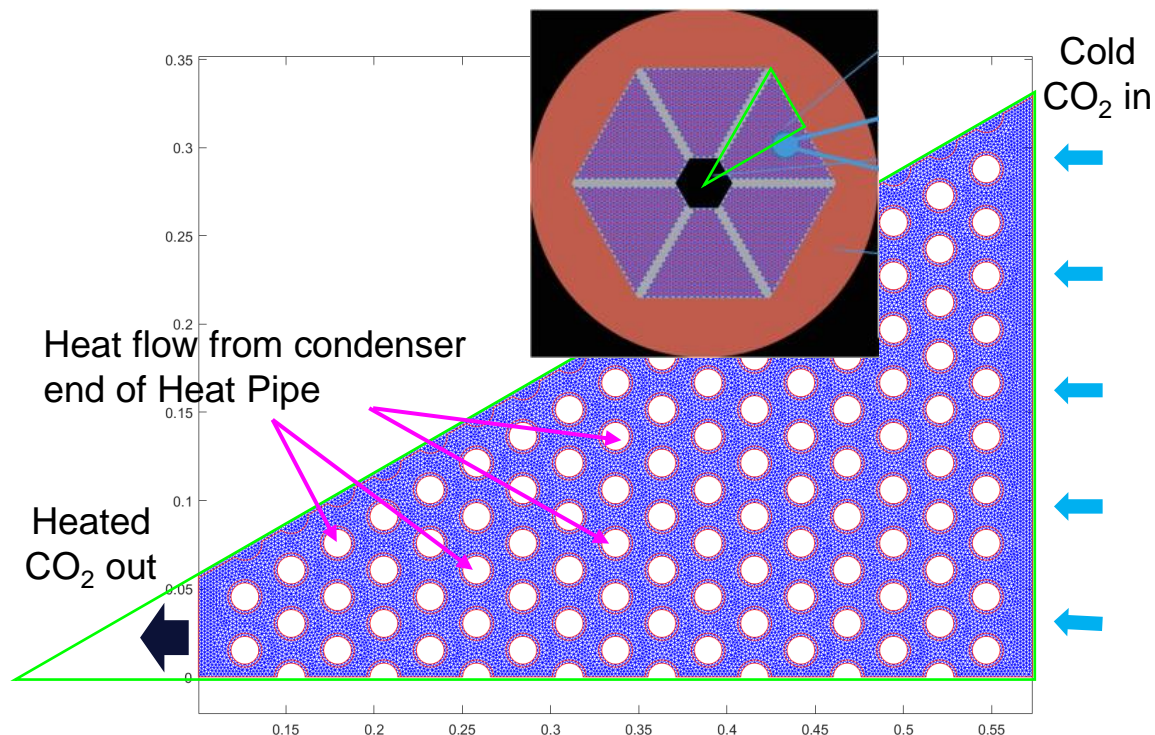
There is minimal interaction between heat pipes – even under conditions of radially varying evaporator temperatures all heat pipes provide similar rate of heat transfer.

PCHE Integration Heat Exchanger

- Developed a component model of a cross-flow printed circuit heat exchanger where CO₂ coolant flows through micro-channels and around embedded heat pipes.
- Utilizing a homogenization approach to pressure drop and heat transfer within the micro-channels.
- Allows investigation into operating conditions, flow configuration, and temperature distribution.



Micro-channel core behavior is described by volume fraction, friction factor, and heat transfer coefficient.

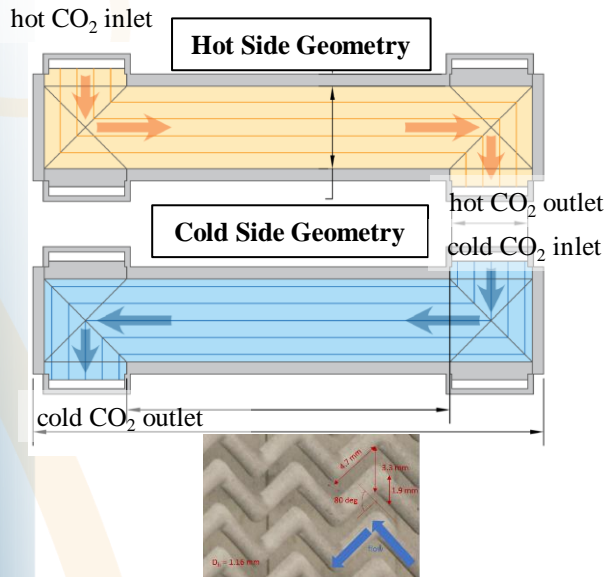


1/12th symmetry mesh of PCHE heat exchanger model.

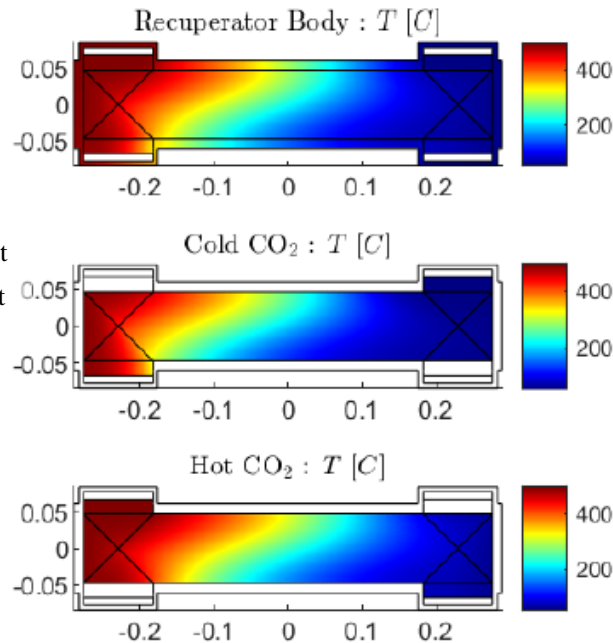
Holes are where heat pipe condenser interfaces.

PCHE Heat Exchanger Model

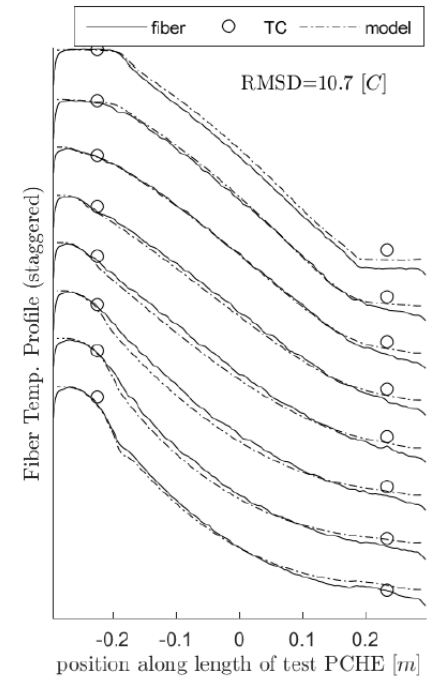
- Modeling technique has been proven for CO₂ recuperator applications through experimental comparison [7].
- Verified correlations for micro-channel pressure drop and heat transfer.
- Model predictions matched steady state experimental data over a large range of flow (1,000-64,000 Reynolds number).



Zig-zag channel PCHE flow layout and micro-channel geometry



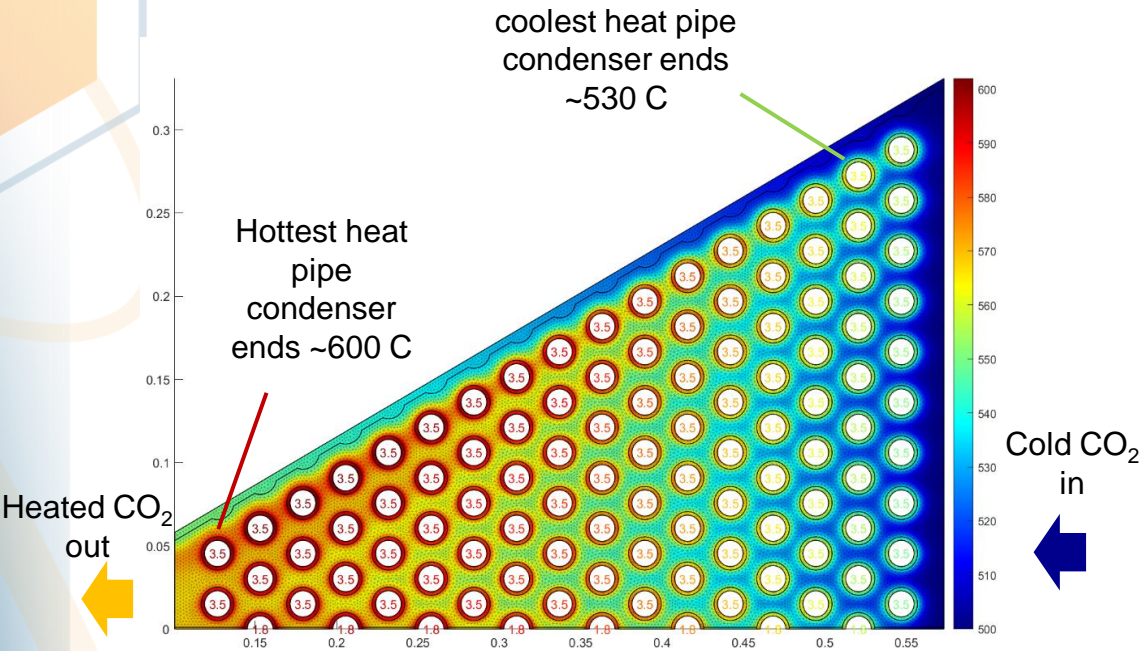
Homogenized model results for PCHE recuperator Body, cold and hot stream CO₂, temperatures (at design flow 0.0336 kg/s , 5,131-6,097 Re)



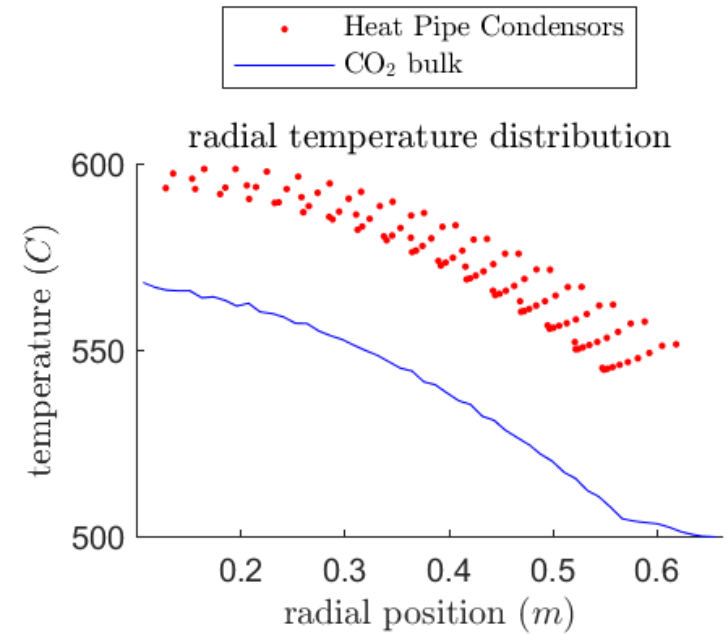
Comparison of PCHE internal temperatures as predicted by model and measured using fiber-optic and TC probes (at design flow

PCHE Integration Heat Exchanger

- Preliminary results for open channel design.



Distribution of heat exchanger and heat pipe interface temperature at 5 MW of reactor input and 60 kg/s of CO₂ coolant flow.



CO₂ bulk and condenser temperatures as a function of radial position

Progress Towards Milestones for Year 1

Milestone 1: Development of Balance of System Models

- Due: 9/30/22
- Deliverable: Technical report
- Progress: Cycle model are 50% done. Heat pipe model complete and integrated with EES. Microreactor model complete and efforts are underway to develop surrogate model suitable for integration with EES.

Milestone 2: PCHE Integration Heat Exchanger Model Complete

- Due: 6/30/22
- Deliverable: Technical report
- Progress: Modeling tool complete but not integrated with balance of system components. Modeling tool needs to be integrated with optimizer to allow design studies.

Milestone 3: Baseline PCHE Design Complete

- Due: 3/31/23
- Deliverable: Technical report
- Progress: Will begin once all modeling tools are available.

Future Work and Conclusions

Short term:

- Complete development of modeling tools and integrate.
- Develop design methodology.
- Complete initial design of sCO₂ and air heat exchangers.
- Pass relevant data on to INL for technoeconomic assessment.

Longer term:

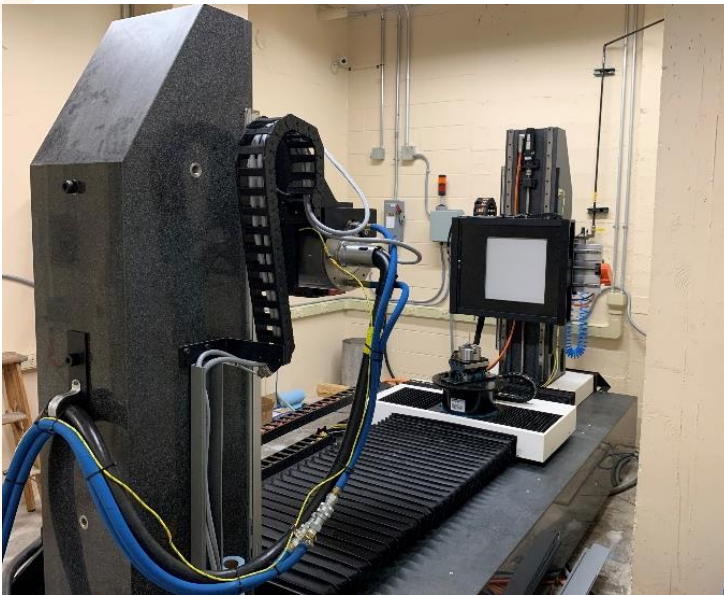
- Complete technoeconomic analysis.
- Develop sub-scale designs and procure test articles.
- Instrument and install test articles in sCO₂ loop (UW) and MAGNET (INL).

Open questions:

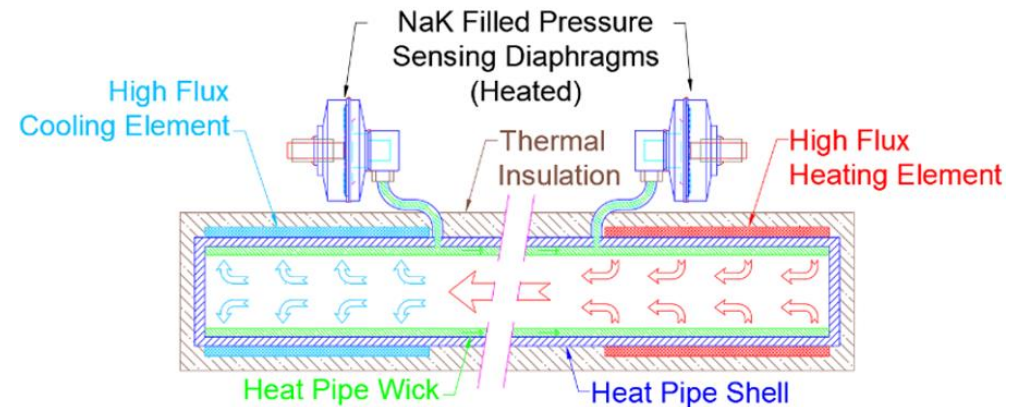
- Heat pipe to heat exchanger interface. High conductivity bonding/joining processes.
- Access to heat pipe codes .
 - SockEye
 - New version of HTPIPE, we have tested an older version (Prenger, 1979 [5])

Planned Heat Pipe Testing

- Measurement of heat pipe temperature profile in both steady-state and transient start-up operation.
- Use FO-DTS sensors for high-resolution measurements of internal temperature distribution.
- Measurement of heat pipe pressure profile will be challenging and will require Na-filled pressure transducers.
- Imaging of heat pipe in operation using 450 kV X-ray facility.



450 kV X-ray CT scanner



Schematic of pressure transducer measurement

References

- [1] Abou-Jaoude, A., A. Foss, Y. Arafat, and B. Dixon, *An Economics-by-Design Approach Applied to a Heat Pipe Microreactor Concept*, INL/EXT-21-63067 (2021).
- [2] Klein, S.A., *EES – Engineering Equation Solver*, Version 11.303, F-Chart Software, <https://fchartsoftware.com>
- [3] Dyreby, J., S. Klein, G. Nellis, and D. Reindl, “Design Considerations for Supercritical Carbon Dioxide Brayton Cycles with Recompression,” *J. of Eng. For Gas Turbines and Power*, Vol. 136(10), (2014).
- [4] Prenger, F.C., *Heat Pipe Computer Program (HTPIPE), User’s Manual*, LA-8101-M, November (1979).
- [5] Matthews, C., B. Wilkerson, R. Johns, H. Trelue, and R.C. Martineau, *Task 1: Evaluation of M&S tools for micro-reactor concepts*, LA-UR-19-22263, (2019).
- [6] Morton, T.J., *Integrated Energy Systems Development*, INL/MIS-20-59847D, Sep. (2020).
- [7] Jentz, I. and M. H. Anderson, “Coupled Heat Transfer and Hydraulic Modeling of an Experimental Printed Circuit Heat Exchanger Using Finite Element Methods,” *Journal of Thermal Science and Engineering Applications*, Vol. 13(3), 2021.
- [8] Chi, S. W.. *Heat pipe theory and practice: A sourcebook*. Hemisphere Publishing Corporation, Washington, D. C., (1976).
- [9] Teng, W., X. Wang, X., and Y. Zhu, “Experimental investigations on start-up and thermal performance of sodium heat pipe under swing conditions,” *Int. J. of Heat and Mass Transfer*, Vol. 152, (2020).

Questions



MRP Microreactor
Program